MEASUREMENT MODEL AND EVALUATION OF ULTRA WIDEBAND PROPAGATION LOSS IN AN INDOOR ENVIRONMENT FOR SHORT RANGE WIRELESS SYSTEMS

SENGALOUN KEOALOUNXAY

A THESIS SUBMITTED IN PARTIAL FULFILLMENT

OF THE REQUIREMENT FOR THE DEGREE OF

MASTER OF ENGINEERING IN INFORMATION ENGINEERING

FACULTY OF ENGINEERING

KING MONGKUT'S INSTITUTE OF TECHNOLOGY LADKRABANG

2009

KMITL-2009-EN-M-230-010

หัวข้อวิทยานิพนธ์	แบบจำลองการวัดและการประเมินผลของการสูญเสียในการแพร่กระจายคลื่นแบบแถบกว้างยิ่งในสภาวะแวดล้อมภายในอาคารสำหรับระบบแบบไร้สายระยะสั้น.
นักศึกษา	นายแสงอรุณ แก้วอรุณไชย์
รหัสประจำตัว	50061013
ปริญญา	วิศวกรรมศาสตรมหาบัณฑิต
สาขาวิชา	วิศวกรรมสารสนเทศ
พ.ศ.	2552
อาจารย์ที่ปรึกษาวิทยานิพนธ์	รศ. นิกร สุขุตมตันติ
อาจารย์ที่ปรึกษาวิทยานิพนธ์ร่วม	อาจารย์ สถาพร พรมวงศ์

บทคัดย่อ

วิทยานิพนธ์ฉบับนี้ได้วิเคราะห์ประสิทธิภาพของช่องสัญญาณการส่งผ่านสัญญาณแบบแถบกว้างยิ่ง และได้ทำการวัดและทดสอบจริงของค่าการสูญเสียในการส่งผ่านช่องสัญญาณในสภาวะแวดล้อมภายในอาคาร โดยใช้สายอากาศแบบกรวยคู่ทั้งด้านส่งและด้านรับ ทำการวัดฟังก์ชันถ่ายโอนความถี่ของช่องสัญญาณวิทยุโดยใช้เครื่องวิเคราะห์โครงข่ายแบบเวกเตอร์ซึ่งเป็นอุปกรณ์หลักในการวัดโดยวัดที่ช่วงความถี่จาก 3 กิกะเฮิร์ต ถึง 11 กิกะเฮิร์ต และได้ใช้รูปคลื่นสัญญาณส่งแบบแถบผ่านสี่เหลี่ยม โดยทำการวัดภายในห้องเรียนซึ่งเป็นห้องใหญ่ที่มีขนาดของห้อง 12.40 x 20.00 m สำหรับการทดลองในงานวิจัยนี้ได้แยกการวัดออกเป็น 4 แบบดังนี้:

แบบที่ 1 วางสายอากาศทางด้านส่งเป็นแนวตั้ง-วางสายอากาศทางด้านรับเป็นแนวตั้ง

แบบที่ 2 วางสายอากาศทางด้านส่งเป็นแนวตั้ง-วางสายอากาศทางด้านรับเป็นแนวนอน

แบบที่ 3 วางสายอากาศทางด้านส่งเป็นแนวนอน-วางสายอากาศทางด้านรับเป็นแนวนอน

แบบที่ 4 วางสายอากาศทางด้านส่งเป็นแนวนอน-วางสายอากาศทางด้านรับเป็นแนวตั้ง

จากนั้นจะนำผลที่ได้จากการวัดมาประเมินหาค่าพารามิเตอร์ต่างๆของวิทยุอิมพัลส์แบบแถบกว้างยิ่งโดยประยุกต์ใช้สูตรการส่งผ่านสัญญาณของฟรีส ทางด้านรับได้พิจารณาใช้เครื่องรับสัญญาณแม่แบบ โดยผลที่ได้จากการวัดจะถูกนำไปวิเคราะห์เพื่อหาค่าพารามิเตอร์ต่างๆ ที่แสดงให้เห็นถึงผลการเปลี่ยนแปลงของช่องสัญญาณแบบแถบกว้างยิ่งอันเนื่องมาจากทิศทางของการวางสายอากาศในแต่ละแบบอาทิเช่นค่าการสูญเสียเชิงวิถี, ค่าเฉลี่ยเวลาประวิงและการแผ่ประวิง RMS, ค่าอัตราความผิดพลาดบิต และสุดท้ายได้แสดงผลการเปรียบเทียบค่าการสูญเสียเชิงวิถีระหว่างแบบจำลองการวัดทั้งสี่แบบ และ ทำการเปรียบเทียบค่าค่าอัตราความผิดพลาดบิตแต่ละตำแหน่งในสี่แบบ จากการวิจัยนี้จะเป็นประโยชน์ในการออกแบบระบบวิทยุอิมพัลส์แถบกว้างยิ่งสำหรับระบบโครงข่ายแบบไร้สายระยะสั้นในสภาวะแวดล้อมภายในอาคารในอนาคต

Thesis Title	Measurement Model and Evaluation of Ultra Wideband Propagation Loss in an Indoor Environment for Short Range Wireless Systems
Student	Mr. Sengaloun Keoalounxay
Student ID.	50061013
Degree	Master of Engineering
Program	Information Engineering
Year	2009
Thesis Advisor	Assoc. Prof. Nikorn Sukutamatanti
Thesis Co-Advisor	Mr. Sathaporn Promwong

ABSTRACT

Ultra wideband (UWB) technology is developed very fast in the past few years. It offers many competitive advantages. In communications, it can provide high data rate performance in multi-user network application. UWB thus, communication systems have been subjected to extensive research and development projects. This thesis focuses on the propagation loss in UWB system. This analysis emphasizes on propagation path loss consideration between transmitter and receiver based on parametric measurement. The research considers using the short range wireless systems in an indoor environment. The concept of model, we suppose the transmitter is an access point and receiver is general electric appliance for example television, camcorder, notebook, PDA and other appliances that can received signal from the access point. The transfer functions of channels are experimented in the large lecture room by using a vector network analyzer (VNA). The antennas used for transmitting and receiving are biconical antennas. The polarization of the Tx and Rx antennas designs are as follows:

Polarization 1: Tx Vertical – Rx Vertical

Polarization 2: Tx Vertical – Rx Horizontal

Polarization 3: Tx Horizontal – Rx Horizontal

Polarization 4: Tx Horizontal – Rx Vertical

The results from VNA are brought to analyze the parameters in UWB system. The results of this study are useful for the design of UWB IR propagation channel in an indoor environment for short range wireless systems.

ACKNOWLEDGMENTS

This endeavor was truly a life learning experience. Thanks are due to many people for their interactions and collaborations.

First of all, I would like to express my sincere appreciation and great gratitude to JICA for a financial support through generous grants under the AUN/SEED-Net project and thank to AUN/SEED-Net for offering me this opportunity to study a Masters degree under a prestigious scholarship which lovers everything since I commenced my study here. I would also like to thank all staff at AUN/SEED-Net who provided supports during my studies here.

I would also like to thank Associate Professor Nikorn Sukutamatanti, my advisor for his guidance and support throughout my thesis. I thank him for all of his valuable suggestions, discussions and all equipments that I used during my study.

I would also like to thank Dr. Sathaporn Promwong, a Head of the Department of Information Engineering who is also my co-advisor, for his guidance, insights and supports during the development of the thesis's topic and for the time he dedicated to this thesis. He patiently discussed all the technical ideas and knowledge with me and gave indispensable suggestions for my research. I am Thankful of for all detailed explanations he provided in order to clarify my doubts during my days in his department. He also helped me with all of my publications. I really feel indebted to him.

I would also like to thank Professor Dr. Jun-ichi Takada, my co-advisor from Tokyo Institute of Technology, Japan. I have benefited from his wisdom, suggestions and comments. I respect him for his rigorous attitude towards scientific research, which led to many improvements of this dissertation.

I would also like to thank my entire teachers at the Department of Information Engineering especially, teachers in wireless communication research group (WCRG) who shared with me lots of interesting ideas and knowledge which help me improve my knowledge. I also thank them for their suggestions, encouragement and understandings during my study period.

There are so many friends and colleagues who were really helpful to me throughout the year that I would also like to thank, especially Mr. Narongsak Manositthichai, Mr. Sanit Teawchim, and other people that I didn't mention in this thesis. They also assisted with my

experiments, such as showing me how to setup and calibrate VNA, run a program when I moved each point, and solve the program when I have any problems. I am very grateful for all of their supports when I was in difficult times during my studies. Without them my work might have been more difficult than what I have experienced.

I would like to thank all committee members who helped reviewing my dissertation, and for their patience in answering all the questions that I asked. I also thank them for their time to serve as my advisory committee members and attend to my thesis defend.

Last but most important I would also like to thank my family and my parents who have continuously encouraged and supported me to studies, my wife's family for all of their tremendous support and their helps to take care of my son and daughter during my absence. I cannot imagine being successful in my studies without them. I am forever indebted to them. This dissertation is a dedication for their love.

I especially would like to thank my wife, Khampheng Phonsavat, for her patience, care, support and her unconditional love even she had difficult times during my studies here. She was pregnant when I first came to study and has to look after or take care of our son which was only one and half years but she still worked hard and gave me her supports. It has been and it is still being extremely difficult to be away and I recognize that. I cannot imagine life without her. I am forever indebted to her. This dissertation is a dedication for her love.

Thank you all.

Sengaloun Keoalounxay

TABLE OF CONTENTS

TABLE OF CONTENTS (CONT.)

TABLE OF CONTENTS (CONT.)

TABLE OF CONTENTS (CONT.)

LIST OF TABLES

LIST OF FIGURES

LIST OF FIGURES (CONT.)

LIST OF FIGURES (CONT.)

LIST OF ABBREVIATIONS

AWGN	:	Additive White Gaussian Noise
BER	:	Bit Error Rate
C.F.R	:	Code of Federal Regulations
DLP	:	Digital Light Processor
EIRP	:	Effective Isotropic Radiated Power
erfc	:	Complementary error function
ETSI	:	European Telecommunications Standards Institute
FAA	:	Federal Aviation Administration
FCC	:	Federal Communications Commission
FD	:	Frequency Domain
FFT	:	Fast Fourier Transform
GPIB	:	General Purpose Interface Bus
GPS	:	Global Positioning Systems
HDTV	:	High Definition Television
IEEE	:	Institute of Electrical and Electronics Engineers
IF	:	Intermediate Frequency
IR	:	Impulse Radio
ITU	:	International Telecommunication Union
LOS	:	Line-of-Sight
MAC	:	Media Access Control
MB-OFDM	:	Multi-Band Orthogonal Frequency Division Multiplexing
NLOS	:	Non Line-of-Sight
NOI	:	Notice of Inquiry
OFDM	:	Orthogonal Frequency Division Multiplexing
PAM	:	Pulse Amplitude Modulation
PC	:	Personal Computer
PDP	:	Power Delay Profile
PL	:	Path Loss
PSD	:	Power Spectral Density

LIST OF ABBREVIATIONS (CONT.)

RF	:	Radio-Frequency
RMS	:	Root Mean Square
SNR	:	Signal to Noise Ratio
SS	:	Spread Spectrum
TG	:	Task Group
UWB	:	Ultra Wideband
UWBWG	:	Ultra Wide Band Working Group
VNA	:	Vector Network Analyzer
WBAN	:	Wireless Body Area Networks
WLAN	:	Wireless Local Area Networks
WMAN	:	Wireless Metropolitan Area Networks
WPAN	:	Wireless Personal Area Networks

LIST OF SYMBOLS

A	:	Pulse amplitude
B	:	Noise equivalent bandwidth of the receiver
dB	:	Decibel
c	:	Speed of light [$3x10^8$ m/s]
d	:	Distance of the transmitter-receiver link
E_b	:	Average energy per bit
f_H	:	Highest cut-off frequency of the UWB bandwidth
f_L	:	Lowest cut-off frequency of the UWB bandwidth
f	:	Frequency
G_r	:	Gain of receive antenna
G_t	:	Gain of transmit antenna
G_f	:	Free space propagation gain
k	:	Boltzmann's constant
P_r	:	Received power
P_t	:	Transmitted power
R_b	:	Bit rate
Rx	:	Receiver antenna
Tx	:	Transmitter antenna
z	:	Correlation receiver output
Hz	:	Hertz
GHz	:	Gigahertz
m	:	Meter
s	:	Second
ns	:	Nanosecond
W	:	Watt
mW	:	Milliwatt
B_f	:	Fractional bandwidth
$H(\omega)$	:	Frequency transfer function
N_{smp}	:	Sampling number

LIST OF SYMBOLS (CONT.)

S_{21}	:	Transmission coefficient
t	:	Time
α	:	Attenuation
$\delta(t)$	:	Dirac delta function
λ	:	Wavelength
η	:	Intrinsic impedance, $\eta = \sqrt{\mu/\varepsilon}$
ε	:	Permittivity, $\varepsilon = \varepsilon_0 \varepsilon_r$
ε_r	:	Dielectric constant
ε_0	:	Permittivity of constant, $\varepsilon_0 \approx 1/36\pi \times 10^{-9}$
μ	:	Permeability, $\mu = \mu_0 \mu_r$
μ_0	:	Permeability of free space, $\varepsilon_0 \approx 400\pi \times 10^{-9}$
μ_r	:	Relative Permittivity
$\bar{\tau}$	:	Mean excess delay
σ_r	:	RMS delay spread
$\rho(d)$	:	Correlation coefficient
v_t	:	Transmitted signal
v_r	:	Received signal
$v_i(t)$	:	Input signal

Chapter 1

Introduction

1.1 Introduction

Recently, ultra wideband (UWB) radio technology has become an important topic for microwave communication because its potential high data rates, low cost and low power consumption properties. The UWB is different from other radio frequency (RF) technologies. As usual, the demands for data higher price, higher security and contact information more quickly. Therefore, new technologies have to find places in overcrowded radio frequency spectrum and use it in an efficient way. UWB is a technology based on the signal spreads across a wide bandwidth, a fact that could bring several advantages compared with other communication systems is narrow. It can coexist with a system of radio stations, as illustrated in figure 1.1[1].

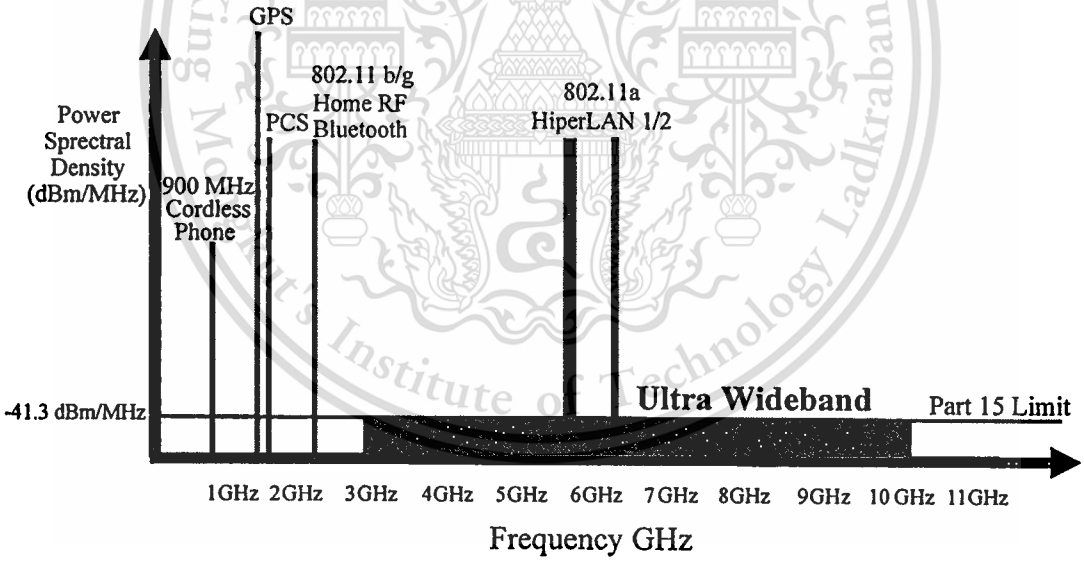

Figure 1.1 Comparison of occupied bandwidths by UWB and other wireless technologies

UWB communication systems are widely used for a variety of applications due to their exceptionally attractive features. The objectives of this technology are low power, low-cost equipment, high data rates, precise positioning capability and low interference.

However, UWB is not a new technology. UWB was first used in the beginning of the twentieth century, by transmitting Morse code sequences with spark gap radio devices [2],

[3]. Later, in the late twentieth century, UWB radar systems have been used primarily in military applications, to work under classified programs such as highly secure communications. Due to the recent improvements in micro-processing and fast switching technologies, UWB has commercial applications. In 2002, a remarkable step in the history of UWB communications has been taken, as in the United States the Federal Communications Commission (FCC) allows the commercial use of UWB applications with limited power limits. Multiple users can use the unlicensed UWB spectrum on a non-interfering basis with other communications systems. The european telecommunications standards institute (ETSI) is currently working in the definition of the UWB standard. However, there are many challenges such as UWB regulatory problems to avoid interference with other systems, and there is no clear global consensus on a standard technology with technical issues and the implementation yet.

UWB communications have been planned for high data rates over short ranges for applications such as wireless personal area networks (WPANs) and high-speed broadband internet access. Even the work is being done for UWB applications in the localization with high accuracy, high resolution ground-penetrating radar, through-wall imaging, precision navigation or asset-tracking radio frequency identification (RFID) for inventory purposes objects [4]. Although more than 80% of commercial UWB applications are planned for indoor use, due to the low transmitting power allowed for UWB communications, UWB may also be used for the physical layer of sensor, ad hoc or mesh or other outdoor communication networks.

1.2 Background and Motivation

In 2002, the FCC allocated 7.5 GHz spectrum from 3.1 GHz to 10.6 GHz for UWB devices. A few years later there have been a significant increase in research activity in both the industry and academic circles in the field of UWB systems for short range indoor communications [5]. UWB communications involves transmitting data using very short pulses thus occupying very large bandwidth. The energy of the UWB signals is spread over a large spectrum thus having the inherent property of being overlaid over existing systems in that frequency range. The advantage of using short pulses is fine timing resolution thus more channel multipaths can be resolved.

Reliable communication is becoming increasingly important day by day. High bit error rate (BER) is not allowed in most commercial applications. In some UWB applications planned such as imaging systems, sensor networks and motorsports radar systems, errors in communications may have disastrous consequences. The FCC [6] specified that UWB has a frequency spectrum ranging from 3.1 to 10.6 GHz and a fractional bandwidth greater than 0.20 or occupied bandwidth greater than 500 MHz. The power density of the UWB signal is considered to be noise for other communication systems because its power spectral density is below the part 15 noise limit. Therefore, UWB radio technology can coexist with other RF technologies without interference. Moreover, UWB radio technology can be utilized for commercial, short-range, low power consumption, low cost for indoor communication systems such as WPANs [7].

This thesis measurement based on parametric modeling by considering pathloss, and evaluated bit error rates; the research propose a template waveform instead of a conventional matched filter technique. In the proposed scheme, the template waveform is considered at the receiver side to maximize the signal to noise ratio (SNR). The transmission waveform and the receiver template waveform are keys for the extension of the Friis' transmission formula to UWB system. An experiment is carried out using biconical antennas for UWB operation in the classroom.

1.3 Research Approach

This thesis analysis the effective spread of channel UWB impulse radio (UWB-IR) and testing quality of transmission channel in an indoor environment measurement based parametric channel modeling by using biconical antenna at the transmitter and receiver, this technique is applied to 121 points at the receiver side each point is 40 cm apart, the nearest point between the transmitter and the receiver is 2.90 m and the furthest between the transmitter and the receiver is 6.66 m. The location used for measurements is a large classroom within a 12 floors building of the Department of Information Engineering, Faculty of Engineering, King Mongkut's Institute of Technology Ladkrabang (KMITL). The measurement is implemented by using matlab simulation for path loss, delay characteristic, and BER.

1.4 Scope of thesis

This thesis focuses on the effectiveness of UWB-IR propagation channel in an indoor environment by conducting a real measurement of a biconical antenna at the transmitter and receiver side set up in 4 models (Polarizations) as follows:

Polarization model	Polarization of Tx and Rx antennas	
	Tx antenna	Rx antenna
1	Vertical	Vertical
2	Vertical	Horizontal
3	Horizontal	Horizontal
4	Horizontal	Vertical

In chapter 2, UWB communication systems and the background information on UWB are provided. This background is needed for the chapters that follow.

In chapter 3, the theory and analysis of UWB channel propagation in an indoor environment are studied, where impulse radio, the institute of electrical and electronics engineers (IEEE) standard, some parameters used for analysis and extension of Friis transmission formula for UWB are briefly reviewed and presented.

In chapter 4, the experimental setup and channel measurement model are presented while chapter 5, focuses on evaluating the performance and presenting the results of experiment.

Finally, Chapter 6 provides conclusions and recommendations for future works.

Chapter 2

Ultra Wideband Communication Systems

2.1 Introduction

Today, most computers and consumer electronic devices from a digital camcorder and DVD player to a mobile PC and a high definition TV (HDTV) require wires to record, play or exchange data. UWB will eliminate these wires, allowing people to "unwire" their lives in new and unexpected ways. Due to a very large bandwidth (7.5 GHz) of free spectrum, FCC recently legalized UWB for commercial use spectrum allocation overlays existing users, but its allowed power level is very low in order to minimize the interference with very high data rates at 10 meters. The data rate of approximately 110 Mbps and possibly 480 Mbps can be achieved at a distances of 3 m under current regulations transmitters which is suitable for battery operated devices.

UWB also has several applications all the way from wireless communications to radar imaging, and vehicular radar (figure 2.1 below). The ultra wide bandwidth and the wide variety of material penetration capabilities allow UWB to be used for radar imaging systems, including ground penetration radars, wall radar imaging, through wall radar imaging, surveillance systems, and medical imaging. Images within or behind obstructed objects can be obtained with a high resolution using UWB.

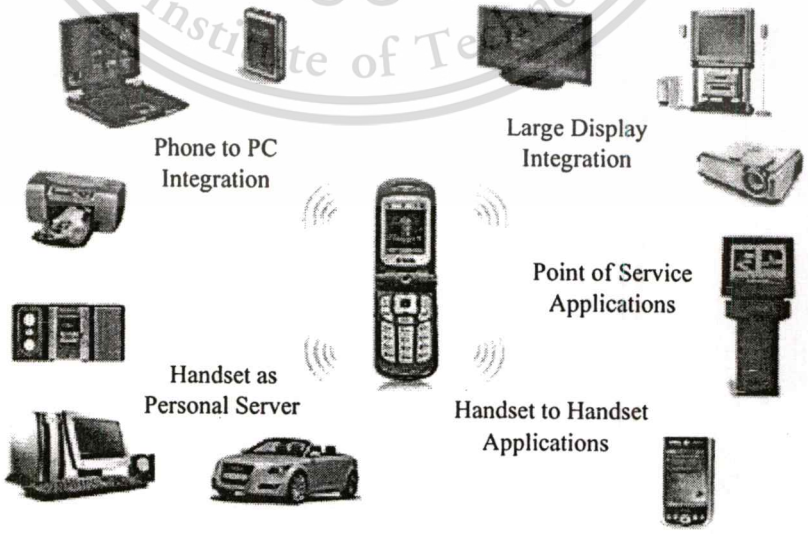

Figure 2.1 UWB communication system devices

Similarly, the excellent time resolution and accurate ranging capability of UWB can be used for vehicular radar systems for collision avoidance, guided parking, etc. Positioning location and relative positioning capabilities of UWB systems are other great applications that have recently received significant attention.

2.2 History

Genesis of UWB technology was originated from work in time-domain electromagnetic that began in 1962 [8]. The concept was to characterize linear time-invariant (LTI) systems by their output response to an impulse excitation, instead of the more conventional means of swept frequency response (i.e., amplitude and phase measurements versus frequency). This output response is known as impulse response $h(t)$. Output response $y(t)$ of a LTI system to any input response $x(t)$ is determined by the convolution integral [9]:

$$y(t) = \int_{-\infty}^{\infty} h(\tau)\, x(t-\tau) d\tau \qquad (2.1)$$

However, it was not possible to measure the impulse response directly until the impulse excitation and measurement techniques were developed. Once these techniques were in place it was obvious that these could be used for short pulse radar and communication systems. In 1978 Ross and Bennett [10] applied these techniques for radar and communication applications.

The development of the sampling oscilloscope occurred in the early 1960s and the corresponding techniques for generating sub-nanosecond baseband pulses sped up the development of UWB. Impulse measurement techniques were used to characterize the transient behavior of certain microwave networks. From measurement techniques the main focus moved to developing radar and communications devices. In particular, radar was given a lot of attention because of the accurate results that could be obtained. The low-frequency components were useful in penetrating objects, and ground-penetrating radar.

UWB communications was awarded the first US patent in 1973 leading to further development of UWB field. The field of UWB had moved in a new direction. Other applications, such as automobile collision avoidance, positioning systems, liquid-level sensing and altimetry were also developed. However, most of the applications and development still occurred in the military or tasks funded by the US Government under

classified programs. For the military, accurate radar and low probability of intercept communications were the driving forces behind UWB research and development. It is interesting to note that in these early days, UWB was referred to as baseband, carrier-free and impulse technology. The US Department of Defense is believed to be the first to have started to use the term UWB.

The late 1990s saw the move to commercialize UWB communication devices and systems. Companies such as Time Domain and in particular startups like XtremeSpectrum were formed around the idea of consumer communication using UWB.

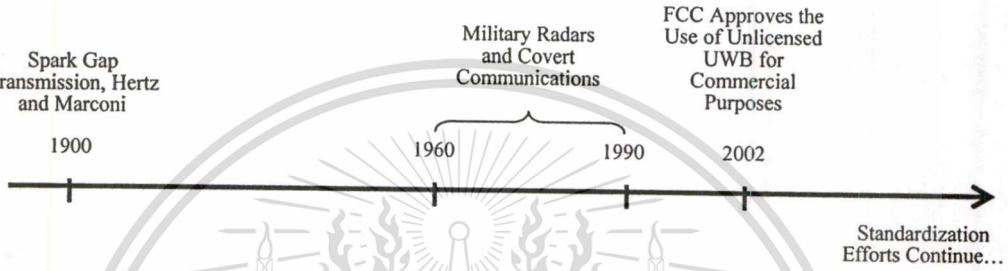

Figure 2.2 History of UWB developments

2.3 UWB Regulation

2.3.1 UWB Regulation in the USA

Before the FCC's first report and order (Federal Communications Commission, 2002a,b), there was significant effort by industrial parties to convince the FCC to release UWB technology under the FCC Part 15 regulation limitations, and to allow licensed-free use of UWB products. The FCC Part 15 Rules permit the operation of classes of radio frequency devices without the need for a licensed or the need for frequency coordination "47 C.F.R. 15.1" (Title 47 of the Code of Federal Regulations). The FCC Part 15 Rules attempt to ensure a low probability of unlicensed devices causing harmful interference to other users of the radio spectrum (47 C.F.R. 15.5). Within the FCC Part 15 Rules, intentional radiators are permitted to operate within a set of limits (47 C.F.R. 15.209) that allow signal emissions in certain frequency bands. They are not permitted to operate in sensitive or safety-related frequency bands, which are designated as restricted bands (47 C.F.R.15.205). UWB devices are intentional radiators under FCC Part 15 Rules.

In 1998, the FCC issued a notice of inquiry (NOI) (Federal Communications Commission, 1998). Despite the very low transmission power levels anticipated, proponents

of existing systems raised many claims against the use of UWB for civilian communications. Most of the claims related to the anticipated increase of interference level in the restricted frequency bands (e.g. TV broadcast bands and frequency bands reserved for radio astronomy and GPS). The Federal aviation administration (FAA) expressed concerned about the interference to aeronautical safety systems. and direction finding of UWB transmitters.

The organizations that support UWB technology see large scale possibilities for new innovative products utilizing the technology. The FCC NOI and comments can be found on the Internet (Ultra-Wideband Working group, 1998, 1999, 2004).

When UWB technology was proposed for civilian applications, there were no definitions for the signal. The defense advanced research projects agency (DARPA) provided the first definition for UWB signal based on the fractional bandwidth (B_f) of the signal. The first definition provided that a signal can be classified as an UWB signal if B_f is greater than 0.25. The fractional bandwidth can be determined as (Taylor, 1995).

$$B_f = 2\frac{(f_H - f_L)}{(f_H + f_L)} \tag{2.2}$$

Where

f_L is the lower and f_H is the higher -3 dB point in a spectrum, respectively.

CURRENT UWB DEFINITION

In February 2002, the FCC issued the FCC UWB rulings that providing the first radiation limitations for UWB, and also permitted the technology commercialization. The final report of the FCC First Report and Order (FCC, 2002a,b) was publicly made available in April 2002. The document introduced four different categories for allowing UWB applications, and setting the radiation masks for them.

The prevailing definition has decreased the limited of B_f at the minimum of 0.20, defined using the equation above. Also, according to the FCC UWB rulings the signal is recognized as UWB if the signal bandwidth is 500MHz or more. In the formula above, f_H and f_L are the higher and lower -10 dB bandwidths, respectively. The radiation limits by FCC for indoor and outdoor data communication applications are presented in Table 1.1.

Spectral masks are in place to protect the existing users operating within the spectrum. UWB signals may be transmitted at power spectral density (PSD) levels up to -41.3 dBm per MHz, which complies with general guideline Part 15 Emission Limits to Control Radio

Interference. Figure 2.3 and figure 2.4 show spectral masks for indoor and outdoor operations respectively. Outdoor operation has a higher degree of attenuation than the indoor operation at the out-of-band region to protect the GPS receivers, centered at 1.6 GHz.

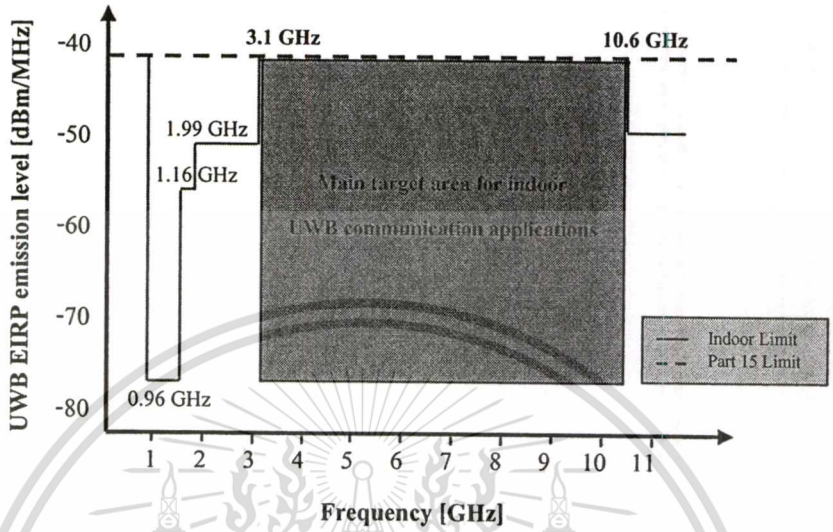

Figure 2.3 Spectral mask for indoor application

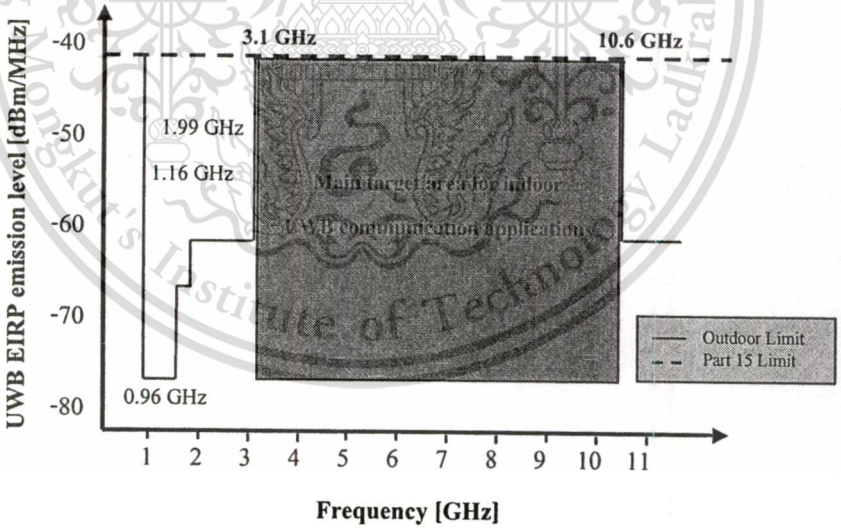

Figure 2.4 Spectral mask for outdoor application

Table 1.1 FCC radiation limits for indoor and outdoor communication applications

Frequency in MHz	Indoor	Outdoor
	EIRP in dBm	EIRP in dBm
960-1610	-75.3	-75.3
1610-1990	-53.3	-63.3
1990-3100	-51.3	-61.3
3100-10600	**-41.3**	**-41.3**
Above 10600	-51.3	-61.3

2.3.2 UWB Regulation in Europe

The European Commission (EC) has finally issued details of the licensing regulations for UWB networking in Europe, albeit with some restrictions that are due to be lifted early in 2008. The WiMedia Alliance is an industry association that promotes and enables the adoption, regulating, standardization and multi-vendor interoperability of UWB worldwide. Its 250-plus members include consumer electronics, mobile devices, personal computers, and software manufacturers. The alliance is supported by several complementary organizations including the 1394 Trade Association, Bluetooth SIG and the USB-IF.

Table 1.2 Restriction applied to EC UWB spectrum allocation

The isotropic radiated power (EIRP) of UWB device are strictly regulated

Frequency range (MHz)	Maximum mean EIRP density (dBm/MHz)	Maximum peak EIRP density (dBm/50 MHz)
Below 1600	-90.0	-50.0
1600-3400	-85.0	-45.0
3400-3800	-85.0	-45.0
3800-4200	-70.0	-30.0
4200-4800	-41.3 (until December 31, 2010) -70.0 (beyond December 31, 2010)	0.0 (until December 31, 2010) -30.0 (beyond December 31, 2010)
4800-6000	-70.0	-30.0
6000-8500	-41.3	0.0
8500-10600	-65.0	-25.0
Above 10600	-85.0	-45.0

Source: European Commission, Radio Spectrum Policy Unit

What is known is that an amendment due in the first quarter of 2008 is designed to relieve the restrictions and take into account a number of new studies covering UWB compatibility in automotive and railway environments, the compatibility with aeronautical radar in the 2.7 to 3.4-GHz band, the 8.5 to 9.0-GHz radar band and the work done on "detect-and-avoid" and other interference mitigation techniques.

Other niche or sector-specific applications to use UWB have already been considered by the EC. Decisions have already been adopted for 24 GHz and 79 GHz short-range radar for cars while frequencies for ground/wall probing radar and building materials analysis should be implemented this year. Other applications such as object discrimination, location tracking and level probing are under consideration.

At an 'open house' during the WiMedia Alliance member meeting in Brussels a number of companies demonstrated prototypes. A Mercedes-Benz R500 took pride of place and was enabled with the ability to stream high-definition video live from a consumer electronic device using UWB to a rear seat entertainment system. The vehicle's UWB system incorporated the Intel Wireless UWB Link 1480 MAC silicon and an Alereon AL4000 WiMedia RF Transceiver to create the wireless USB connection.

2.4 Characteristics of UWB

UWB technology has the following significant characteristics:

- **High Data Rates**

UWB technology can do things that the existing wireless networking systems cannot do. Most importantly, UWB can handle more bandwidth-intensive applications such as a streaming video, than either 802.11 or Bluetooth because it can send data at much faster rates. UWB technology has a data rate of roughly 100 megabits per second, with speeds up to 500 megabits per second; This is compared with a maximum speeds of 11 megabits per second for 802.11b (often referred to as Wi-Fi) which is the technology currently used in most wireless LANs; and 54 megabits per second for 802.11a, which is Wi-Fi at 5 MHz. Bluetooth has a data rate of about 1 megabit per second.

- **Low Power Consumption**

When transmitting data, UWB devices consume less than several tens of microwatts. That is a huge saving and the reason is that UWB transmits short impulses constantly instead of transmitting modulated waves continuously like most narrowband systems do. UWB

chipsets do not require RF to Intermediate Frequency (IF) conversion, local oscillators, mixers, and other filters. The low power consumption makes UWB ideal for use in battery-powered devices like cameras and cell phones.

➢ **Interference Immunity**

Due to low power and high frequency transmission, UWB's aggregate interference is "undetected" by narrowband receivers. Its power spectral density is at or below narrowband thermal noise floor. The low power level thus causes no irritating interferences to existing home wireless systems. According to its First Report and Order, the FCC requires that indoor UWB devices transmit only when operating with a receiver. A device connected to AC power is not constrained to reduce or conserve power by ceasing transmission, so this restriction will eliminate unnecessary emissions. Additional tests conducted by the FCC have also demonstrated conclusively that UWB devices may be permitted to operate under a proper set of standards without causing harmful interference to other radio operations.

➢ **High Security**

UWB's white-noise-like transmissions enhance security since receivers without the specific code cannot decode it. Different coding schemes, algorithms, and modulation techniques can be assigned to different users for data transmissions. Security can also be realized at the media access control (MAC) level by allowing two devices to communicate with each other. Although currently no formal security standard is available for UWB, the study group of IEEE 802.15.3 has defined AES-128 symmetric security for payload protection and integrity.

➢ **Reasonable Range**

IEEE 802.15.3a Study Group defined 10 meters as a minimum range at a speed of 100Mbps. However, UWB can go further. The Philips company has used its digital light processor (DLP) technology in UWB device so it can operate beyond 45 feet at 50 Mbps for four DVD screens.

➢ **Low Complexity, Low Cost**

The most attractive features of UWB are low system complexity and cost. Traditional carrier based technologies modulate and demodulate complex analog carrier waveforms. In contrast, UWB systems are made of "all-digital" with minimal RF or microwave electronics. The inherent RF simplicity in UWB designs make the systems highly frequency adaptive and enable them to be positioned anywhere within the RF spectrum. Also home UWB

wireless devices do not need transmitting power amplifier. This is a great advantage over narrowband architectures that require amplifiers with significant power back-off to support high-order modulation waveforms for high data rates. The cost of placing UWB technology inside a consumer electronics device is $20, compared with $40 for 802.11b and $65 for 802.11a.

2.5 UWB Standardization by IEEE

The IEEE established the 802.15.3a study group to define a new physical layer concept for short range and high data rate applications. This ALTernative PHYsical (ALT PHY) is intended to serve the needs of groups wishing to deploy high data rate applications. With a minimum data rate of 110 Mbps at 10 m, this study group intends to develop a standard to address such applications as video or multimedia links, or a cable replacement. While not specifically intended to be a UWB standards group, the technical requirements very much lend themselves to the use of UWB technology. The study group has been the focus of significant attention recently as the debate over competing UWB physical layer technologies has raged. The work of the Study Group also includes analyzing the radio channel model proposal to be used in the UWB system evaluation.

The purpose of the study group is to provide a higher speed PHY for the existing approved 802.15.3 standard for multimedia applications which involve. The main desired characteristics of the alternative PHY are:

- Co-existence with all existing IEEE 802 physical layer standards
- Target data rate in excess of 100 Mbits/s for consumer a applications
- Robust multipath performance
- Location awareness
- Use of additional unlicensed spectrum for high rate WPANs.

The IEEE established the 802.15.4a task group to define a physical layer concept for low data rate applications utilizing a UWB air interface. The task group addresses new applications which require only moderate data throughput, but requires a long battery life. Example applications are low-rate wireless personal area networks, sensors and small networks, as described in [11] and [12]. In most cases, centimeter accuracy ranging is the key feature brought by UWB to address these new applications. A baseline proposal was accepted by unanimous vote on March 2005 and the standard is now in a drafting stage.

2.6 IEEE 802.15.3a

The indoor wireless standards effort can be broadly categorized into three standards groups. The first of which is IEEE 802.11, responsible for WLAN standards. The IEEE 802.16 group is responsible for wireless metropolitan area networks (WMAN) standards. This body is concerned with fixed broadband wireless access systems, also known as "last mile" access networks. IEEE 802.15, of which we are concerned with, is responsible for WPAN standards.

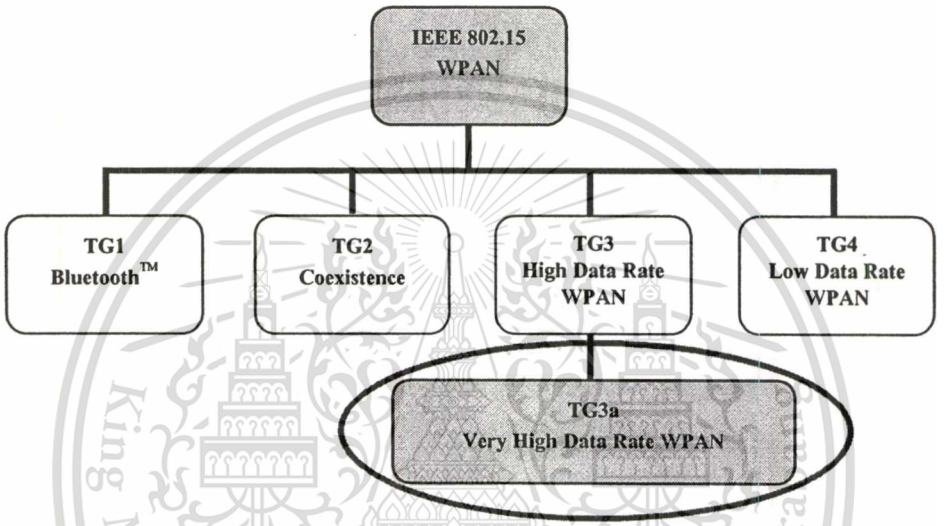

Figure 2.5 IEEE 802.15, standards group responsible for WPAN standards.

The efforts of IEEE 802.15 are divided up into four main areas (as shown in figure 2.5):

(1) Task Group 1 (TG1) is creating a WPAN standard based on Bluetooth™ to operate in the 2.4 GHz ISM band;

(2) TG2 is concerned with the coexistence of unlicensed spectrum devices;

(3) TG3 is responsible for high data rate (in excess of 20 Mbps) WPAN standards; and

(4) TG4 is creating a low data rate, low power WPAN standard.

An additional group, TG3a, was created to investigate physical layer alternatives for high data rate WPAN systems (i.e. alternatives for the IEEE 802.15.3 physical layer).

TG3a established technical requirements and selection criteria for a WPAN physical layer in December 2002. TG3a has set out to develop a flexible standard which will enable high data rate WPAN (110 Mbps at 10m, 200 Mbps at 4m, and 480 Mbps at 2m) over a cost

effective architecture. This new standard will enable a broad range of applications including the wireless transmission of images and video.

The IEEE 802.15.3a task group has evaluated a number of popular indoor channel models to determine which model best fits the important characteristics from realistic channel measurements using UWB waveforms. The goal of the channel model is to capture the multipath characteristics of typical environments where IEEE 802.15.3a devices are expected to operate. The model should be relatively simple to use in order to allow PHY proposers to use the model and, in a timely manner, evaluate the performance of their PHY in typical operational environments.

Furthermore, it should be reflective of actual channel measurements. Since it may be difficult for a single model to reflect all of the possible channel environments and characteristics, the group chose to try matching the following primary characteristics of the multipath channel:

- RMS delay spread
- Power decay profile
- Number of multipath components (defined as the number of multipath arrivals that are within 10 dB of the peak multipath arrival)

Note that the actual channels resulting from the model may have several paths that are much weaker than 10 dB from the peak, while the above characteristic was simply used to compare to measurement results.

However, on January 19, 2006 IEEE 802.15.3a task group (TG3a) members voted to withdraw the December 2002 project authorization request (PAR) that initiated the development of high data rate UWB standards. The process was in total deadlock. There were two technology proposals on the table backed by two different industry alliances. One of them was backed by the majority of the industry; the other was only supported by a small minority but had sufficient votes to block forward progress. The task group finally agreed to duke it out in the market place. The Working Group concurred. The technology at the time also faced significant regulatory hurdles, which have been resolved in 2008. This was not a factor in this decision but from a standards perspective it probably was too early to write a UWB standard. The main proposal was adopted by the WiMedia Alliance, and eventually by the USB-IF and Bluetooth SIG.

2.7 UWB applications

UWB technology is popular for its multipath immunity, high data throughput, better wall penetration, low power consumption, and low probability of interception and detection. Because of all these features UWB technology has become increasingly accepted for numerous applications in civilian and military field. Some of the applications that can be integrated with UWB are listed below

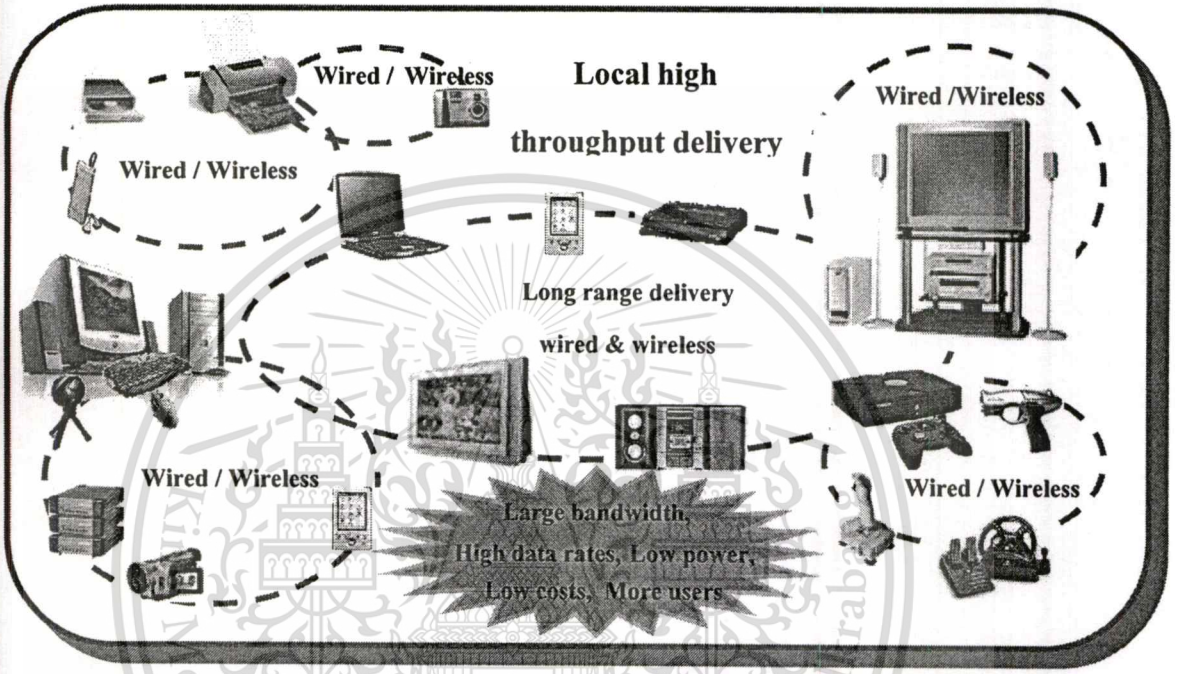

Figure 2.6 UWB application in the digital home networks.

➢ **Precision Location**

Modern day global positioning satellite systems (GPS) suffer from numerous sources of errors. But these can be improved and location can be precisely estimated within 1-2 meters using differential GPS system for outdoor application. But using UWB in addition to these technologies is a viable solution for extending the location finding capabilities to the indoor. And even in the vicinity of buildings and large topographic features GPS receivers have major problems due to multipaths. But a UWB augmented GPS system can work really well in these kinds of situations.

➢ **Through-wall Sensing System**

To detect the motion of a person or objects that are placed on the other side of a wall, high resolution is required. Precision time gating is required to track multiple targets at

longer ranges as in. And an UWB system is a reliable solution in providing this kind of resolution and through-wall penetration capabilities.

➢ **UWB Radar**

UWB pulses are short in time duration and thus millions of pulses could be sent in a second so that a near perfect image of the target is obtained. Advantage in using UWB in this application is that due to its inherent time resolution property it reduces post detection signal processing as is required in narrowband radars to improve the detected image.

UWB underground penetrating radars can be used to find live things in a pile of rubble. And these kinds of radars could also be used to check if any under-ground cables or pipes are present before digging. Thus these kinds of radars can be used in numerous applications like target specific application, civil engineering applications, geophysical application, and many more.

➢ **Sensor Networks (IEEE 802.15.4a)**

Sensor networks are currently used for surveillance, automobiles, and medical situations and for numerous other applications. If a wired network is used it is very cumbersome, expensive, and uncomfortable in situations where wires are visible and in the way of work. UWB is a viable solution as a wireless communication link in these kinds of application so that although the work is being done, but the network is still unnoticeable and invisible to others. And sometimes UWB signal itself can be used as a sensor.

UWB technology applications are not limited. As there is more improvement in source, receiver and antenna technologies UWB would find more and more applications so that there exists a wires free world

2.8 Conclusion

This chapter discussed communication fundamentals using UWB pulses. The regulatory issues and some applications of UWB technology in communication area were also examined. The fact that UWB technology has been around so many years and has been used for a variety of applications is strong evidence of the viability and flexibility of Technology. The simple transmit and receive structures, which can make this a potentially powerful technology for low-complexity, low-cost communications. How is will be discussed in later chapters, the physical properties of the signal support Location and tracking capabilities of UWB much lighter than existing close volume technologies.

The severe restrictions on the transmission power (less than 0.5mW maximum power) have significantly limited the range of applications of UWB in the short-distance high data rate low data rate or longer-distance applications. The great potential of UWB is flexible transition between these two extremes, without the need for substantial changes to the transceiver.

UWB is still the subject of considerable debate, there is no doubt that the Technology is able to achieve very high data rates and is an alternative to existing technology for WPAN, short-range, high data rate communications, multimedia applications, and cable replacement. A large part of the current debate centers the PHY layer(s) to adopt the development of a standard, and issues of coexistence and Interference.

Chapter 3

Theory and analysis of UWB channel propagation in an indoor environment

3.1 Introduction

This chapter explain about theory and principle of UWB channel propagation in an indoor environment for wireless communication system by emphasize in reflection and scatter of UWB system, Friis' transmission formula and other parameters that affect to the quality of the UWB impulse radio propagation channel such as reduction of power and distortion which all substance has necessity for study and predict UWB impulse radio propagation channel.

3.2 Multipath channel modeling in UWB system

Multipath is the name given to the phenomenon at the receiver whereby after transmission an electromagnetic signal travels by various paths to the receiver. See figure 3.1 for an example of multipath propagation within a room. This effect is caused by reflection, absorption, diffraction, and scattering of the electromagnetic energy by objects in-between the transmitter and the receiver. If there were no objects to absorb or reflect the energy, this effect would not take place and the energy would propagate outward from the transmitter, dependent only on the transmit antenna characteristics. However, in the real world objects between the transmitter and the receiver cause the physical effects of reflection, absorption, diffraction, and scattering, and this gives rise to multiple paths. Due to the different lengths of the paths, pulses will arrive at the receiver at different times, with the delay proportional to the path length.

UWB systems are often characterized as multipath immune or multipath resistant. Examining the pulses described previously, we can see that if pulses arrive within one pulse width they will interfere, while if they are separated by at least one pulse width they will not interfere. If pulses do not overlap, then they can be filtered out in the time domain or, in

other words, ignored. Assuming one symbol per pulse, they will not produce interference with the same symbol. Alternatively the energy can be summed together by a rake receiver.

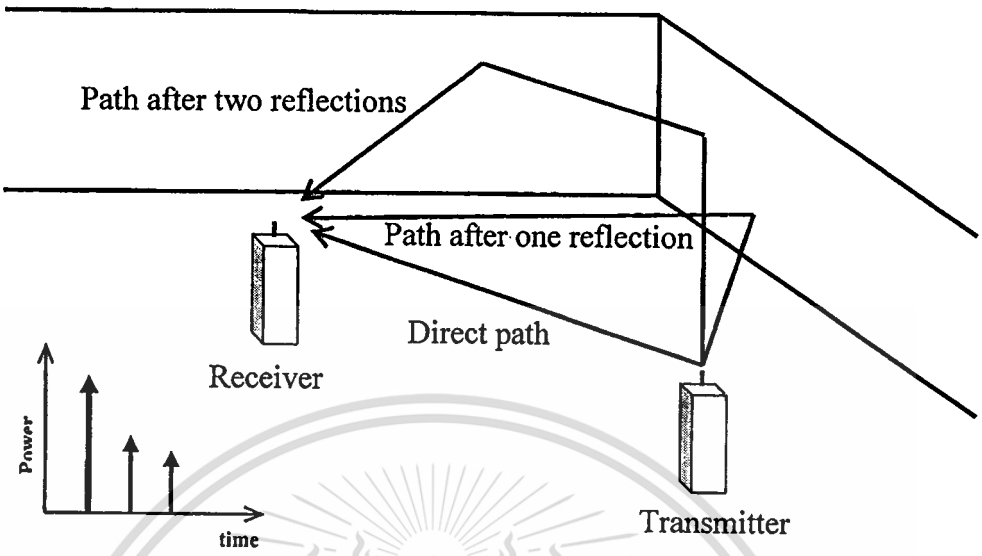

Figure 3.1 A typical indoor scenario in which the transmitted pulse is reflected off objects within the room, thus creating multiple copies of the pulse at the receiver with different delays.

3.3 Path loss model

Path loss by definition is the attenuation undergone by an electromagnetic wave in transit between a transmitter and a receiver in a communication system [13]. UWB propagation has peculiar characteristics that should be reflected in path loss models. Models coherent with the characteristics of the channel are, therefore, very important to simulate propagation in UWB environments.

3.3.1 Path loss model background

It is well known that path loss increases with distance for free space environments, nonetheless, different attenuations can be experienced in the communication due to effects such as reflection, refraction, diffraction, scattering, clutter and absorption from buildings, structures or any other obstructions in the path. Reflection and refraction can occur when a propagating electromagnetic wave faces an object that is much larger than the signal's wavelength. Diffraction occurs when the surface encountered by the electromagnetic wave has irregularities such as sharp edges. Scattering occurs when the medium through which the electromagnetic wave propagates contains a large number of objects smaller than the

wavelength. Wave clutter is due to disorganized wave propagation due to rough surfaces or interfaces. Absorption is due to conversion of transmitted energy into another form, usually thermal in the transmission of electrical, electromagnetic or acoustic signals. Wireless communications and specifically UWB communications are characterized by this propagation effects.

The path loss (*PL*) is defined as

$$PL_{(dB)} = P_{t[dB]} - P_{r[dB]} \tag{3.1}$$

where P_t is the power fed to the transmitting antenna and P_r is the power available at the receiving antenna.

3.3.2 Free space path loss

In communication systems, free space path loss is the loss in signal strength of an electromagnetic wave that would result from a line-of-sight (LOS) path through free space, with no obstacles nearby to cause reflection or diffraction. It does not include factors such as the gain of the antennas used at the transmitter and receiver, nor any loss associated with hardware imperfections. A discussion of these losses may be found in the article on link budget.

There have been several proposed path loss models in the literature. Assuming perfect isotropic radiating antennas at the transmitter and receiver the received power as a function of frequency can be expressed as following:

$$\frac{P_r}{P_t} = G_t G_r G_f \tag{3.2}$$

$$P_r = \frac{P_t G_t G_r c^2}{(4\pi d)^2 f^2} \tag{3.3}$$

where:

P_r - Receive power

P_t - Average transmit power spectral density

G_t - Transmitter gain

G_r - Receiver gain

G_f - Free space propagation gain (less than unity in practice)

$$G_f = \left(\frac{\lambda}{4\pi d}\right)^2 \tag{3.4}$$

where

$\lambda = \frac{c}{f}$ - is the wavelength (meters)

f - is the operating frequency (hertz)

d - is the distance between transmitter and receiver antennas (meters)

c - is the speed of light [$3 \times 10^8 m/s$]

A convenient way to express free space path loss is in terms of dB:

$$L_{dB} = 10\log(P_t) - 10\log(P_r) \tag{3.5}$$

$$= 32.44 + 20\log(f) + 20\log(d) - 10\log(G_t) - 10\log(G_r)$$

3.4 Extension of Friis' Transmission Formula for UWB transmission System

In narrowband systems, the link budget of the free space propagation loss is usually estimated by using Friis' transmission formula [14]. However, it is not directly applicable to the UWB impulse radio transmission system, as the formula is expressed as a function of the frequency. Moreover, the waveform may be distorted due to the frequency characteristics of the antenna. Ref. [15] treats the special cases of the constant gain and the constant aperture, but no general discussion had been made although it suggested the use of the time-domain antenna effective length.

The Friis' transmission formula has been widely used, and can be applied to the calculation of these LOS channels.

$$G_{Friis}(f) = \frac{P_r(f)}{P_t(f)} = G_f(f)G_r(f)G_t(f) \tag{3.6}$$

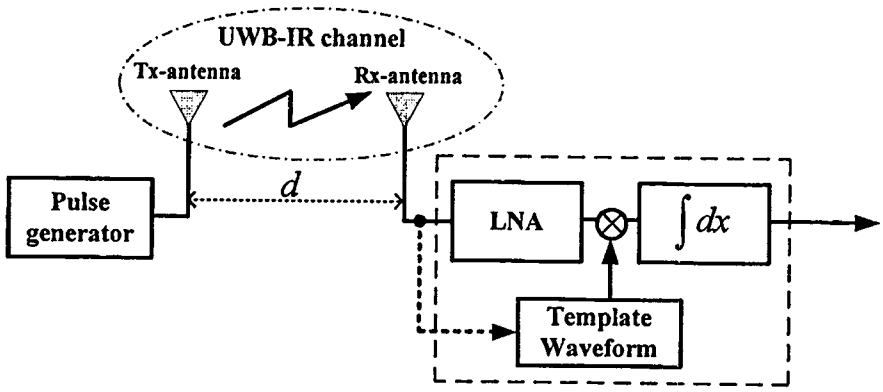

Figure 3.2 Block diagram of transmission system for UWB signals [16].

It is noted, however, that Eq. (3.6) is satisfied only at some certain frequency, and is not directly applicable to UWB systems. The Friis' transmission formula shall be extended to take into account the transmission signal waveform and its distortion as well [17], [18].

Input signal $v_{\mathrm{i}}(t)$ at the transmitter port is expressed as the convolution of an impulse input and the pulse shaping filter $h_{\mathrm{i}}(t)$ as

$$v_{\mathrm{i}}(t) = E_{\mathrm{i}}\delta(t) * h_{\mathrm{i}}(t) \tag{3.7}$$

where

$$\int_{-\infty}^{\infty} h_{\mathrm{i}}^2(t)dt = \int_{-\infty}^{\infty} |H_{\mathrm{i}}(f)|^2 df = 1 \tag{3.8}$$

Friis' formula is extended taking into account the transmission waveform, the channel transfer function H_{c} is express as

$$H_{\mathrm{c}}(f) = \frac{V_{\mathrm{r}}(f)}{E_{\mathrm{i}}} = H_{\mathrm{f}} H_{\mathrm{i}} \mathbf{H}_{\mathrm{r}} \cdot \mathbf{H}_{\mathrm{t}} \tag{3.9}$$

where

$$\begin{aligned} \mathbf{H}_{\mathrm{a}} &= \mathbf{H}_{\mathrm{a}}(\theta_{\mathrm{a}}, \varphi_{\mathrm{a}}, f) \\ &= \hat{\theta}_{\mathrm{a}} H_{\mathrm{a}\theta}(\theta_{\mathrm{a}}, \varphi_{\mathrm{a}}, f) + \hat{\varphi}_{\mathrm{a}} H_{\mathrm{a}\varphi}(\theta_{\mathrm{a}}, \varphi_{\mathrm{a}}, f) \\ \mathrm{a} &= \mathrm{r\ or\ t} \end{aligned} \tag{3.10}$$

where $\hat{\theta}_{\mathrm{a}}$, $\hat{\varphi}_{\mathrm{a}}$ - polar angels and azimuth angles of Tx or Rx antenna

is a complex transfer function vector of the antenna relative to the isotropic antenna,

$$H_f = \frac{\lambda}{4\pi d} \exp(-jkd) \tag{3.11}$$

is the free space transfer function

Where $$k = \frac{2\pi}{\lambda} \tag{3.12}$$

is the propagation constant.

3.5 Correlation receiver

Let us consider a correlation receiver shown in figure 3.2. The output SNR is dependent on the choice of the template waveform. The correlate output $v_0(\tau)$ is therefore expressed as

$$v_0(\tau) = \int_{-\infty}^{\infty} v_r(t) h_w(t-\tau) dt \tag{3.13}$$

Where $v_0(\tau)$ is the receiver input waveform which is inverse Fourier transform, and $h_w(t)$ is the template waveform. τ corresponds to the timing of the template waveform, and the optimum timing τ_0 is chosen as

$$\tau_0 = \arg\max v_0(\tau) \tag{3.14}$$

Hereafter $h_w(t)$ is normalized as

$$\int_{-\infty}^{\infty} |h_w(t)|^2 dt = 2B \tag{3.15}$$

Where B is the signal bandwidth, so that the output noise power is constant as $N_0 B$, where $\frac{N_0}{2}$ is power spectral density of AWGN.

Under the constraint of Eq. (3.15), $h_{wm}(t)$ maximizes $v_0(\tau_0)$ when $h_{wm}(t)$ is a time-reversed and scaled version of $v_r(t)$, i.e.

$$h_{\mathrm{wm}}(t) = \frac{\sqrt{2B}v_{\mathrm{r}}(\tau_0 - t)}{\sqrt{\int_{-\infty}^{\infty}|v_{\mathrm{r}}(t)|^2 dt}} \tag{3.16}$$

where τ_0 is usually chosen so that $h_{\mathrm{wm}}(\mathrm{t}) = 0$ for $\mathrm{t} < 0$ to satisfy the causality. $h_{\mathrm{wm}}(\mathrm{t})$ is called the optimum template waveform hereafter. It is noted that the link budget evaluation is identical to that in Ref. [19] when $h_{\mathrm{wm}}(\mathrm{t})$ is used as the receiver template.

3.6 Isotropic correlation receiver

It is obvious from Eq. (3.16) that the optimum template waveform is not the simple time-reversed version of the transmitter waveform, but the channel characteristics including the antennas and the free space propagation. Therefore, it is not always feasible to adapt the template waveform to the angular-dependent antenna characteristics, since the waveform shall be generated at the clock rate of tens of gigahertz. Therefore, we consider a canonical template waveform $h_{\mathrm{wc}}(t)$. In this paper we have chosen $h_{\mathrm{wc}}(t)$ that is optimum for the isotropic and the constant gain antennas, i.e.

$$h_{\mathrm{wc}}(t) = \frac{\sqrt{2B}v_{\mathrm{r-iso}}(\tau_0 - t)}{\sqrt{\int_{-\infty}^{\infty}|v_{\mathrm{r-iso}}(t)|^2 dt}} \tag{3.17}$$

Where

$$v_{\mathrm{r-iso}}(t) = \int_{-\infty}^{\infty} H_{\mathrm{f}}(f)V_{\mathrm{t}}(f)\exp(j2\pi f t)df \tag{3.18}$$

Is the receiver input voltage for isotropic antenna including. The difference between the optimum and the isotropic templates indicates quantitatively the distortion of the waveform.

3.7 Power delay profile

The power delay profile (PDP) gives the intensity of a signal received through a multipath channel as a function of time delay. The time delay is the difference in travel time between multipath arrivals. The abscissa is in units of time and the ordinate is usually in decibels. It is easily measured empirically and can be used to extract certain channel's parameters such as the delay spread. Otherwise, we can use for consider the effect to time dispersion that composed of mean excess delay and RMS delay spread.

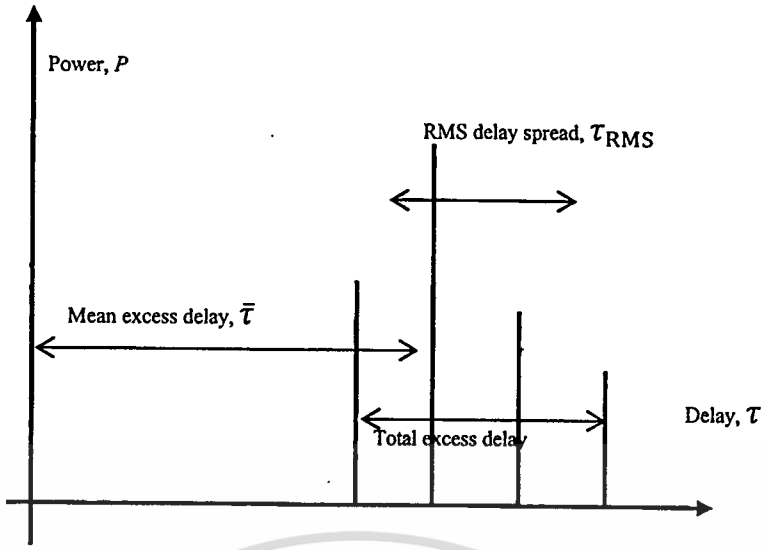

Figure 3.3 Example of power delay profile.

$$\bar{\tau} = \frac{\sum_{i=1}^{n} a_i^2 \tau_i}{\sum_{i=1}^{n} a_i^2} = \frac{\sum_{i=1}^{n} P(\tau_i)\tau_i}{\sum_{i=1}^{n} P(\tau_i)} \tag{3.19}$$

$$\tau_{RMS} = \sqrt{\overline{\tau^2} - (\bar{\tau})^2} \tag{3.20}$$

$$\overline{\tau^2} = \frac{\sum_{i=1}^{n} a_i^2 \tau_i^2}{\sum_{i=1}^{n} a_i^2} = \frac{\sum_{i=1}^{n} P(\tau_i)\tau_i^2}{\sum_{i=1}^{n} P(\tau_i)} \tag{3.21}$$

3.8 Path loss

In the wireless communication system the important parameter use for analyze the channel propagation that is path loss. Due to propagation channel by consider the propagation of UWB signals in indoor environments is an important issue with significant impacts on the future direction and scope of the UWB technology and its applications.

$$PL[dB] = 20\log\left(\frac{v_t(t)}{v_r(t)}\right) \tag{3.22}$$

where

v_t - is transmitted signal level

v_r - is received signal level

For UWB path loss we consider at transmitted signal maximum power and received signal maximum power as function of distance d

$$PL_{\mathrm{UWB}}(d)[dB] = 20\log\left(\frac{max|v_{\mathrm{t}}(t)|}{max|v_{\mathrm{r}}(t)|}\right) \quad (3.23)$$

From (3.23) we define the transmitted signal equal 1 therefore we can rewrite equation as following

$$PL_{\mathrm{UWB}}(d)[dB] = -20\log(max|v_{\mathrm{r}}(t)|) \quad (3.24)$$

3.9 Correlation coefficient

The most commonly used measure for linear relationship between two variables is the Pearson correlation coefficient. The two variables must be measured by interval or ratio scale. The values of the coefficient can range from -1 to +1. If there is no linear relationship between two variables, the value of coefficient is 0. If there is a perfect positive relationship, the value is +1. If there is a perfect negative relationship, the value is -1. The correlation coefficient can be expressed as

$$\rho(d) = \frac{\max|r_{\mathrm{ab}}(\tau)|}{\max|\sqrt{r_{\mathrm{a}}(\tau)r_{\mathrm{b}}(\tau)}|} \quad (3.25)$$

$$r_{\mathrm{ab}} = \int_{-\infty}^{\infty} v_{\mathrm{t}}(\tau)v_{\mathrm{r}}(t+\tau)dt \quad (3.26)$$

$$r_{\mathrm{a}} = \int_{-\infty}^{\infty} v_{\mathrm{t}}(\tau)v_{\mathrm{t}}(t+\tau)dt \quad (3.27)$$

$$r_{\mathrm{b}} = \int_{-\infty}^{\infty} v_{\mathrm{r}}(\tau)v_{\mathrm{r}}(t+\tau)dt \quad (3.28)$$

where

$r_{\mathrm{ab}}(\tau)$ - is the cross correlation function between signal a and b

$r_{\mathrm{a}}(\tau)$ - is the auto-correlation of signal a

$r_{\mathrm{b}}(\tau)$ - is the auto-correlation of signal b

3.10 Bit error rate (BER)

The BER can consider from correlation coefficient between received signals with template waveform. The correlation coefficient of correlation coefficient of template waveform C_c can show as

$$C_c = \frac{\max|r_{v_r h_c}(\tau)|}{\sqrt{\max|r_{v_r}(\tau)| \cdot \max|r_{h_c}(\tau)|}} \quad (3.29)$$

The BER can be express as equation 3.30

$$BER = Q\left(\sqrt{2C_c(E_b/N_o)}\right) \quad (3.30)$$

where

E_b/N_o - is the energy per bit to noise power spectral density ratio

3.11 Conclusion

This chapter discusses theory and some parameters used for UWB channel propagation in an indoor environment for wireless communication systems such as Friis' transmission formula and path loss model. Other parameters, for example, power delay profile, path loss, correlation coefficient and bit error rate, were used to analyse some effects from power loss, distortion of signal and so on. These effects are caused by reflection, absorption, diffraction, and scattering of the electromagnetic energy by objects which are in between the transmitter and the receiver.

Chapter 4

Experimental setup and channel measurement model For UWB impulse radio propagation

4.1 Introduction

This chapter describes the method used in the experiment and real measurement of UWB-IR in the large lecture room - E12-1101 within the Faculty of Engineering, King Mongkut's Institute of Technology Ladkrabang, Thailand. The research studied characteristics of UWB-IR channel modeling and analysed the effectiveness of the spread of UWB-IR channel, as well as testing the quality of the transmission channel in an indoor environment. This measurement is based on the parametric channel modeling by using biconical antenna at the transmitter and receiver. This technique is applied to 121 points at the receiver side. Each point is 40 cm apart. The nearest between transmitter and receiver is 2.90 m and farthest between the transmitter and receiver is 6.66 m.

This thesis also considered the effect of antenna polarization as we setup four various polarizations in one model and parameters used for analyze are same. The polarization of the Tx and Rx antennas design as follows:

Polarization 1: Tx Vertical – Rx Vertical

Polarization 2: Tx Vertical – Rx Horizontal

Polarization 3: Tx Horizontal – Rx Horizontal

Polarization 4: Tx Horizontal – Rx Vertical

For the concept of model, we suppose the transmitter is an access point and the receiver is a general electric appliance such as a television, a camcorder, a notebook, a PDA or other appliances that can receive signal from the access point. We measure and store data by using the vector network analyzer (VNA) followed by matlab simulation and analysing serveral parameters that we want to know such as power delay profile, RMS delay spread, correlation coefficient, path loss, and bit error rate.

4.2 Tool of experiment

4.2.1 Vector network analyzer (VNA)

Vector network analyzer (VNA) comprises of the vector network circuit analyzer model HP-8510C, S-parameter test set model HP-8514B and frequency synthesized sweeper model HP-83620A is main instrument show as figure 4.1.

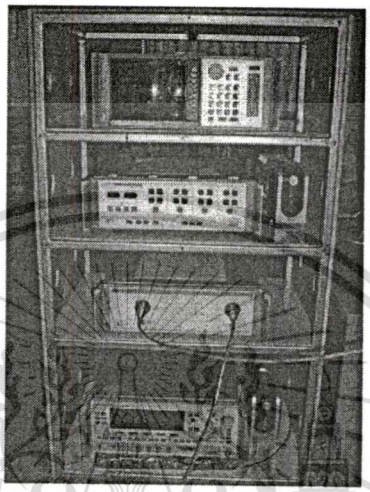

Figure 4.1 Vector network analyzer (VNA)

4.2.2 Biconical antenna

In wireless communication, antenna is very important equipment for transmitting and receiving signal. The antenna is a transducer designed to transmit or receive electromagnetic waves. In a transmitting antenna, the signal from an electronic circuit causes electrons in the antenna to oscillate; these moving electrons generate electromagnetic radiation, which is transmitted through the air and space. Waves distribution depend on the design of the antenna. The transmitting antennas of a radio station might be designed to emit waves in all directions, while an antenna used for radar or space communications would be designed to focus the waves in a single direction. In a receiving antenna electromagnetic waves cause the electrons to oscillate, inducing a signal that can be detected by an electronic circuit.

There are two fundamental types of antenna directional patterns, which, with reference to a specific three dimensional (usually horizontal or vertical) plane are either:

1 Omni-directional (radiates equally in all directions), such as a vertical rod or

2 Directional (radiates more in one direction than in the other).

In this research a biconical antenna was used [20]. A biconical antenna consisted of an arrangement of two conical conductors, which sre driven by potential, charge, or an alternating magnetic field (and the associated alternating electric current) at the vertex. The conductors have a common axis and vertex. The two cones face in opposite directions. Biconical antennas are broadband dipole antennas, typically exhibiting a bandwidth of 3 octaves or more. The radiation pattern of biconical antenna is omni-directional and the frequency satisfies range 3.1 GHz to 10.6 GHz for UWB system approved by Federal Communication Commission (FCC) in year 2002. The characteristic of this antenna is illustrated in figure 4.2 to figure 4.4.

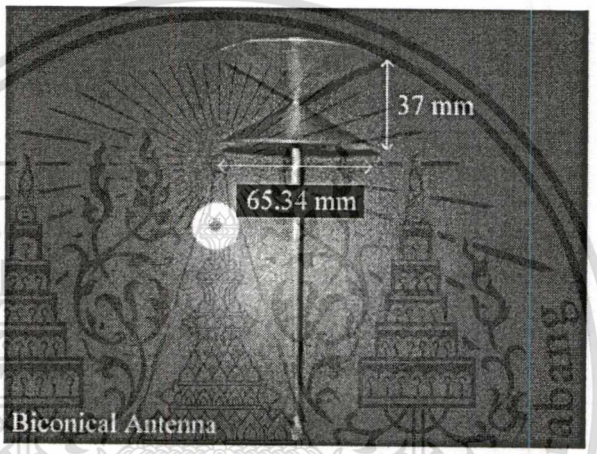

Figure 4.2 Geometry and dimension of the biconical antenna

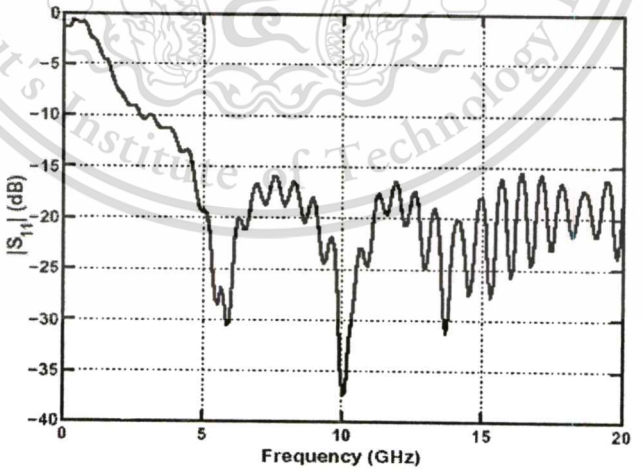

Figure 4.3 Reflection coefficient of biconical antenna

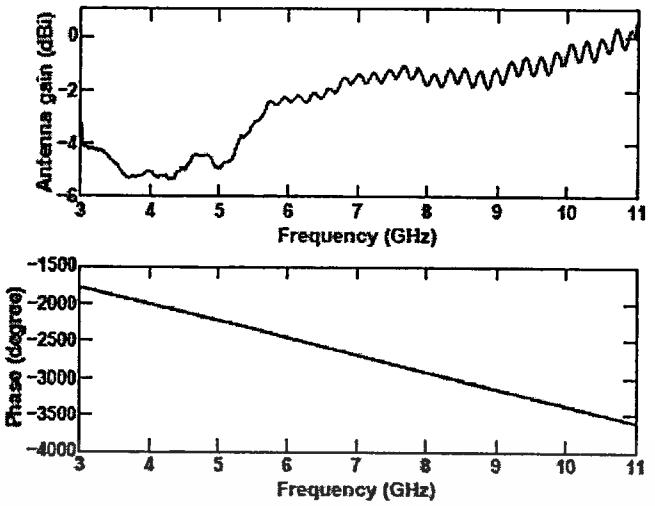

Figure 4.4 Magnitude and Phase of transfer function antenna

4.3 Measurement setup

The measurement system consists of a vector network analyzer (VNA) model HP-8510C, S-parameter test set model HP-8514B and frequency synthesized sweeper model HP-83620A, a biconical antenna pair and a control computer with a Matlab software.

The VNA is operated in response measurement mode, where port1 is a transmitter port (Tx) and port2 is a receiver port (Rx). The antennas used in the measurements are biconical antennas made by our lab. Typical features of the biconical antenna are omni-directional radiation pattern and a constant phase center. Both features are important in the radio channel sounding. Dynamic range mentioned in Table 1. is given as reduced to the output of the Rx antenna. Specified dynamic range for the network analyzer is 100 dB but the cable losses diminished 20 decibels of the dynamic range.

4.4 Parameters used for analysis

The important parameters for the experiments are listed in Table 4.1. It is noted that the calibration is done at the connectors of the cables to be connected to the antennas. Therefore, all the impairments of the antenna characteristics are included in the measured results.

Table 4.1 Experimental setup parameters.

Parameter	Value
Frequency range	3 GHz to 11 GHz
Number of frequency points	801
Dynamic power range	80 dB
Tx antenna height	2.80 m
Rx antenna height	0.70 m
Distance between Tx and Rx	2.90 to 6.66 m
Rx move step	0.4 m

4.5 Calibration

The VNA requires a calibration with the same cables and adapters as will be used in the measurement. To be able to carry out a magnitude and phase information of the transmitted signal the enhanced response calibration is required. Since the amplifier is isolated in reverse direction, it has to be removed from the setup for the time of calibration. After performing the calibration, the amplifier is reconnected. The amplifier frequency response is measured independently and it is taken into account in the post-processing.

4.6 UWB transmission signal waveform model

For UWB transmission signal waveform, the rectangular passband waveform is considered as the UWB transmitted signal. The expression of UWB transmitted signal (v_t) in time domain is given by Equation 4.1. The transmitted signal waveform and spectrum of UWB are shown in figure 4.5 and figure 4.6 respectively.

$$v_t = \frac{1}{f_b}[f_H \text{sinc}(2f_H t) - f_L \text{sinc}(2f_L t)] \qquad (4.1)$$

where

f_H - is maximum frequency [10.6 GHz]

f_L - is minimum frequency [3.1 GHz]

f_b - is occupied bandwidth [$f_b = f_H - f_L = 10.6 - 3.1 = 7.5$ GHz]

$$\text{sinc}(x) = \frac{\sin(\pi x)}{(\pi x)}$$

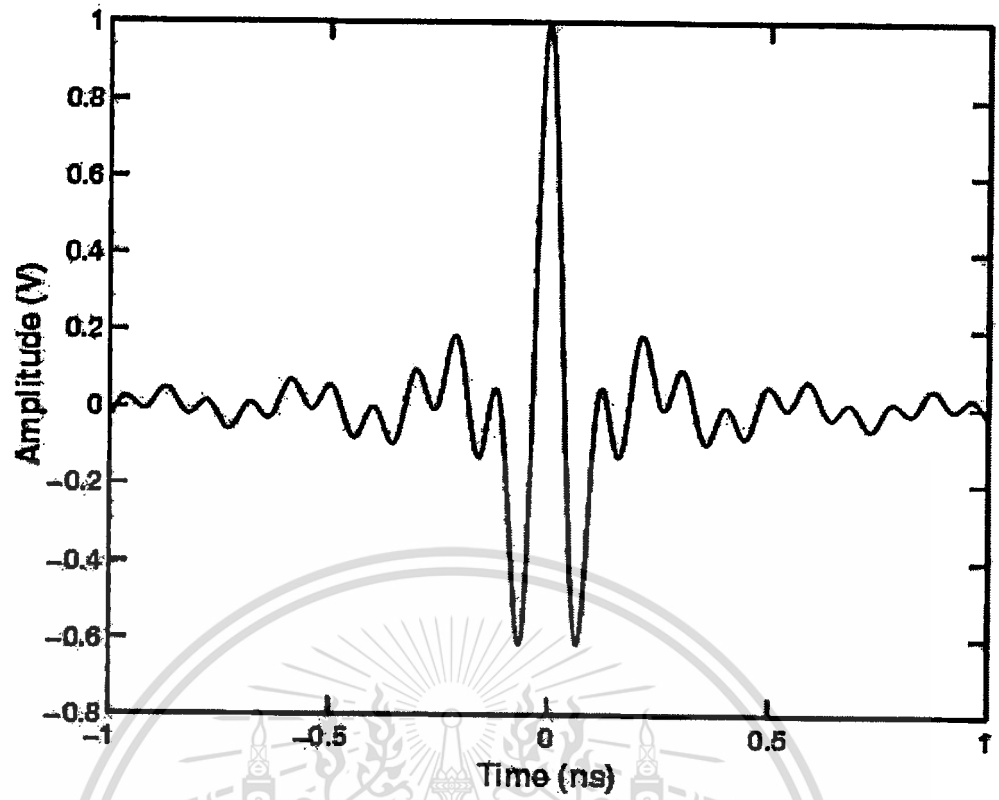

Figure 4.5 The transmitted signal waveform of UWB

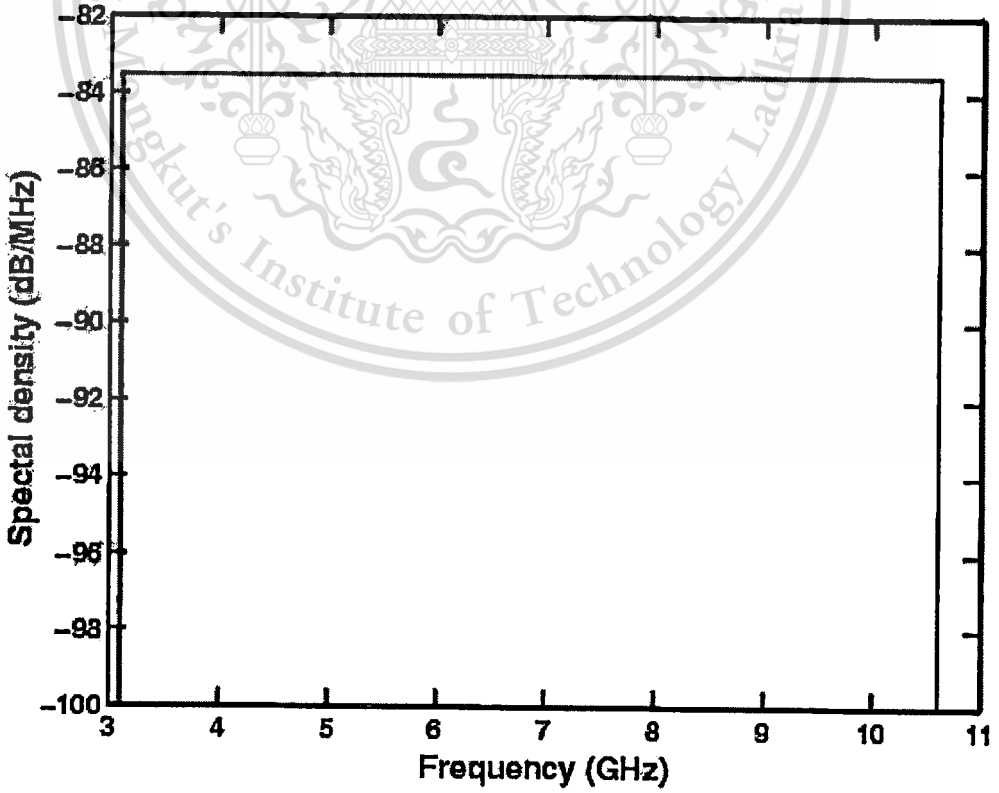

Figure 4.6 The transmitted spectrum of UWB

4.7 UWB channel measurement model

In this experiment we setup 4 various polarizations as mention in above, for step of measurement in each various polarization will show as follows.

4.7.1 Measurement of polarization 1

The VNA is operated in response measurement mode, where port1 is a transmitter port (Tx) connect to transmitter antenna by using Semi-rigid coaxial cables long 3 m and port2 is a receiver port (Rx) connect to receiver antenna by using Semi-rigid coaxial cables 7 m. The antennas used in the measurements are biconical antennas, the polarization of Tx antenna is vertical and polarization of Rx antenna is vertical both of antenna are differences height. The nearest point between the Tx antenna and the Rx antenna is 2.90 m at position (1,6) and the furthest between the Tx antenna and the Rx is 6.66 m at position (11,1) and (11,11). The Tx antenna is fixed point height from floor 2.80 m and the Rx antenna is moved along grid (11x11) totally 121 points and height from floor 0.7 m start from position (1,1) to (1,11) for the first row after that start the second row moved back from position (2,11) to (2,1) for the next row and position also do like this until finished at the last position (11,11). The room used for measurement and setup shown in figure 4.7a, 4.7b and 4.7c.

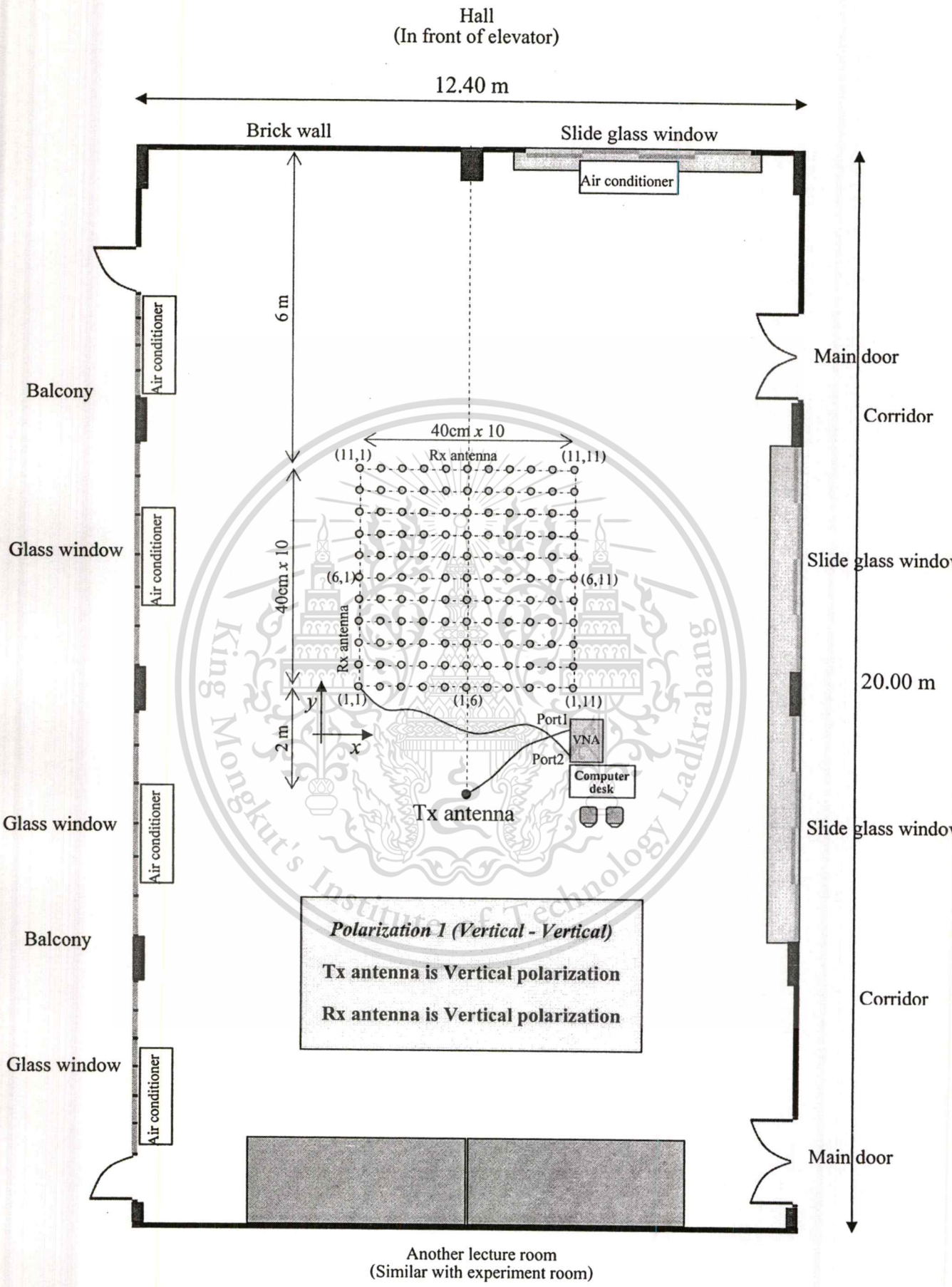

Figure 4.7a Dimension of room and instrument setup positioning – Top view.

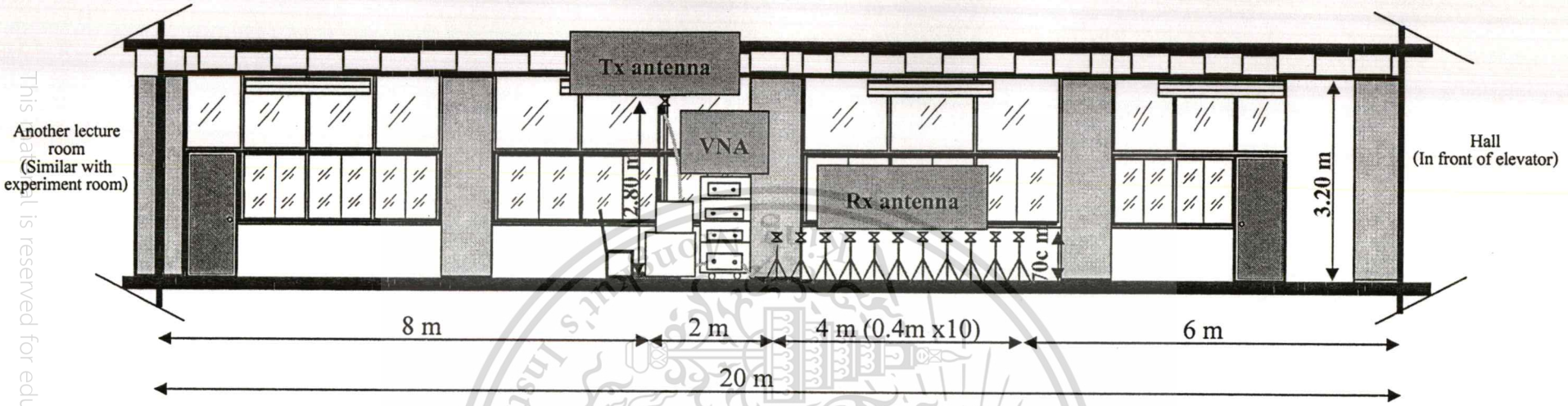

Figure 4.7b Dimension of room and instrument setup positioning – side view.

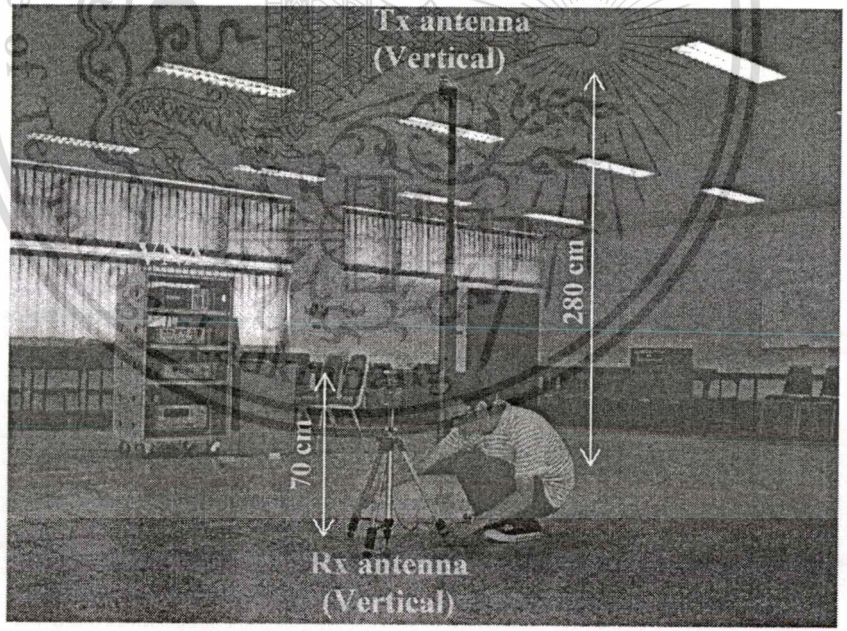

Figure 4.7c The experimental setup.

4.7.2 Measurement of polarization 2

This model every things is the same with model 1 except polarization of antennas. The polarization of antennas in this model we changed only Rx antenna from Vertical polarization to Horizontal polarization for Tx antenna is not change. The room used for measurement and setup in this model shown in figure 4.8a, 4.8b and 4.8c.

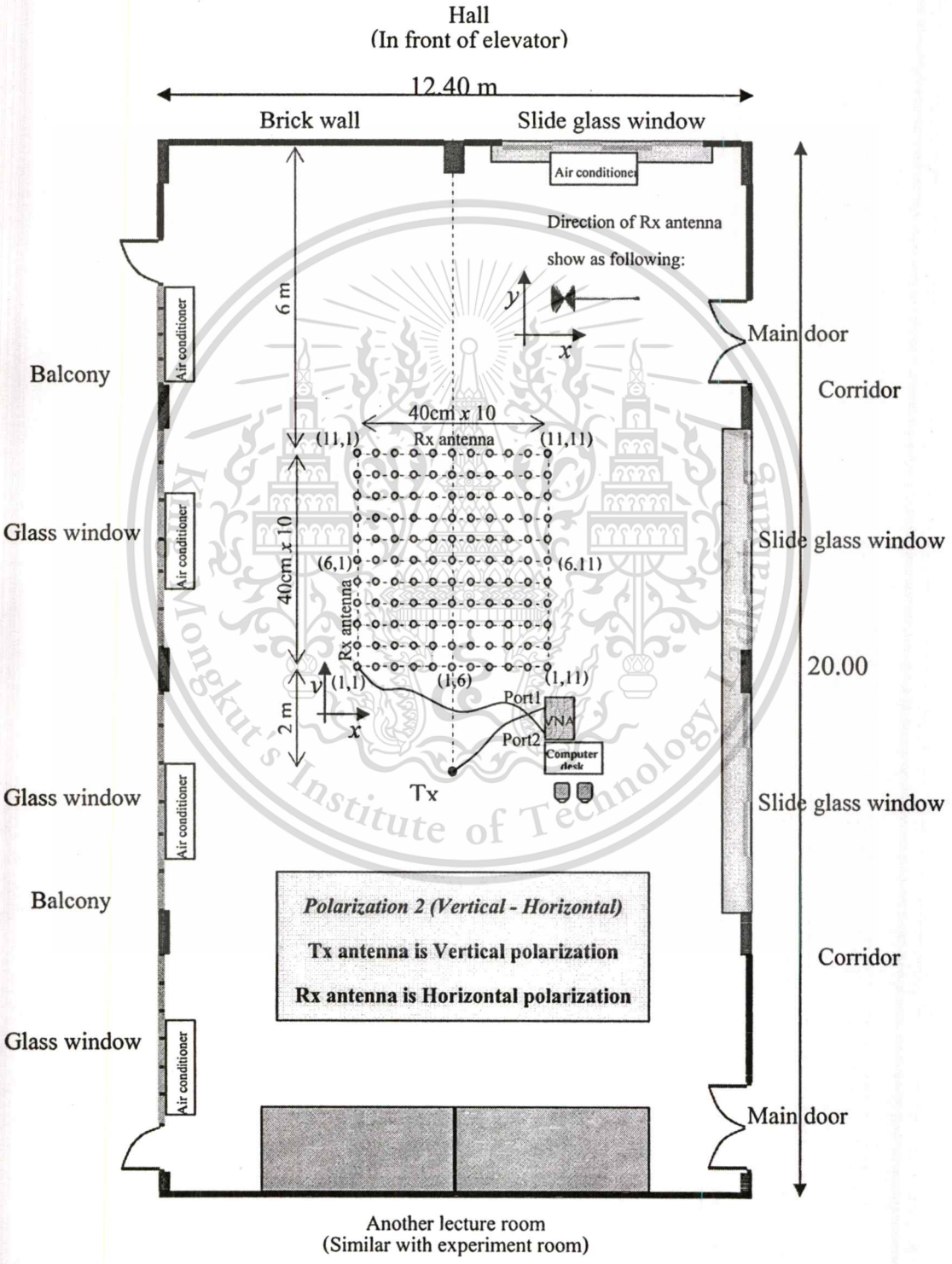

Figure 4.8a Dimension of room and instrument setup positioning – Top view.

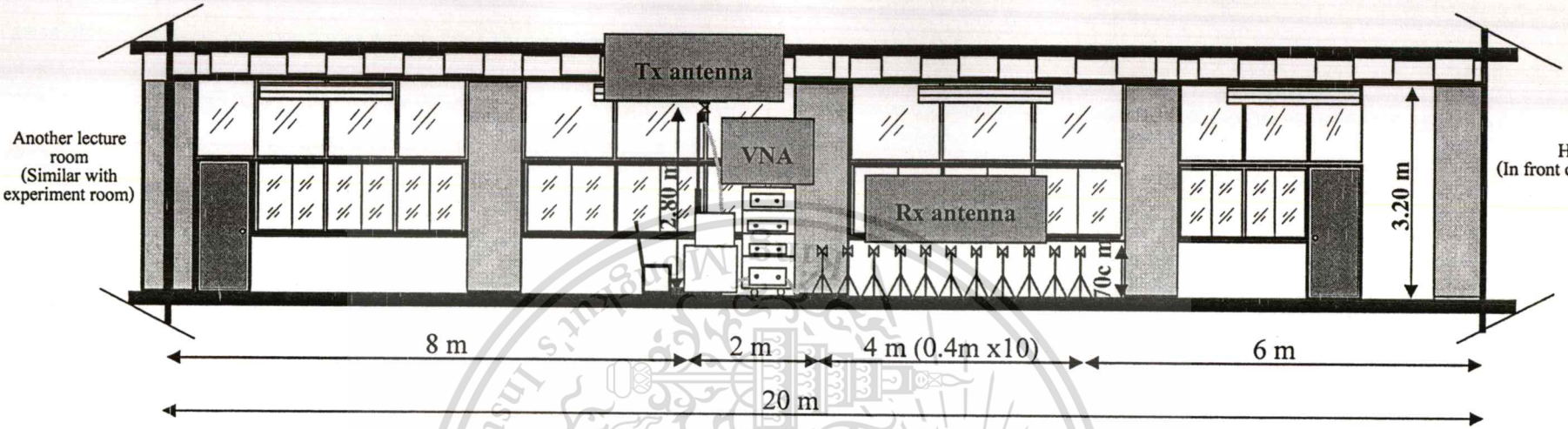

Figure 4.8b Dimension of room and instrument setup positioning – side view.

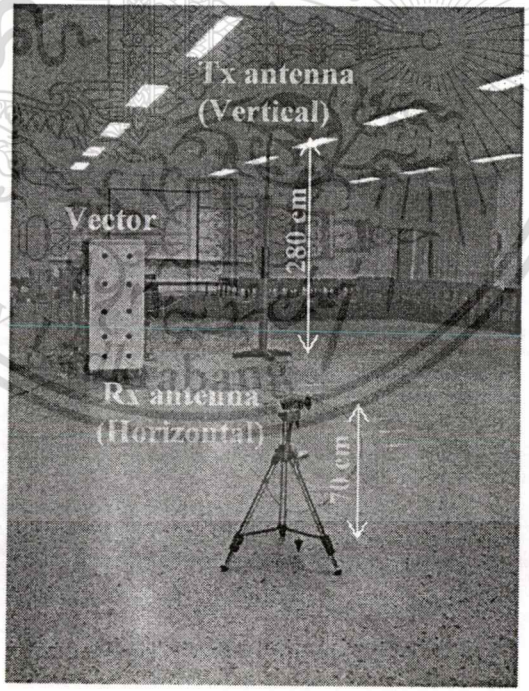

Figure 4.8c The experimental setup.

4.7.3 Measurement of polarization 3

This model every things is the same with model 1 except polarization of antennas. The polarization of antennas in this model we changed Tx antenna from Vertical polarization to Horizontal polarization and Rx antenna change from Vertical polarization to Herizontal. The room used for measurement and setup in this model shown in figure 4.9a, 4.9b and 4.9c.

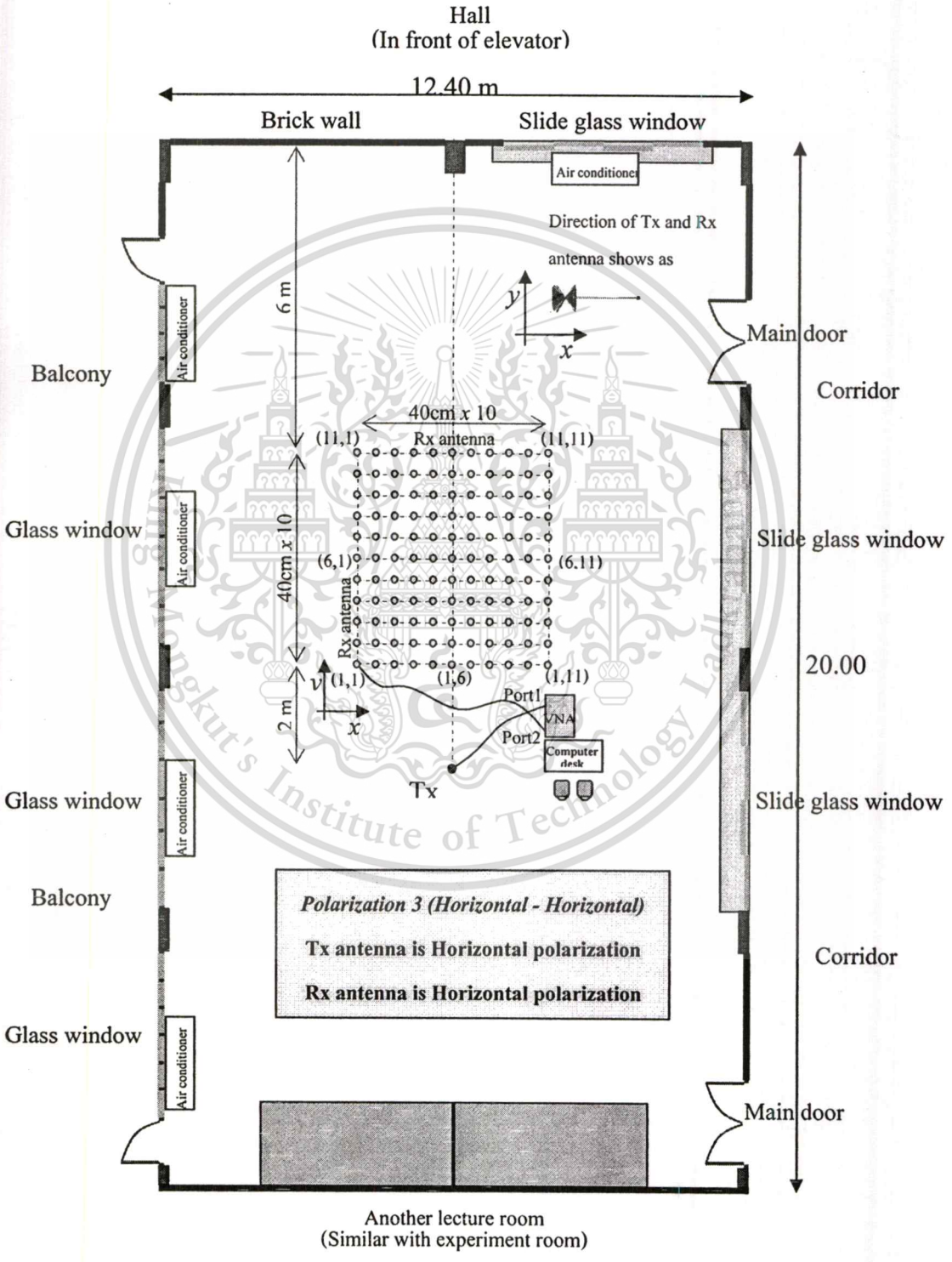

Figure 4.9a Dimension of room and instrument setup positioning – Top view.

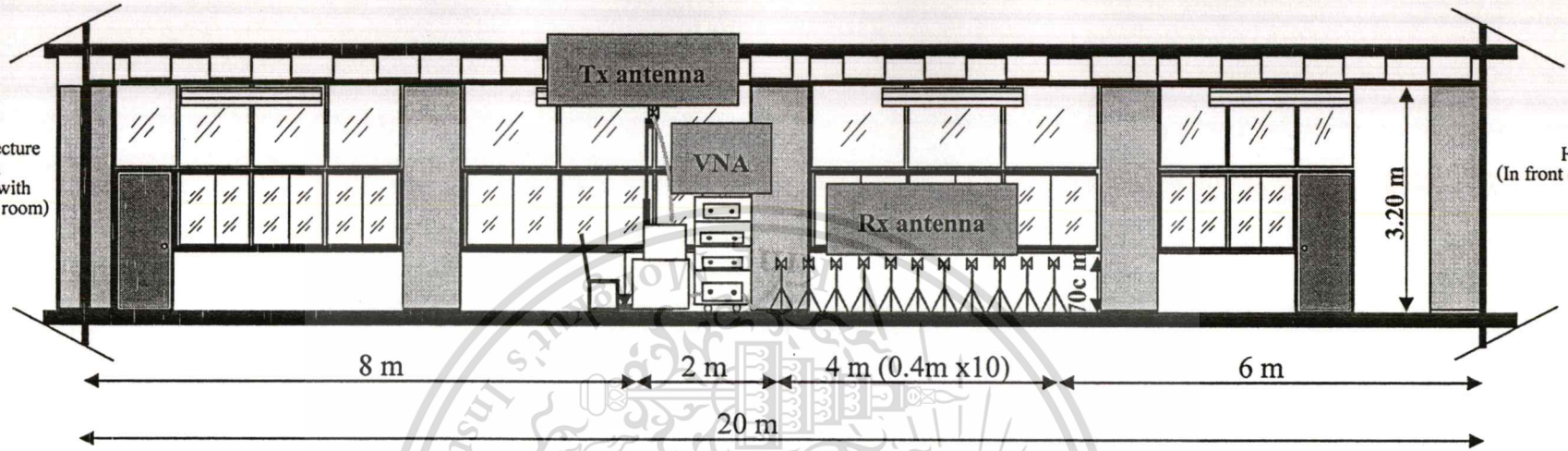

Figure 4.9b Dimension of room and instrument setup positioning – side view.

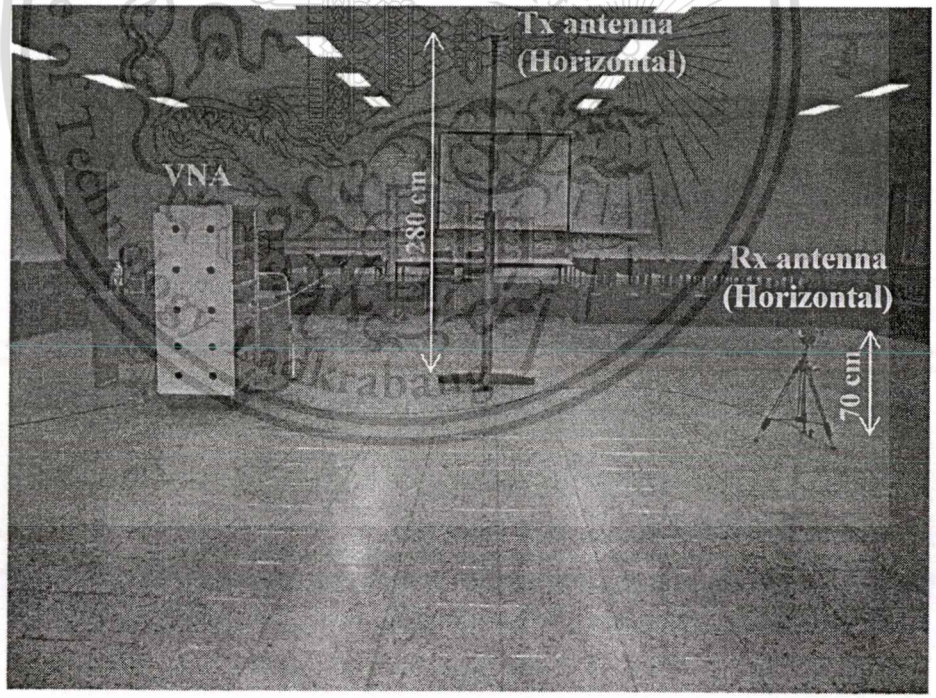

Figure 4.9c The experimental setup.

4.7.4 Measurement of polarization 4

The last model every things is also the same with model 1 except polarization of antennas. The polarization of antennas in this model we changed only Tx antenna from Vertical polarization to Horizontal polarization for Rx antenna is not change. The room used for measurement and setup in this model shown in figure 4.10a, 4.10b and 4.10c.

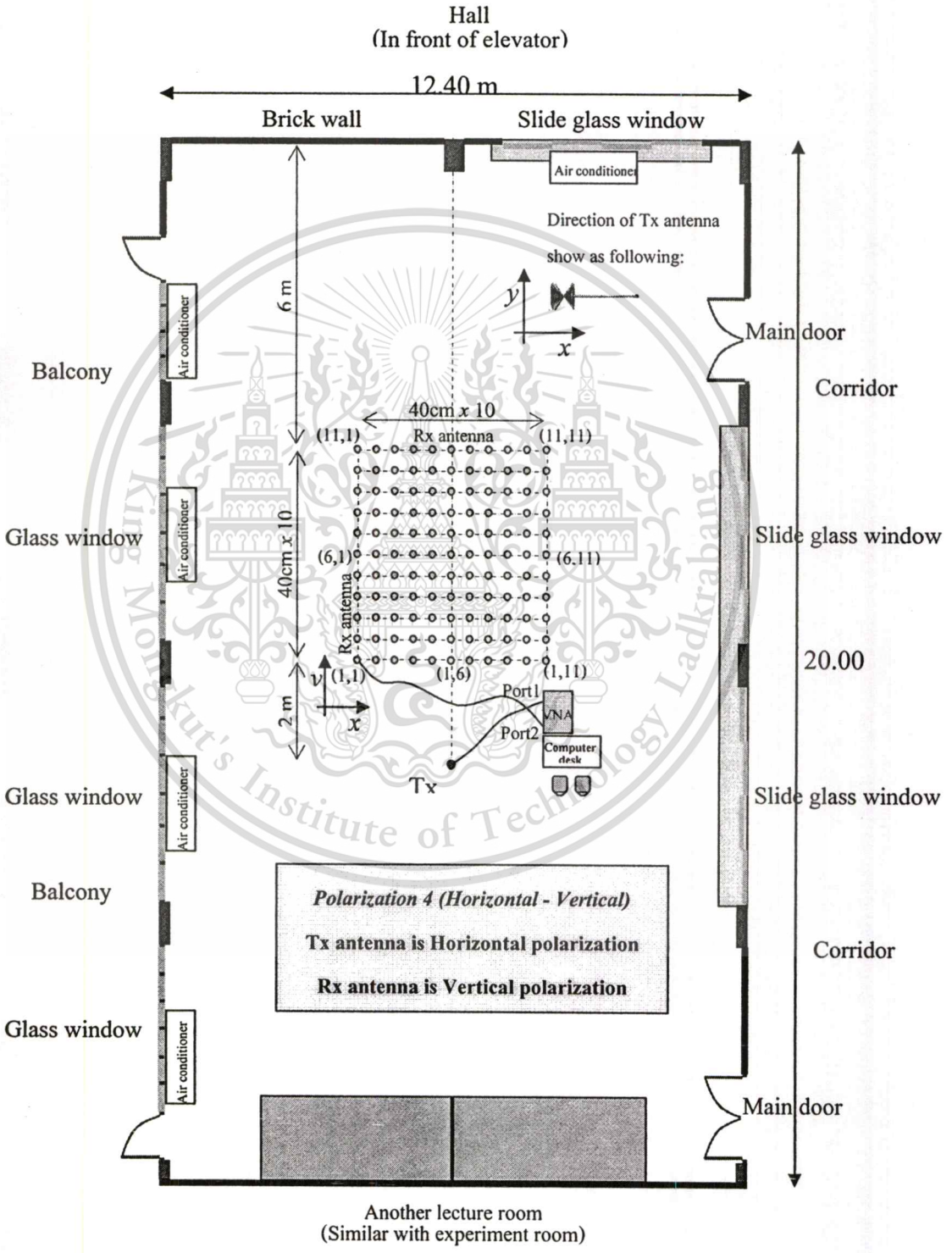

Figure 4.10a Dimension of room and instrument setup positioning – Top view.

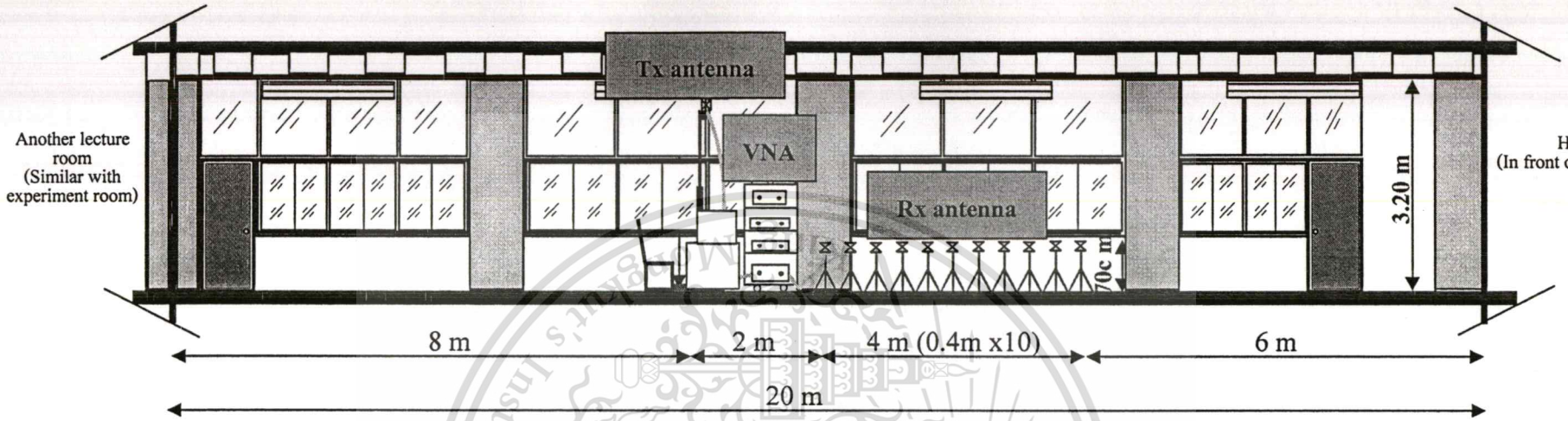

Figure 4.10b Dimension of room and instrument setup positioning – side view.

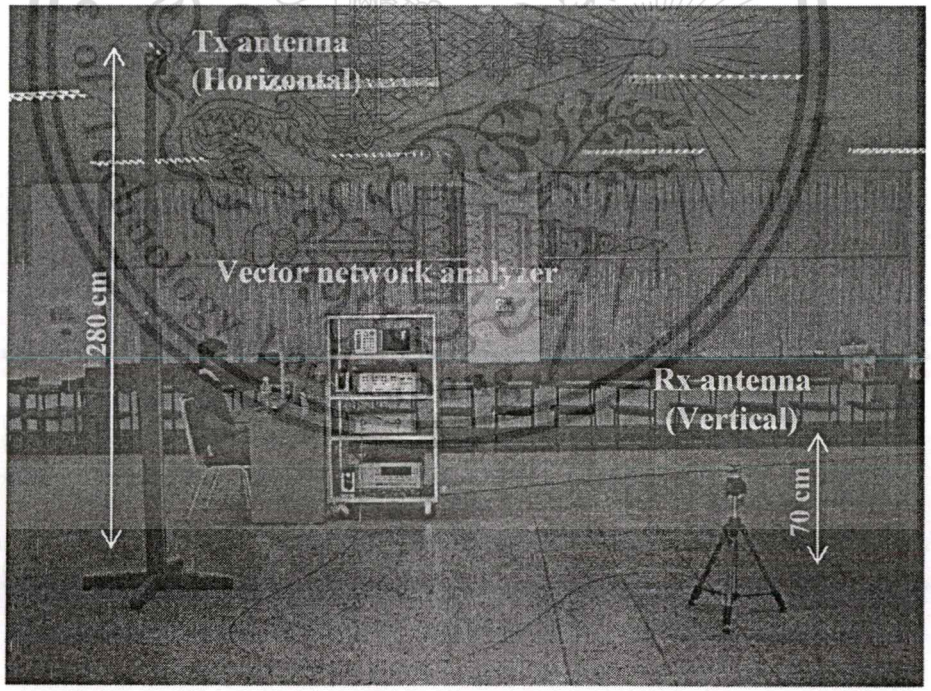

Figure 4.10c The experimental setup.

4.8 Conclusion

In This chapter, we mention the step of experiments in four various polarizations in an indoor environment, the main equipment in this experiment is vector network analyzer. The biconical antennas are used as the transmitter (Tx) and receiver (Rx) antennas. The characteristic of biconical antenna, the parameters used for analysis and also the UWB transmission signal waveform are presented. For the results of experiment in each various polarization and comparisons will discuss and shown in the next chapter.

Chapter 5

Measurement results

Measurement results for the parametric channel modeling by using biconical antennas at the transmitter and receiver are given in this chapter. The results of experimental including power delay profile, RMS delay spread, correlation coefficient, path loss and bit error rate (BER) for each polarization, finally show comparison path loss and BER in four various polarizations.

5.1 Results of experiment

5.1.1 Results of polarization 1 (Tx Vertical – Rx Vertical)

This model of the vector network analyzer is operated in response measurement mode, where port 1 is a transmitter port (Tx) connected to a transmitter antenna by using Semi-rigid coaxial cables 3m long and port 2 is a receiver port (Rx) connect to a receiver antenna by using Semi-rigid coaxial cables 7m long. The antennas used in the measurements are biconical antennas, the polarization of Tx antenna is vertical and polarization of Rx antenna is vertical both of the antennas are differences heights. Tx antenna height is 2.80m from the floor and Rx antennas height is 0.7m from the floor the nearest point between Tx antenna and Rx antenna is 2.90m at position (1,6) and the farthest point between Tx antenna and Rx is 6.66m at position (11,1) and (11,11).

5.1.1.1 Power delay profile

The power delay profile will show in a format of 3 axis which consists of the distance between Tx and Rx antenna, excess delay and power delay profile as figure 5.1. According to the polarization of the Tx and Rx antennas (Tx vertical and Rx vertical), the received signal power is not greatly decreased when the distance between Tx and Rx antennas are increased but the access time is different when Tx and Rx are near and far.

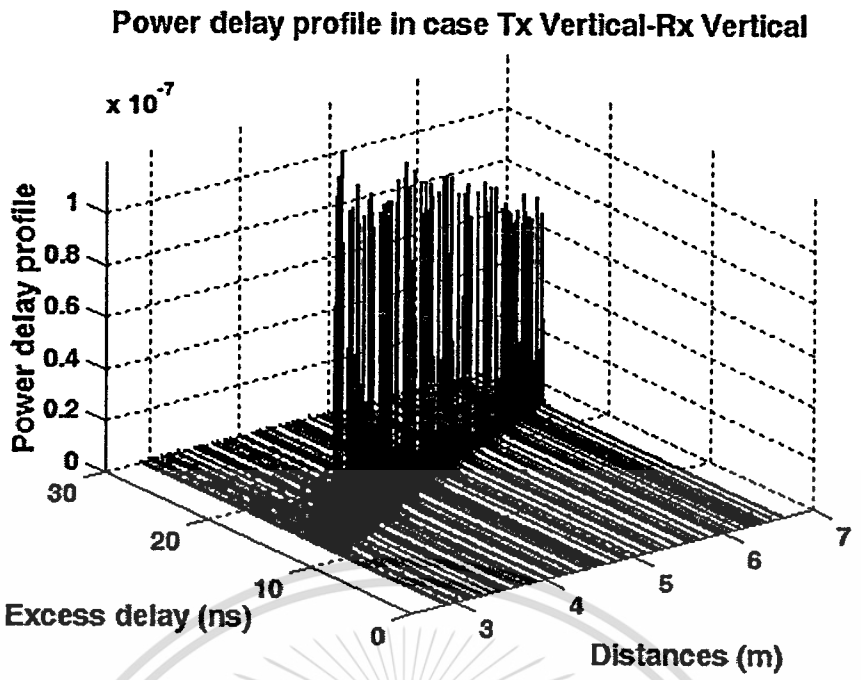

Figure 5.1 Power delay profile in case of (Tx Vertical – Rx Vertical)

5.1.1.2 RMS delay spread

The RMS delay spread shown in figure 5.2. We can see that the value of RMS delay spread is related with the distant between Tx and Rx antennas when the distance is increased the value of RMS delay spread is increased too which is in accordance with figure 5.1.

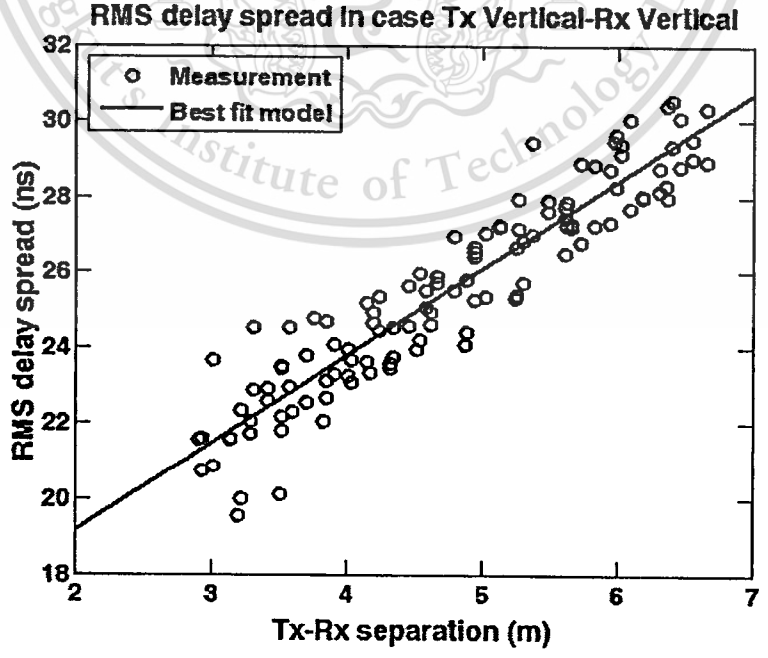

Figure 5.2 RMS delay spread in case of (Tx Vertical – Rx Vertical)

5.1.1.3 Path loss

The path loss is related with the distance between Tx and Rx antennas. When Tx is separated far from Rx the path loss is increased. The effect may come from environment of the room. For example, reflections off walls, ceilings, furniture, people, and other objects that may be present within a room. The path loss of this polarizes shown in figure 5.3 and figure 5.4 respectively.

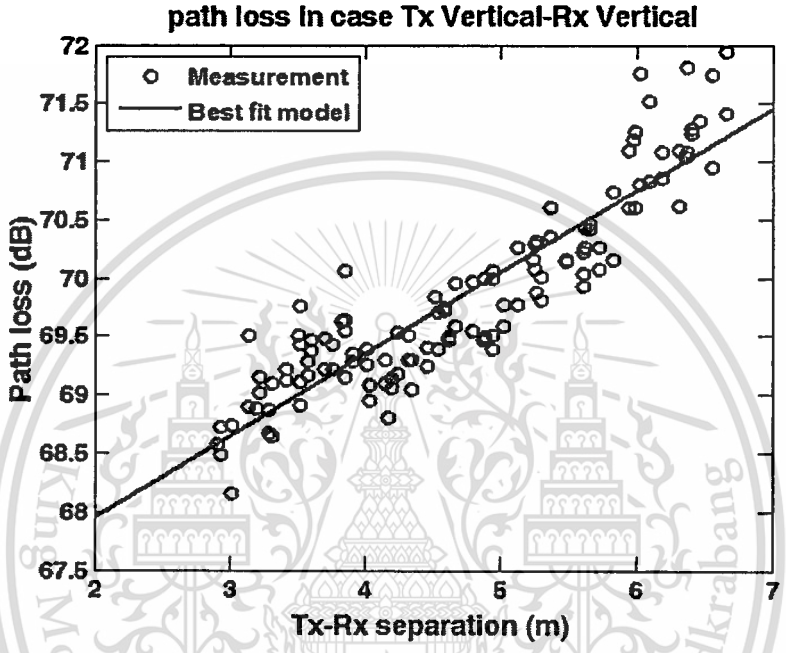

Figure 5.3 Path loss in case of (Tx Vertical – Rx Vertical)

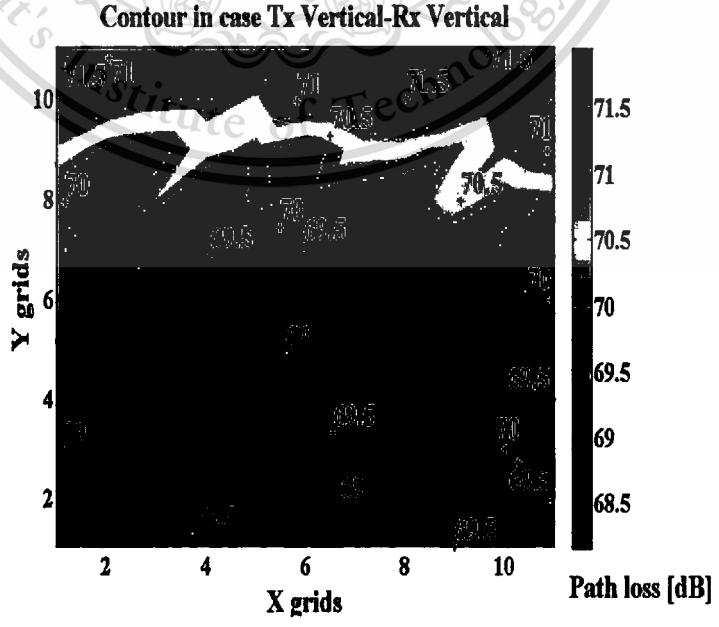

Figure 5.4 Contour show path loss by grid in case of (Tx Vertical – Rx Vertical)

5.1.1.4 Correlation coefficient

The correlation coefficient is performing a distortion of signal. The correlation coefficient between a transmitted signal and a received signal within the distance between Tx and Rx antennas from 2.90m to 6.66m. Normally when Tx is separated far from Rx the correlation coefficient is decreased but in this case we see that when Tx is near with Rx the value of correlation coefficient is alike. It not greatly different if compared with the middle of Tx and Rx antenna. The effect of this case maybe comes from the polarization of the antennas and environment in the room. For example, reflections off walls, ceilings, furniture, people, and other objects that may be present within a room. The correlation coefficient of this polarizes show in figure 5.5.

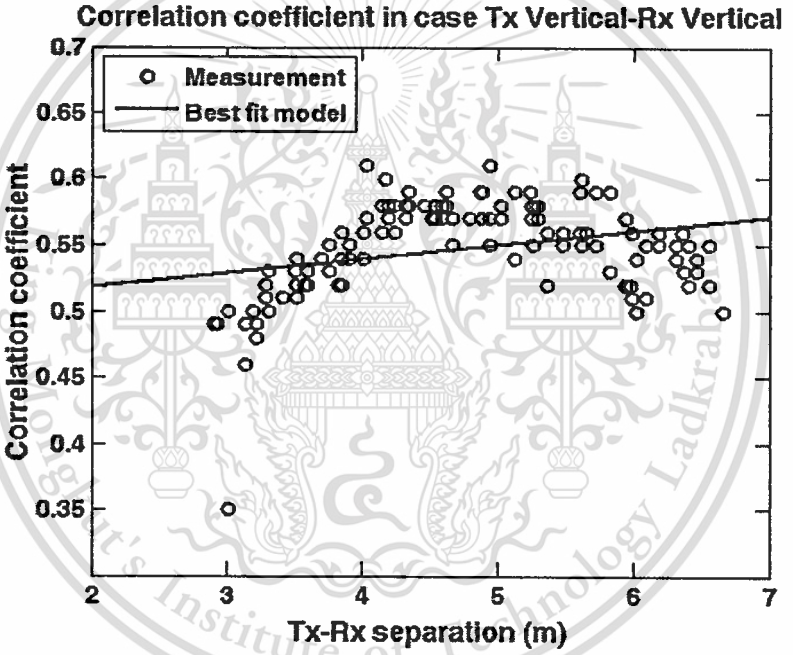

Figure 5.5 Correlation coefficient in case of (Tx Vertical – Rx Vertical)

5.1.1.5 Bit error rate (BER)

From the position of Rx are (1,1), (1,6), (6,1), (6,6), (11,1) and (11,6). We observe the bit error rate (BER) doesn't belong to the distance between Tx and Rx antennas but belong to the polarization of the Tx and Rx antennas and the environment of the room, the BER of each position show in figure 5.6.

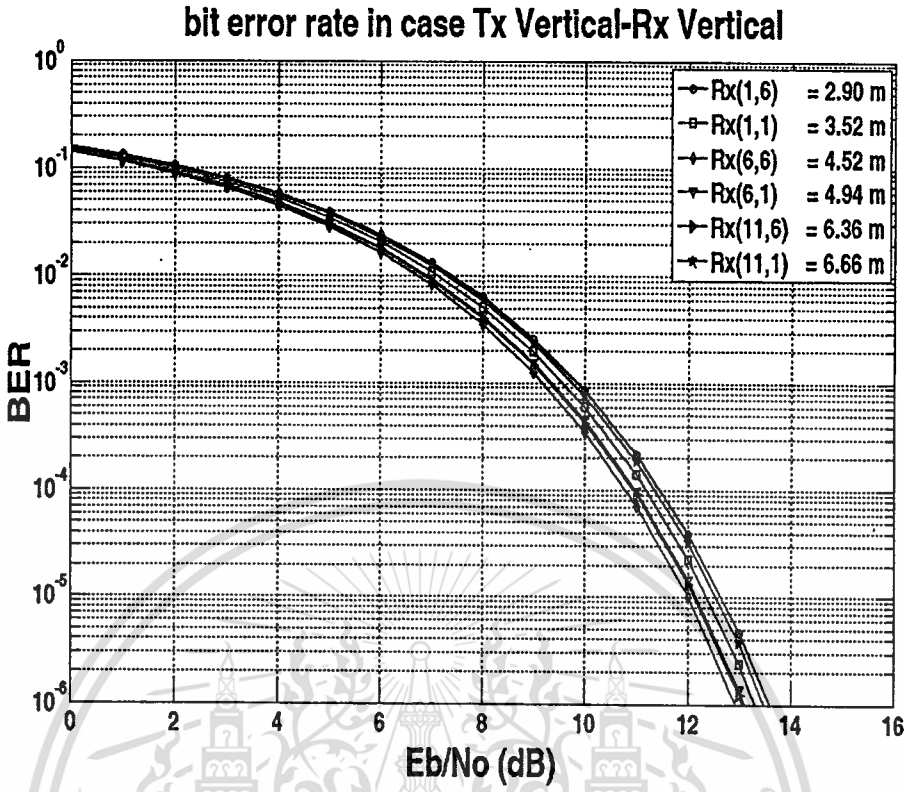

Figure 5.6 BER each position in case of (Tx Vertical – Rx Vertical)

5.1.2 Results of polarization 2 (Tx Vertical – Rx Horizontal)

In this model the polarization of Tx antenna is Vertical and polarization of Rx antenna is Horizontal. For other parameters it is the same with polarization 1.

5.1.2.1 Power delay profile

The power delay profile in this case shown in figure 5.7. According to the polarization of the Tx and Rx antennas (Tx Vertical and Rx Horizontal), the received signal power is decreased when the distance between Tx and Rx antennas is increased and the access time is also different when Tx and Rx are both near and far.

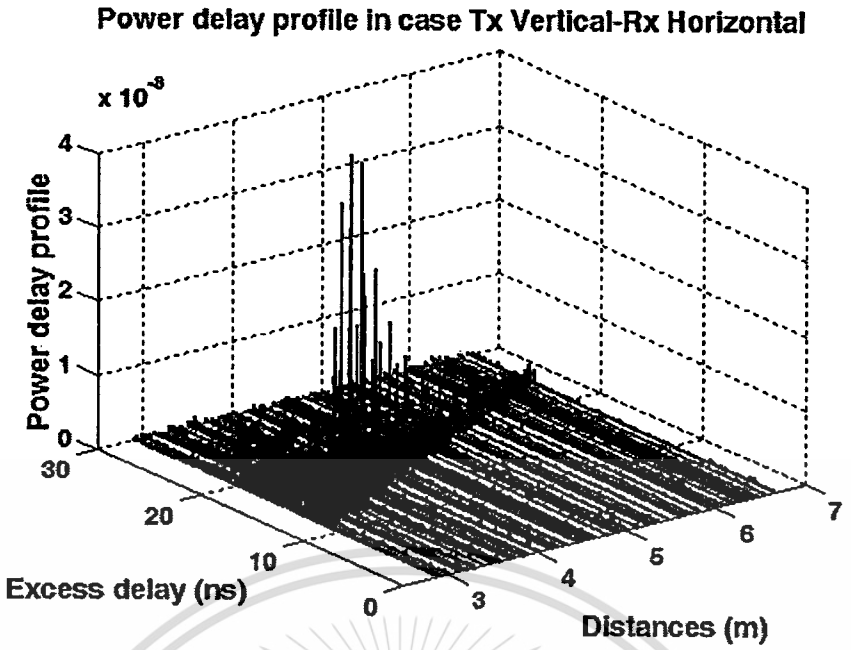

Figure 5.7 Power delay profile in case of (Tx Vertical – Rx Horizontal)

5.1.2.2 RMS delay spread

The RMS delay spread of this model shown in figure 5.8 .We can see that the value of RMS delay spread is related with distance between Tx and Rx antennas when the distance is increased the value of RMS delay spread is increased too which is in accordance with figure 5.7.

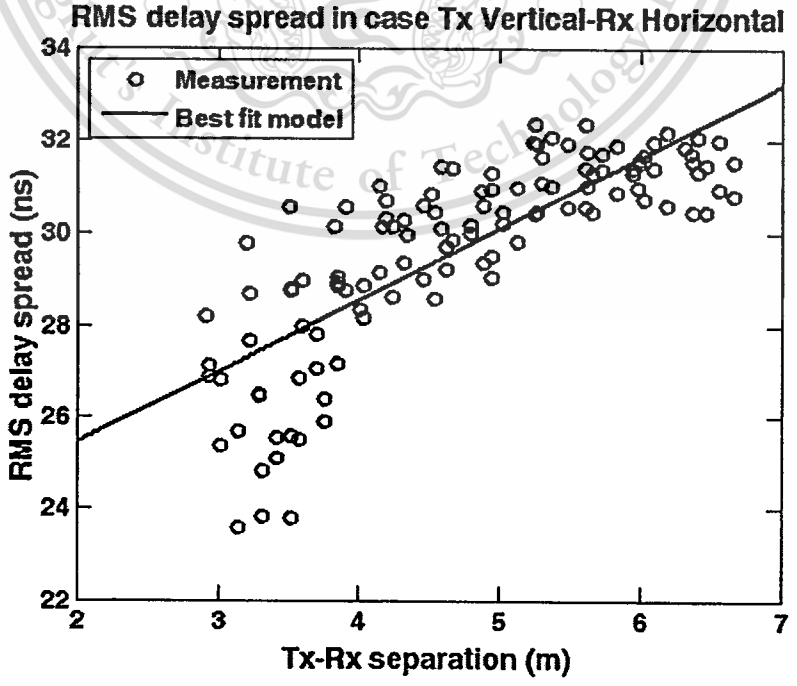

Figure 5.8 RMS delay spread in case of (Tx Vertical – Rx Horizontal)

5.1.2.3 Path loss

The path loss is related to the distance between the Tx and Rx antennas. When Tx is separated far from Rx the path loss is increased. This effect may come from environment of the room. For example, reflections off walls, ceilings, furniture, people, and other objects that may be present within the room. On the other hand due to directivity miss match as show in figure 5.9 and figure 5.10 respectively.

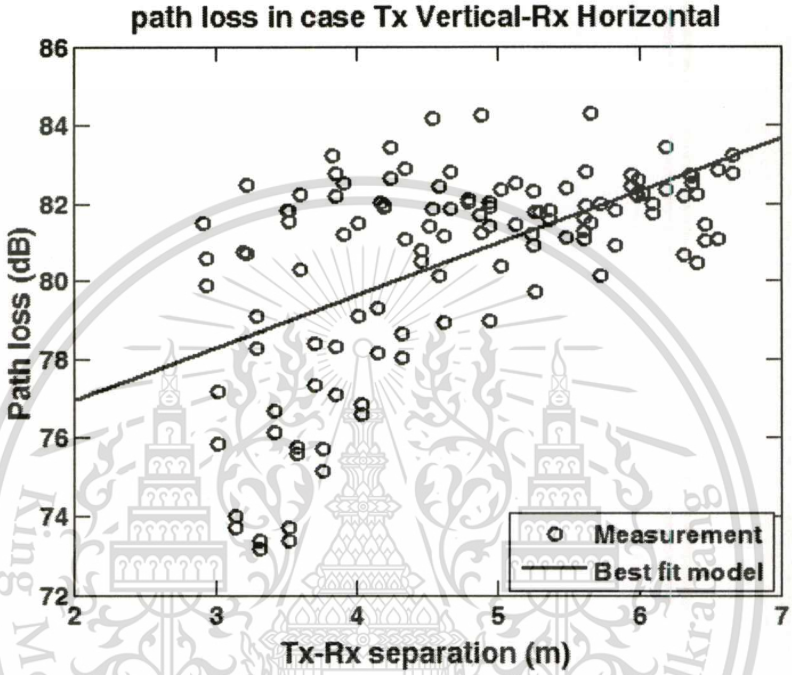

Figure 5.9 Path loss in case of (Tx Vertical – Rx Horizontal)

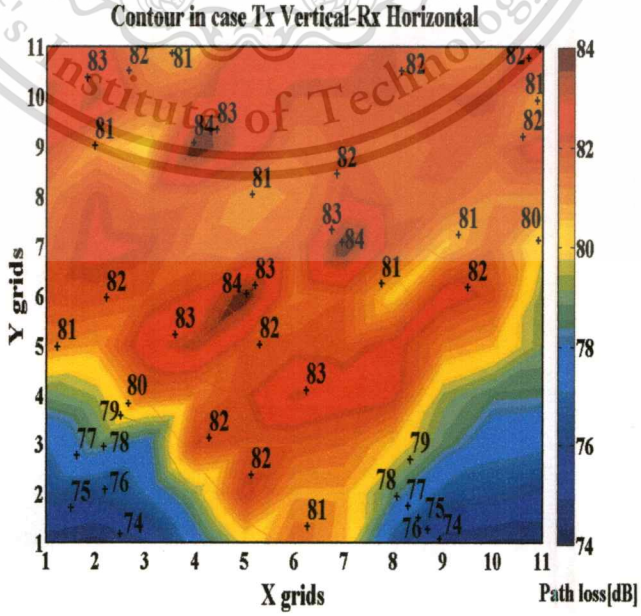

Figure 5.10 Contour show path loss by grid in case of (Tx Vertical – Rx Horizontal)

5.1.2.4 Correlation coefficient

The correlation coefficient in this case is related between Tx and Rx antennas when Tx separated far from Rx the correlation coefficient is decreased as shown in figure 5.11.

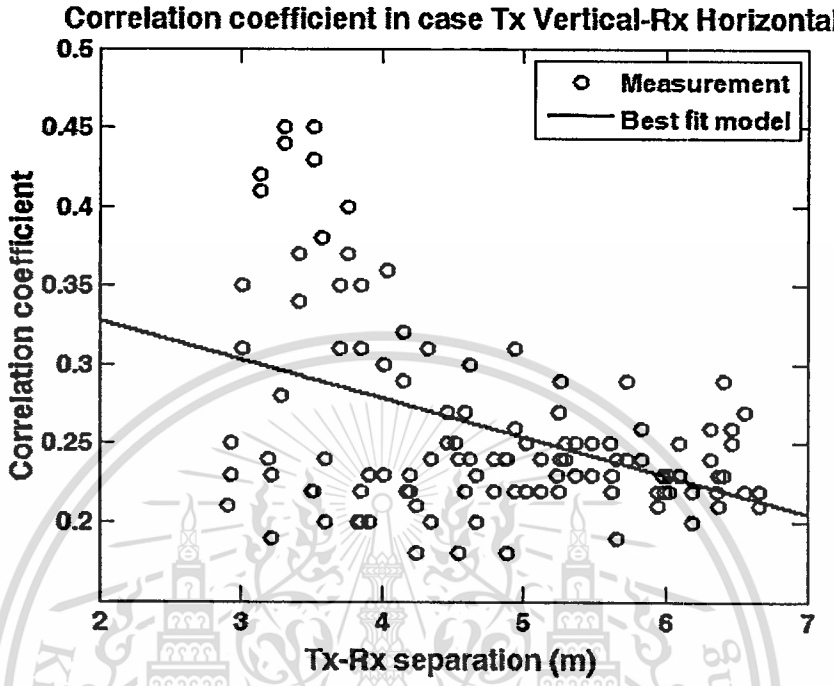

Figure 5.11 Correlation coefficient in case of (Tx Vertical – Rx Horizontal)

5.1.2.5 Bit error rate (BER)

From the position of Rx are (1,1), (1,6), (6,1), (6,6), (11,1) and (11,6). We see that the bit error rate is not belonging to the distance between Tx and Rx antennas but belong to the polarization of the Tx and Rx antennas and environment in the room, the BER of each position show in figure 5.12.

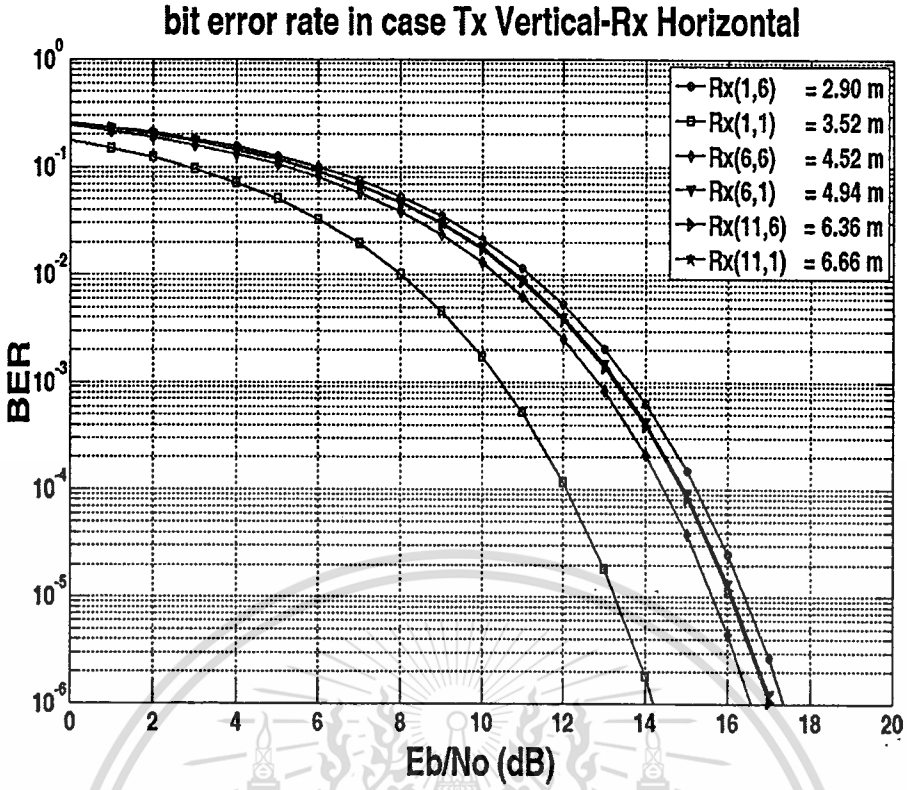

Figure 5.12 BER in case of (Tx Vertical – Rx Horizontal)

5.1.3 Results of polarization 3 (Tx Horizontal – Rx Horizontal)

This model the polarization of Tx antenna is Horizontal and polarization of Rx antenna is Horizontal. For other parameters is the same with polarization 1.

5.1.3.1 Power delay profile

The power delay profile in this case shows in figure 5.13. According to the polarization of the Tx and Rx antennas (Tx Horizontal and Rx Horizontal), the received signal power is decreased when distance between Tx and Rx antennas increased and the access time is also different when Tx and Rx near and far.

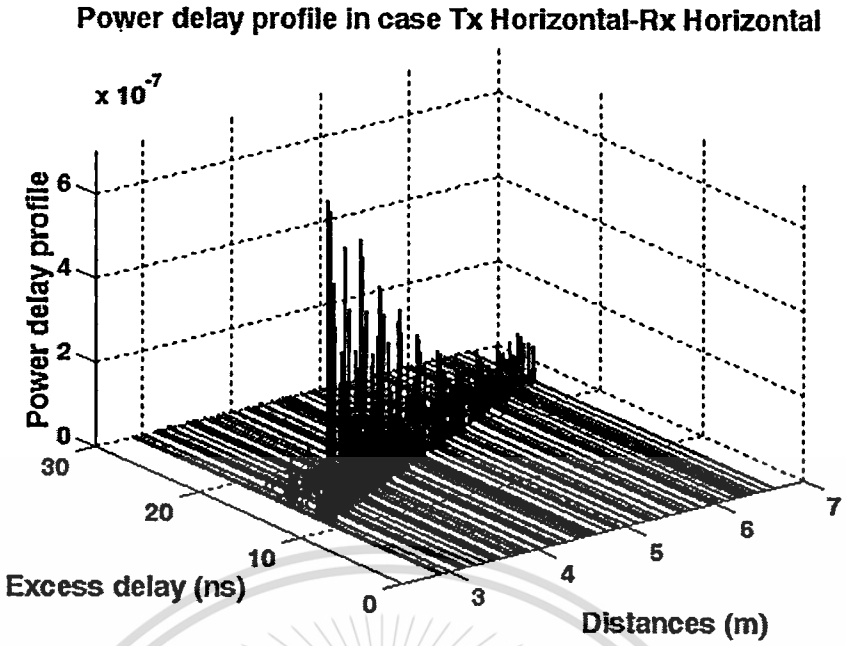

Figure 5.13 Power delay profile in case of (Tx Horizontal – Rx Horizontal)

5.1.3.2 RMS delay spread

The RMS delay spread of this polarize shows in figure 5.14 we can see that the value of RMS delay spread is related with distance between Tx and Rx antennas when the distance of Tx and Rx antennas increased the value of RMS delay spread is increased too which accordant with the figure 5.13.

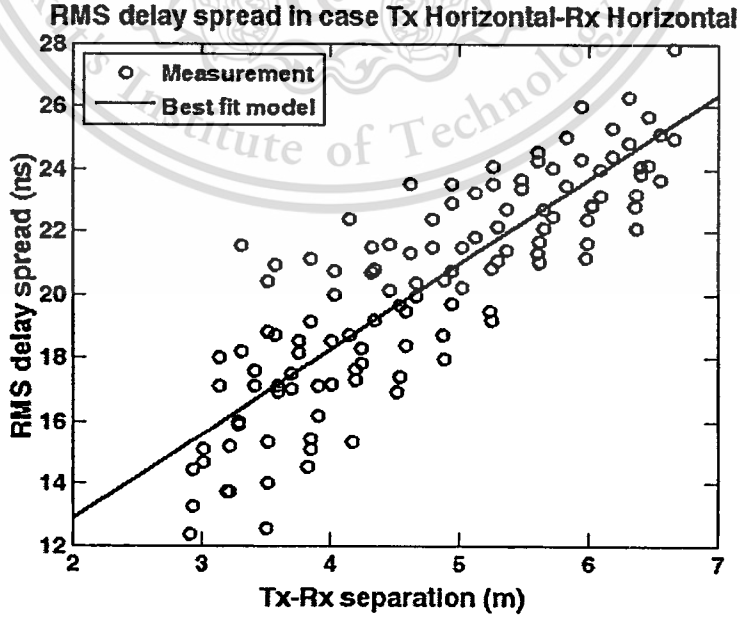

Figure 5.14 RMS delay spread in case of (Tx Horizontal – Rx Horizontal)

5.1.3.3 Path loss

The path loss is related with distance between Tx and Rx antenna, when Tx separated far from Rx the path loss is increased the effected may come from environment in the room. For example, reflections off walls, ceilings, furniture, people, and other objects that may be present within a room. The path loss of this polarize are show in figure 5.15 and figure 5.16 respectively.

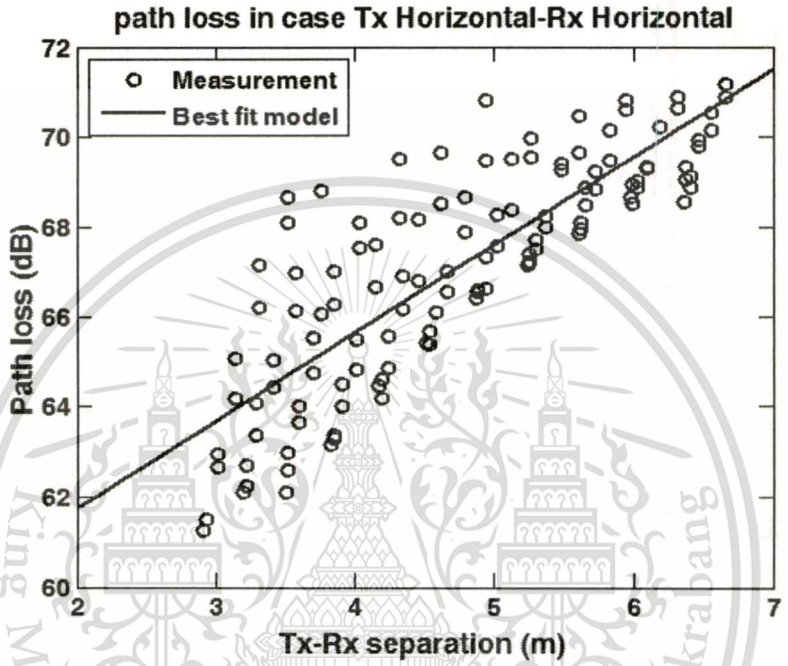

Figure 5.15 Path loss in case of (Tx Horizontal – Rx Horizontal)

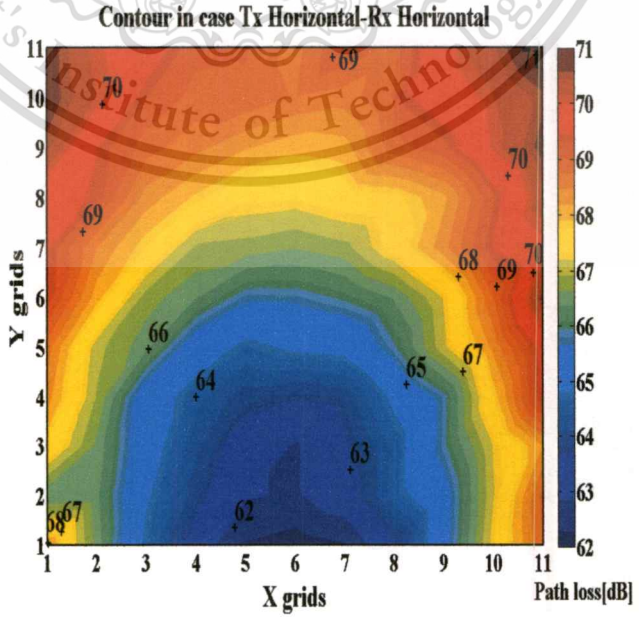

Figure 5.16 Contour show path loss by grid in case of (Tx Horizontal – Rx Horizontal)

5.1.3.4 Correlation coefficient

The correlation coefficient in this case is related between Tx and Rx antennas when Tx separated far from Rx the correlation coefficient is decreased as shown in figure 5.17.

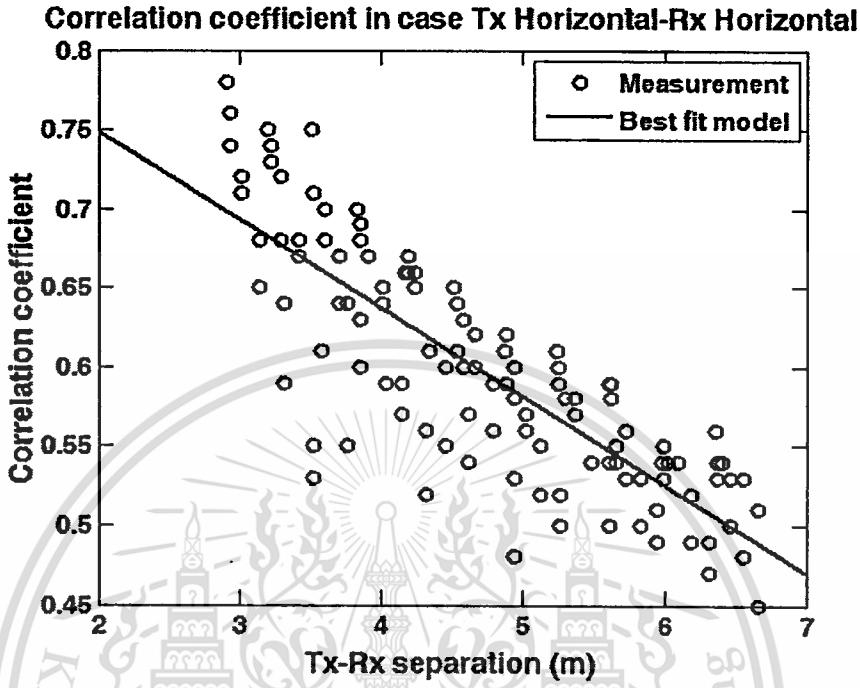

Figure 5.17 Correlation coefficient in case of (Tx Horizontal – Rx Horizontal)

5.1.3.5 Bit error rate (BER)

From the position of Rx are (1,1), (1,6), (6,1), (6,6), (11,1) and (11,6). We see that the bit error rate (BER) is belonging to the distance between Tx and Rx antennas but not at all the BER of each position show in figure 5.18.

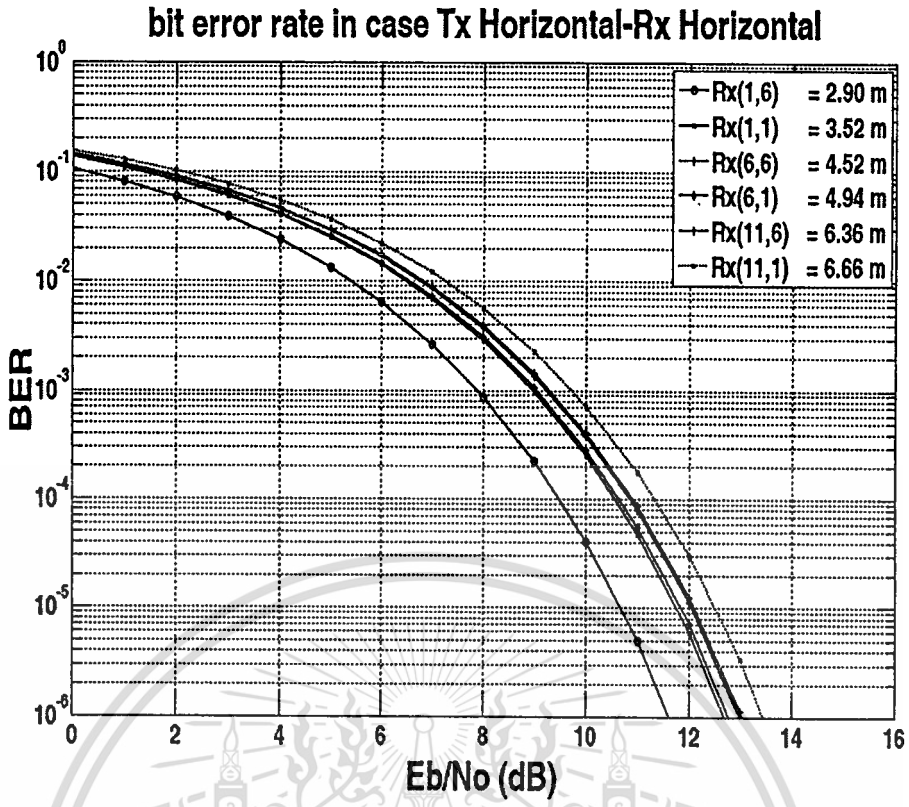

Figure 5.18 BER in case of (Tx Horizontal – Rx Horizontal)

5.1.4 Results of polarization 4 (Tx Horizontal – Rx Vertical)

This model the polarization of Tx antenna is Horizontal and polarization of Rx antenna is Vertical. For other parameters is the same with polarization 1.

5.1.4.1 Power delay profile

The power delay profile in this case shows in figure 5.19. According to the polarization of the Tx and Rx antennas (Tx Horizontal and Rx Vertical), the received signal power is decreased when distance between Tx and Rx antennas increased and the access time is also different when Tx and Rx near and far.

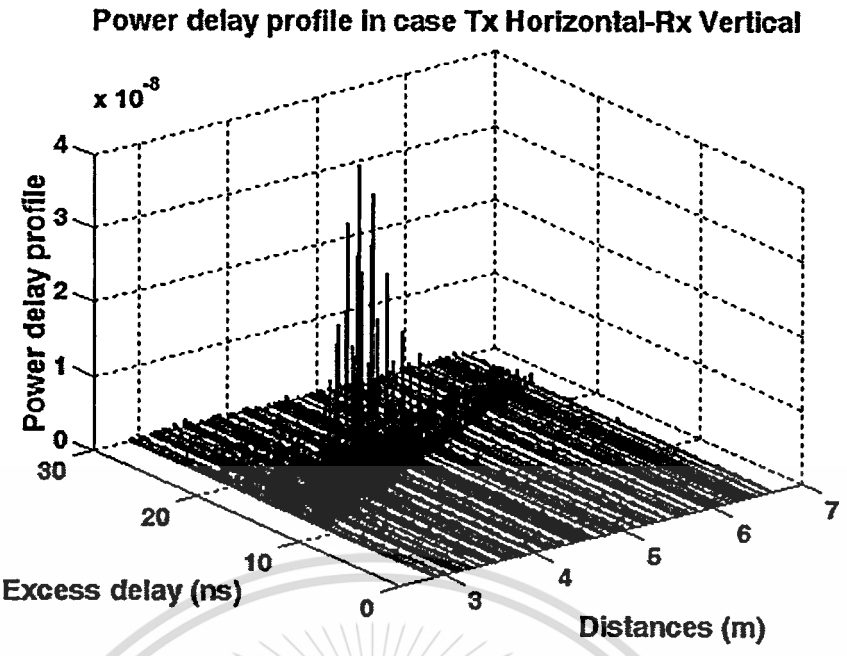

Figure 5.19 Power delay profile in case of (Tx Horizontal – Rx Vertical)

5.1.4.2 RMS delay spread

The RMS delay spread of this model shows in figure 5.20 we see that the value of RMS delay spread is related with distance between Tx and Rx antennas when distance increased the value of RMS delay spread is increased too which accordant with the figure 5.19.

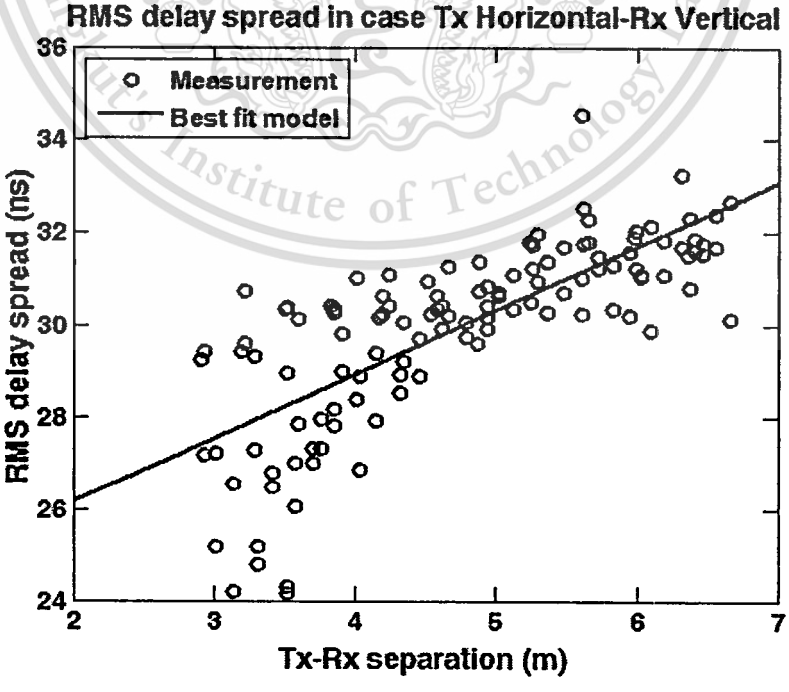

Figure 5.20 RMS delay spread in case of (Tx Horizontal – Rx Vertical)

5.1.4.3 Path loss

The path loss is related with distance between Tx and Rx antennas, when Tx separated far from Rx the path loss is increased but not at all the effected may come from the polarization of the antennas and environment in the room. The path loss of this case shows in figure 5.21 and figure 5.22 respectively.

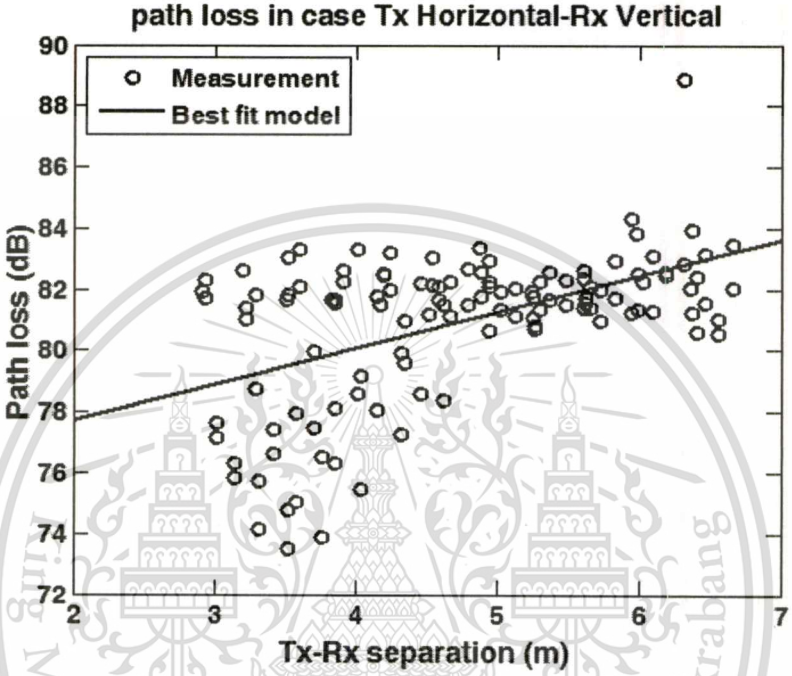

Figure 5.21 Path loss in case of (Tx Horizontal – Rx Vertical)

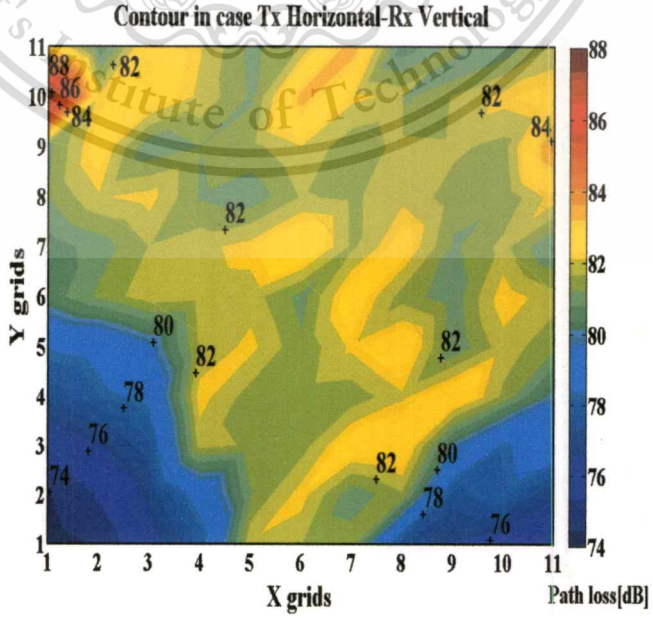

Figure 5.22 Contour show path loss by grid in case of (Tx Horizontal – Rx Vertical)

5.1.4.4 Correlation coefficient

The correlation coefficient in this case shows in figure 5.23. It's related between Tx and Rx antennas when Tx separated far from Rx the correlation coefficient is decreased but not at all the effected may come from the polarization of the antennas and environments in the room.

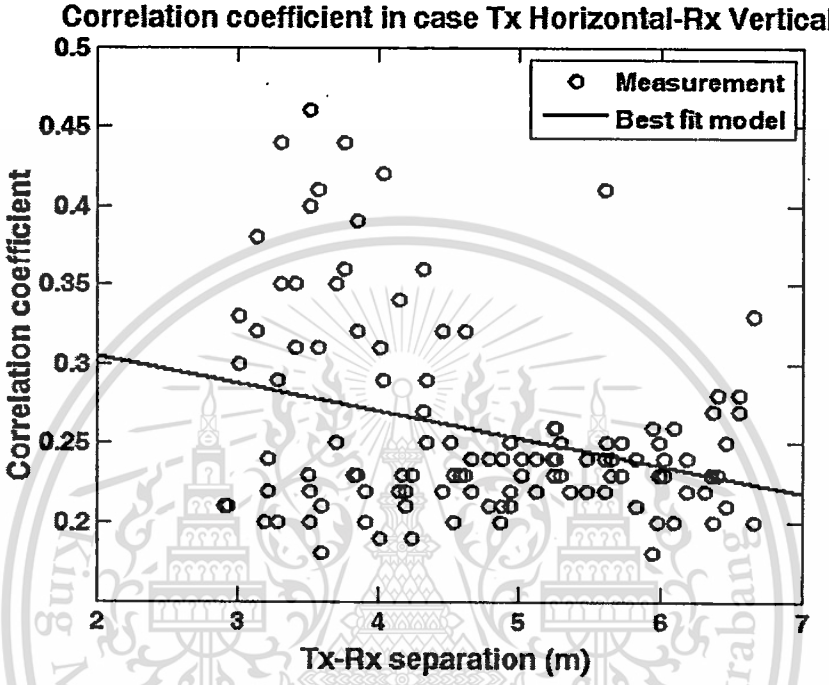

Figure 5.23 Correlation coefficient in case of (Tx Horizontal – Rx Vertical)

5.1.4.5 Bit error rate (BER)

The BER of the position of Rx are (1,1), (1,6), (6,1), (6,6), (11,1) and (11,6) shows in figure 5.24.

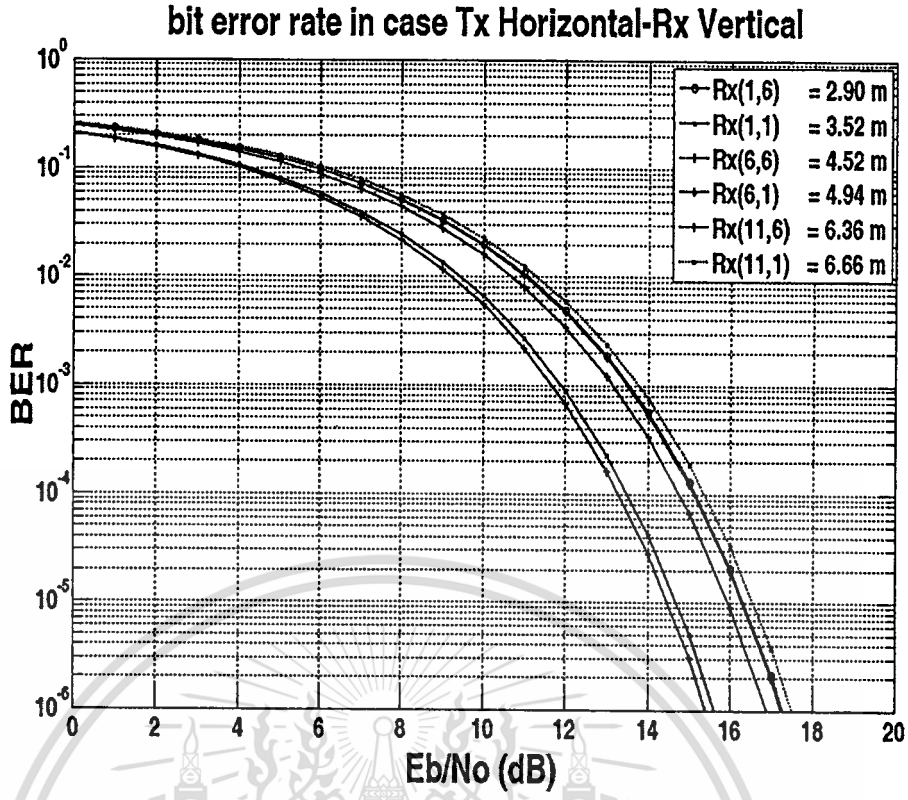

Figure 5.24 BER in case of (Tx Horizontal – Rx Vertical)

5.2 Comparison of the four different polarizations.

5.2.1 Path loss comparison

The path loss of four polarizations is shows in figure 5.25. From figure we can separate 2 groups of polarization. The first group is same polarizations (Vertical-Vertical and Horizontal-Horizontal) and the second group is various polarizations (Vertical-Horizontal and Horizontal-Vertical). We noticeably when Tx and Rx antennas the same polarization in the group then path loss is nearby. Otherwise, if compare path loss between first group and second group we can see that path loss the first group (Vertical-Vertical and Horizontal-Horizontal) is less than path loss of the second group (Vertical-Horizontal and Horizontal-Vertical) due to polarization of the antennas.

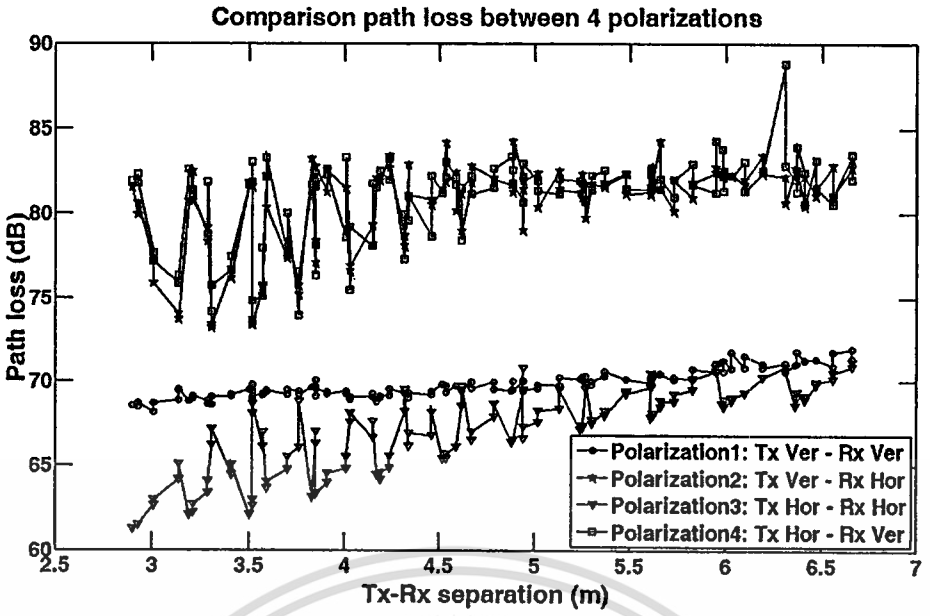

Figure 5.25 comparison of Path loss

5.2.2 Bit error rate (BER) comparison

For bit error rate (BER) in each position of four polarizations are shows in figure 5.26 to figure 5.34. we give an example of position of Rx are (1,1), (1,6), (1,11), (6,1), (6,6), (6,11), (11,1), (11,6) and (11,11) respectively.

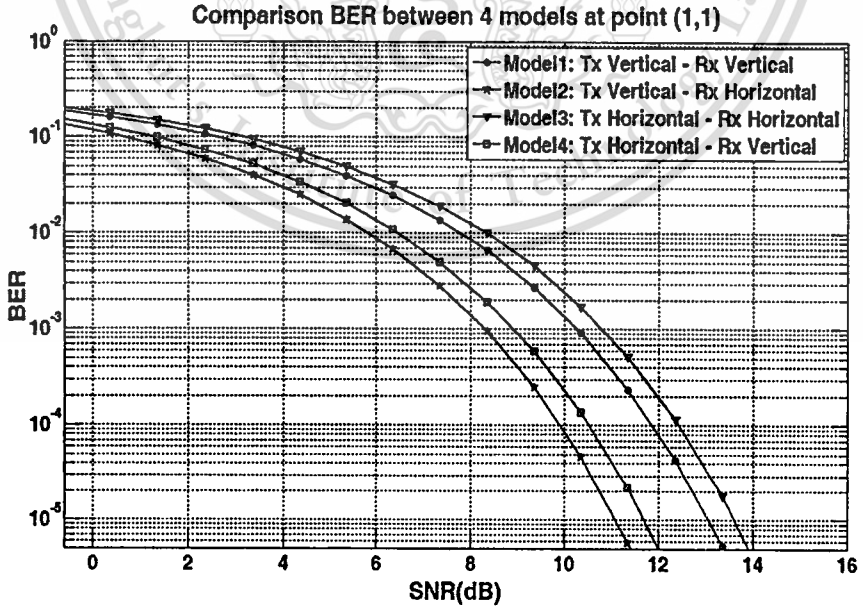

Figure 5.26 BER comparison at point (1,1)

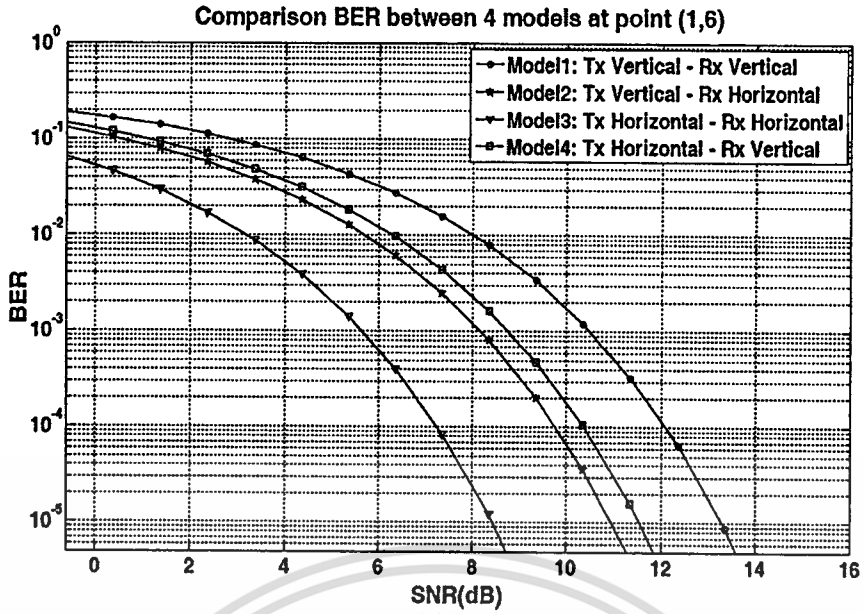

Figure 5.27 BER comparison at point (1,6)

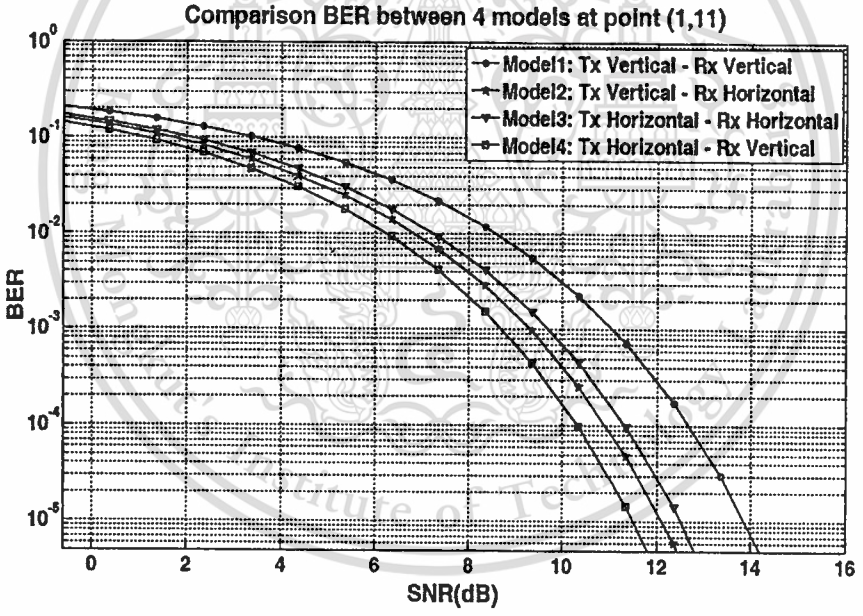

Figure 5.28 BER comparison at point (1,11)

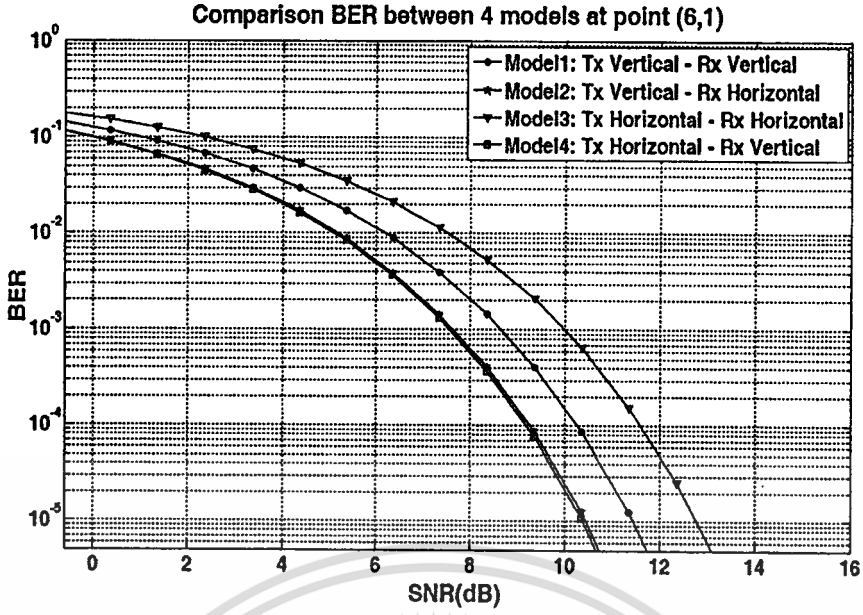

Figure 5.29 BER comparison at point (6,1)

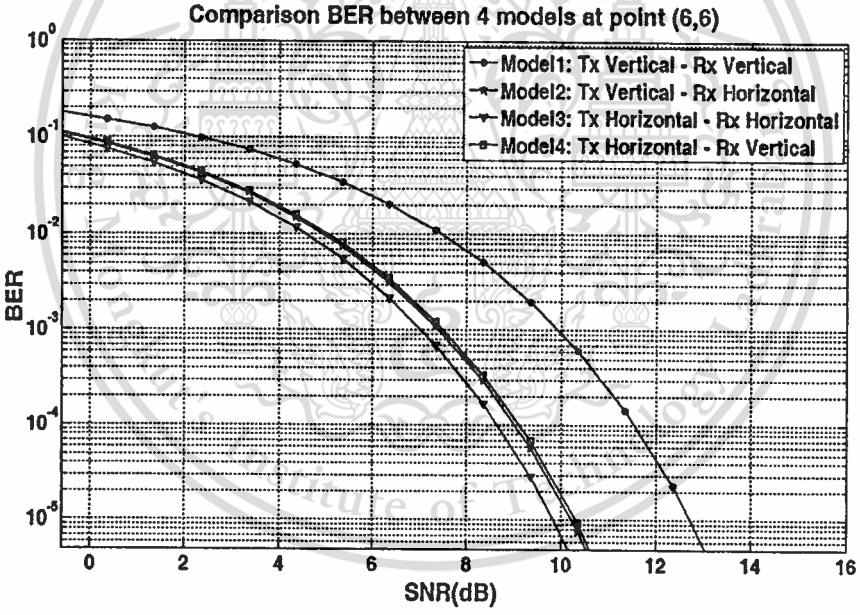

Figure 5.30 BER comparison at point (6,6)

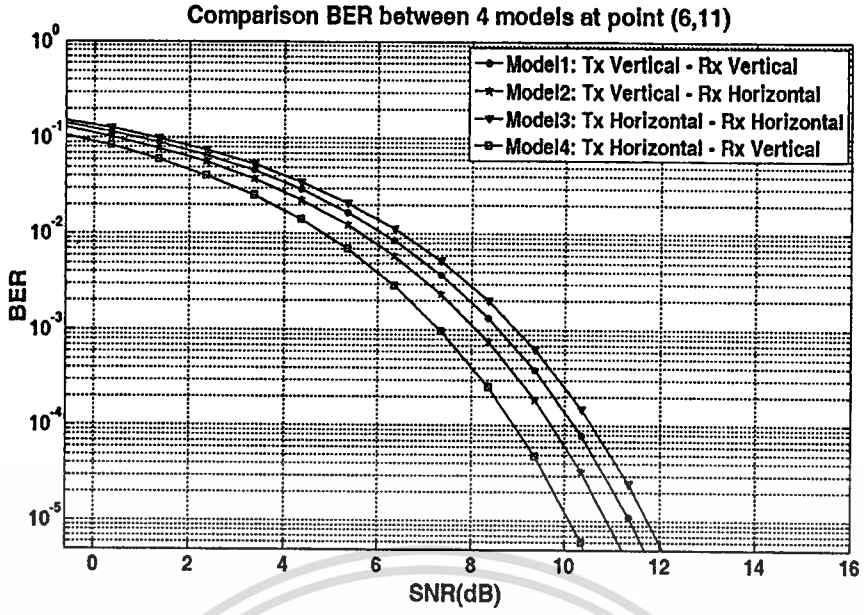

Figure 5.31 BER comparison at point (6,11)

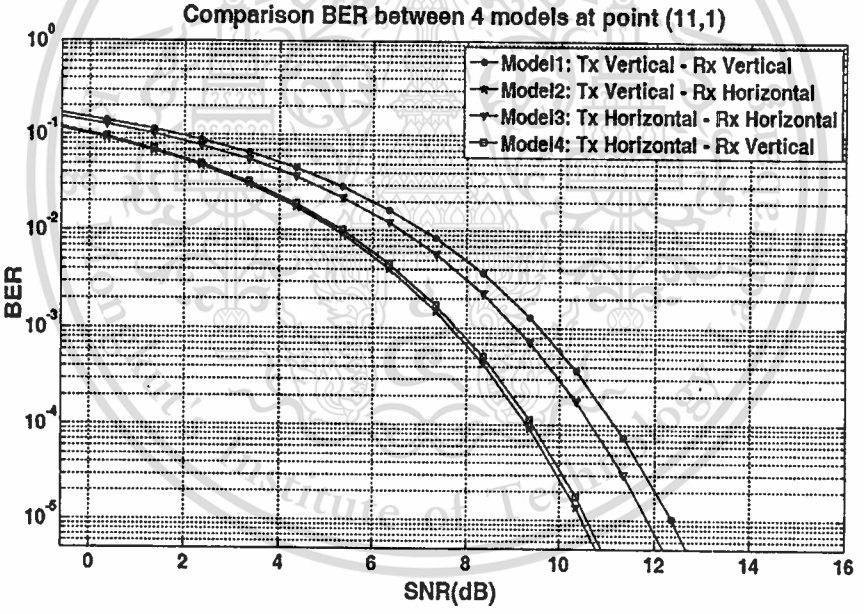

Figure 5.32 BER comparison at point (11,1)

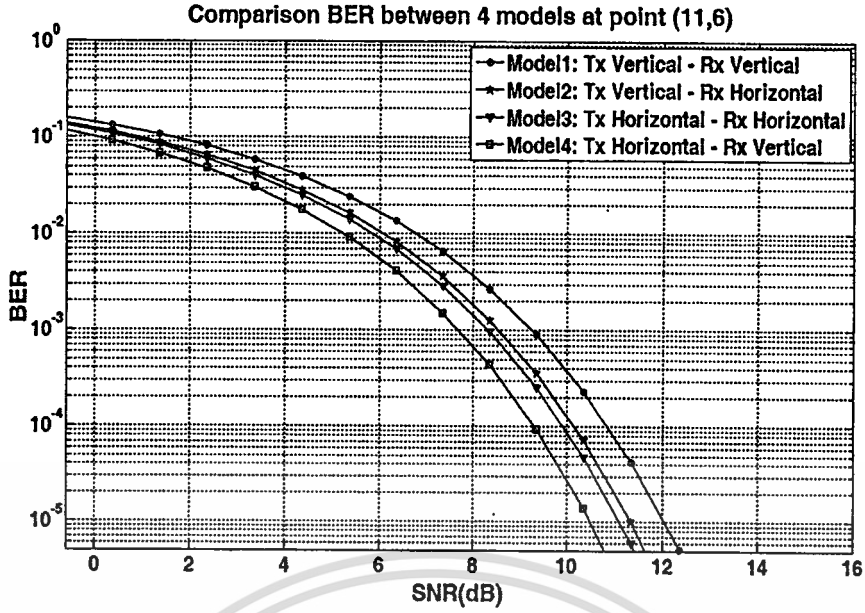

Figure 5.33 BER comparison at point (11,6)

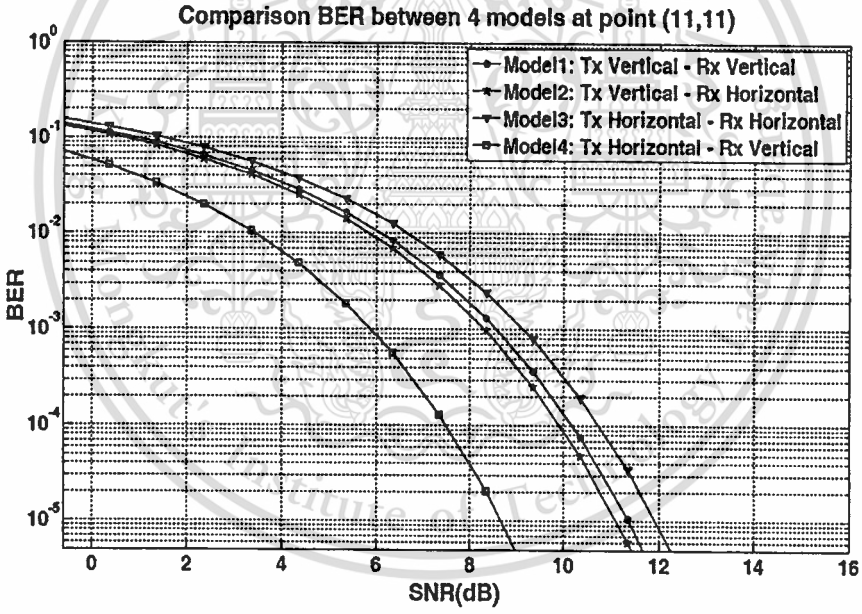

Figure 5.34 BER comparison at point (11,11)

5.3 Conclusion

This chapter presented the results of real measurement in an indoor environment. The experiments carried out on four various polarizations of the antenna, the results of experiment are shows in each polarization consisting of power delay profile, RMS delay spread, correlation coefficient, path loss show by distance and grid, Magnitude of the channel transfer function, phase of the channel transfer function and BER. Finally path loss and BER between various polarizations were compared.

Chapter 6

Conclusions and Recommendations

UWB technology is one of the hot topics of today because of a tremendous promise it holds especially in the field of high data rate and short distance wireless communications. Once realized, UWB can hold its sway over a varied range of applications with the small hardware complexity.

The objective of this thesis we have presented is the UWB impulse radio in an indoor environment to investigate the performance and characteristics of transmission loss by various polarizations of transmitter and receiver antennas. The transmitter and receiver used are biconical antennas. The experiment carried out at the Department of Information Engineering, King Mongkut's Institute of Technology Ladkrabang, Thailand. And the results of experiment are shown in chapter 5.

6.1 Evaluation of each chapter.

In chapter 1, UWB technologies and background are presented. The technologies can take full advantage of the extremely wide bandwidth made available for UWB systems and can also coexist with other existing wireless communication systems. A comparison of occupied bandwidths by UWB and other wireless technologies, motivation and research approach is also provided.

In chapter 2, UWB communication system is presented. In this chapter we explain about history of UWB, UWB regulations in the United State of America (USA) and Europe, characteristics and advantages of UWB such as high data rates, low power consumption, interference immunity, high security, reasonable range and low cost. We also present the UWB IEEE standard and a standard of WPAN is IEEE 802.15 especially IEEE 802.15.3a a new standard for very high data rate for WPAN. And finally we present some applications applied to UWB usage such as precision location, through-wall sensing system, radar and sensor networks.

In chapter 3, Theory and analysis of the UWB channel propagation in an indoor environment is presented. This chapter mentions theory of path loss modeling and multipath channel, which relate to the model of experiment. The block diagram of a transmission

system for UWB signal was shown in figure 3.2 and presented all equations used for analysis including power delay profile, path loss, RMS delay spread, correlation coefficient and BER.

In chapter 4, Experimental setup and channel measurement model for UWB-IR propagation, explains how to setup the model and equipments the step of experiments in 4 polarizations, the main equipment in this experiment is vector network analyzer (VNA). The biconical antennas are used as a transmitter (Tx) and receiver (Rx) antennas. A characteristic of biconical antenna, parameters, UWB transmission signal waveform, and also dimension and environment of experiment room are presented.

In chapter 5, Measurement results for the parametric channel modeling by using biconical antenna at the transmitter and receiver are given in this chapter. The results of experimental including power delay profile, RMS delay spread, correlation coefficient, path loss, magnitude, phase and BER for each polarization, finally is show comparison path loss and BER in four various polarizations.

6.2 Evaluation of experiments

Evaluation and results of experiment in each polarization can conclude as follows:

- **Experiment 1 (Tx Vertical - Rx Vertical)**

This experiment set Tx and Rx antenna are same polarization by using biconical antenna and the polarization of Tx and Rx antenna is vertical. The results of experiment are show as section 5.1.1 in chapter 5.

- **Experiment 2 (Tx Vertical - Rx Horizontal)**

This experiment set Tx and Rx antenna are various polarization by using biconical antenna. A polarization of Tx antenna set vertical polarization whilst polarization of Rx antenna set horizontal. The results of experiment are show as section 5.1.2 in chapter 5.

- **Experiment 3 (Tx Horizontal - Rx Horizontal)**

This experiment set Tx and Rx antenna are same polarization by using biconical antenna and the polarization of Tx and Rx antenna is horizontal. The results of experiment are show as section 5.1.3 in chapter 5.

- **Experiment 4 (Tx Horizontal - Rx Vertical)**

This experiment set Tx and Rx antenna are various polarization by using biconical antenna. A polarization of Tx antenna set horizontal polarization whilst polarization of Rx antenna set vertical. The results of experiment are show as section 5.1.4 in chapter 5.

For comparison results between four polarizations were show and explain in chapter 5, figure 5.25 shown path loss comparisons and figure 5.26, 4.27, 5.28, 5.29, 5.30, 5.31, 5.32, 5.33, and 5.34 were shown BER comparisons. These results for parametric measurement case it's could be useful for designing UWB IR channel propagation in an indoor environments.

6.3 Conclusion

Performance results showed difference value due to the polarization of the antenna. We can see that when Tx and Rx antenna are same polarization (Tx vertical – Rx vertical and Tx horizontal – Rx horizontal) the performance is better than Tx and Rx antenna are various polarization (Tx vertical – Rx horizontal and Tx horizontal – Rx vertical) so a performance of this experiment accurate along to theory of antenna. Beside polarization of the antenna, other factor that may effected to the results of experiment that is environment of experiment room. For example, reflections off walls, ceilings, furniture, people, and other objects that may be present within a room.

UWB IR is a suitable technique to be used in high data rate and short range wireless communications; however, performance of each antenna polarization in the experimental is considered. The Results of this study is useful for designed UWB IR propagation channel in an indoor environment for short range wireless systems.

6.4 Recommendation for future works

Many methods have been studied in determining the network connectivity including our study in which we have considered only one direction under free space propagation model. The recommendations for further research are:

- Range – data rate performance should be studied for different representative indoor environments, ex. home environment, office environments, considering propagation characteristics of such scenarios, using more suitable path loss models.
- Range-data rate performance and specifically the UWB frequency dependent path loss model should consider the frequency dependency of transmitter and receiver antennas.

- Evaluation of the range-data rate performance considering MB-OFDM technique.
- Considerations Time of arrival (TOA).
- Considerations Direction of arrival (DOA) or Angle of arrival (AOA).
- Considerations transmitter and receiver antennas by using various antennas.

REFERENCES

REFERENCES

[1] Ghavami, M., Michael, L.B., Kohno, R., Ultra Wideband Signals and Systems in Communication Engineering, Wiley, 2004.

[2] Benedetto, M., Giancola, G., Understanding Ultra Wide Band Radio Fundamentals, Prentice Hall, 2004.

[3] J. Foerster, E. Green, S. Somayazulu, D. Leeper, "Ultra-Wideband technology for short- or medium-range wireless communications," Intel Technology Journal, 2nd Quarter, 2001, pp. 1 – 11.

[4] Proakis, J., Digital Communications, McGraw-Hill, 3rd edition, 1995

[5] J. R. Foerster, S. Roy, S. Somayazulu, and D. Leeper, "Ultrawideband radio design:The promise of High-Speed, Short-Range Wireless Connectivity," Proceedings of The IEEE, Vol. 92, No. 2, pp. 295-311, Feb. 2004.

[6] Federal Communications Commission, "Revision of Part 15 of the Commission's Rules Regarding UWB Transmission Systems," First Report, FCC 02-48, Apr. 2002.

[7] J. Farserotu, A. Hutter, F. Platbrood, J. Gerrits and A. Pollini, "UWB Transmission and MIMO Antenna Systems for Nomadic User and Mobile PAN," Wireless Personal Communications, no. 22, pp. 197-317, 2002.

[8] R. J. Fontana, "ABrief History of UWB Communications," Multispectral Solutions, Inc. (MSSI), Germantown, MD.

[9] J. G. Proakis and D. G. Manolakis, "Digital Signal Processing: Principles, Algorithms, and Applications," Prentice-Hall, Inc., 3rd edition, 1996.

[10] C. L. Bennett and G. F. Ross, "Time-domain electromagnetics and its applica-tions," Proceedings of the IEEE, Vol. 66, No. 3, pp. 229-318, 1978.

[11] B Allen, "Ultra Wideband Wireless Sensor Networks," IEE UWB Symposium, June 2004.

[12] I. Opperman et al., "UWB Wireless Sensor Networks: UWEN-A practical example, in IEEE Communications Mag., December 2004.

[13] M. Ghavami, L.B Michael, R. Kohno, Ultra Wideband Signals and Systems in Communication Engineering, Wiley, 2004.

[14] H.T. Friis, "A note on a simple transmission formula," Proc. IRE, vol. 34, no. 5, pp. 254–256, May 1946.

[15] United States of America, "Path loss calculations for ultrawideband signals in indoor environments," ITU-R Document 3K/30-E, pp. 1–14, Nov. 2003.

[16] S. Teawchim and S. Promwong, "NOVEL TEMPLATE RECEIVER FOR ULTRA WIDEBAND IMPULSE RADIO," The 1st Joint International Conference on Information Communication Technology (JICT 2007), pp. 296-299, Dec. 19-22, 2007. Vientiane, Lao PDR.

[17] J. Takada, S. Promwong and W. Hachitani, "Extension of Friis' Transmission Formula for Ultra-Wideband Systems," IEICE Tech. Rep., WBS2003-8/MW2003-20, May 2003.

[18] A.H.Mohammadian, A.Rajkotia, and S.S.Soliman, "Characterization of UWB Transmit-Receive Antenna System," Proc. IEEE Conf. Ultra Wideband Syst. Tech. (UWBST) 2003, Nov. 2003.

[19] S. Promwong, and J. Takada, "Free space link budget estimation scheme for ultra wideband impulse radio with imperfect antennas," IEICE Electronics Express, vol. 1, no. 7, pp. 188–192, July 2004.

[20] S. Promwong and W. Hachitani, and J. Takada, "Free Space Link Budget Evaluation of UWBIR Systems," 2004 International Workshop on Ultra Wideband Systems Joint with Conference on Ultra Wideband Systems and Technology (UWBST&IWUWBS), May 2004.

PUBLICATIONS

PUBLICATIONS

[1] Sengaloun Keoalounxay, Sathaporn Promwong, Nikorn Sukutamatanti, and Jun-ichi Takada. "ULTRA WIDEBAND IMPULSE RADIO TRANSMISSION WAVEFORM ANALYSIS WITH HUMAN BODY FOR WIRELESS BODY AREA NETWORKS," The 1st Joint International Conference on Information Communication Technology (JICT 2007), pp. 265-268, Dec. 19-22, 2007. Vientiane, Lao PDR.

[2] Sengaloun Keoalounxay, Sathaporn Promwong, Nikorn Sukutamatanti, Wiphanee Boonsing, and Jun-ichi Takada. "SNR GAIN ANALYSIS OF ULTRA WIDEBAND TEMPLATE RECEIVER FOR WIRELESS PERSONAL AREA NETWORKS," The 14th Asia-Pacific Conference on Communication, Oct. 14-16, 2008. Akihabara, Tokyo, Japan.

ULTRA WIDEBAND IMPULSE RADIO TRANSMISSION WAVEFORM ANALYSIS WITH HUMAN BODY FOR WIRELESS BODY AREA NETWORKS

Sengaloun Keoalounxay[†], *Sathaporn Promwong*[†,††] *Nikorn Sukutamatanti*[†] *and Jun-ichi Takada*[††]

[†]Department of Information Engineering, Faculty of Engineering
King Mongkut's Institute of Technology Ladkrabang, Bangkok 10520, Thailand.
E-mail: sengaloun04@yahoo.com, {kpsathap, ksnikorn}@kmitl.ac.th
[††]Graduate School of Science and Engineering, Tokyo Institute of Technology,
2-12-1-S6-4, O-okayama, Meguro-ku, 152-8550, Tokyo, Japan.
E-mail: takada@ide.titech.ac.jp

ABSTRACT

Ultra wideband impulse radio (UWB-IR) technology is an ideal candidate for wireless networks that can be utilized for short-range, high-speed, low power, and low cost indoor applications. This paper discusses the effects of the human body shadowing on the UWB propagation based on the extended Friis' transmission formula. The matched filter is considered at the receiver side to maximize the SNR for evaluation. The UWB transmission gain are presented. The technique gives very accurate results and is very useful for design and evaluation of UWB impulse radio transmission systems.

Keywords: UWB system, human body shadowing, free space propagation, Friis' transmission formula

1. INTRODUCTION

In UWB communication systems, the antennas are significantly pulse-shaping filters. Any distortion of the signal in the frequency domain causes the distortion of the transmitting pulse shape. Consequently this will increase the complexity of the detection mechanism at the receiver [1]. Moreover, low cost, geometrically small and still efficient structures are required for typical wireless applications. In order to minimize the interference with existent systems, the UWB is expected to be used mainly in wireless personal area networks (WPANs), wireless body area networks (WBANs) and home networks. Therefore the antenna design for UWB signal radiation is one of the main challenges [2, 3].

Even if the channel is in line of sight (LOS), Friis' transmission formula cannot be directly applied to the UWB radio as the bandwidth of the pulse is extremely wide. Furthermore, simple comparison between waveforms of transmitter and receiver is not significant because of the distortion of the waveform caused by the frequency response of the antenna.

In this paper, we discuss the effects of the human body shadowing on the UWB propagation channel. This scheme is based on the Friis' transmission formula, adapted for UWB, in the sense that we would like to derive the equivalent antenna gain for UWB systems. The transmission waveform and the matched filter reception are keys for the extension of the Friis' formula to UWB. An experiment is carried out using the biconical antenna and skycross antenna for UWB operation in the anechoic chamber.

2. FRIIS' TRANSMISSION FORMULA FOR UWB TRANSMISSION SYSTEM

In this study, we focus on the effects of the human body shadowing in free space.

In narrowband systems, the link budget of the free space propagation loss is usually estimated by using Friis' transmission formula [4]. However, it is not directly applicable to the UWB-IR transmission system, as the formula is expressed as a function of the frequency. Moreover, the waveform may be distorted due to the frequency characteristics of the antenna. Ref. [5] treats the special cases of the constant gain and the constant aperture, but no general discussion had been made although it suggested the use of the time-domain antenna effective length.

The Friis' transmission formula has been widely used, and can be applied to the calculation of these LOS channels.

$$G_{\text{Friis}}(f) = \frac{P_r(f)}{P_t(f)} = G_f(f)G_r(f)G_t(f), \qquad (1)$$

where G_r and G_t are Rx and Tx antenna gain,

$$G_f(f) = \left(\frac{\lambda}{4\pi d}\right)^2 \qquad (2)$$

is the free space propagation gain (less than unity in practice), $\lambda = \frac{c}{f}$ is the wavelength, c is the velocity of the light, f is the operating frequency, and d is the separation between transmitter and receiver antennas.

It is noted, however, that Eq. (1) is satisfied only at some certain frequency, and is not directly applicable to UWB systems. The Friis' transmission formula shall be extended to take into account the transmission signal waveform and its distortion as well [6, 7].

Input signal $v_i(t)$ at the transmitter port is expressed as the convolution of an impulse input and the pulse shaping filter $h_i(t)$ as

$$v_i(t) = E_i\delta(t) * h_i(t), \qquad (3)$$

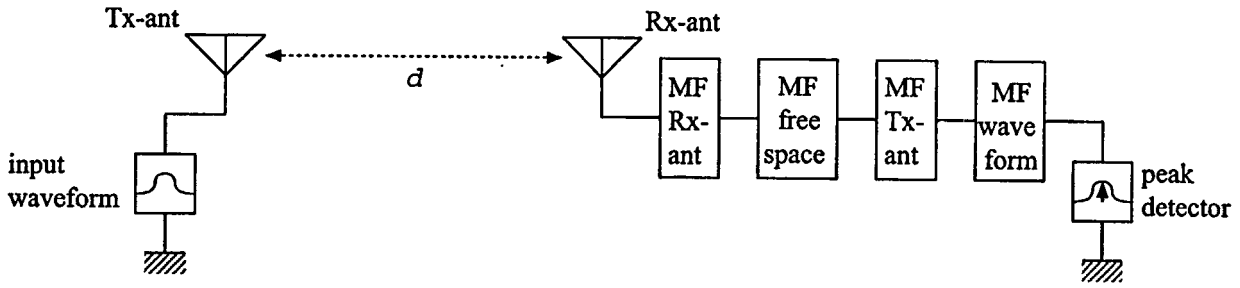

Figure 1. *Block diagram of transmission system for the extension of Friis' transmission formula to treat UWB signal.*

where

$$\int_{-\infty}^{\infty} h_i^2(t)\mathrm{d}t = \int_{-\infty}^{\infty} |\mathrm{H_i(f)}|^2\,\mathrm{df} = 1. \tag{4}$$

Friis' formula is extended taking into account the transmission waveform as

$$H_{\text{c-Friis}}(f) = \frac{V_r(f)}{E_i} = H_f H_i \mathbf{H_r}\cdot\mathbf{H_t}, \tag{5}$$

where

$$\begin{aligned}\mathbf{H_a} &= \mathbf{H_a}(\theta_a,\ \varphi_a,\ \mathrm{f})\\ &= \hat{\theta}_a H_{a\theta}(\theta_a,\ \varphi_a,\ f) + \hat{\varphi}_a H_{a\varphi}(\theta_a,\ \varphi_a,\ f),\\ a &= \mathrm{r}\ or\ \mathrm{t},\end{aligned} \tag{6}$$

is a complex transfer function vector of the antenna relative to the isotropic antenna,

$$H_f = \frac{\lambda}{4\pi d}\exp(-\mathrm{j}kd), \tag{7}$$

is the free space transfer function where

$$k = \frac{2\pi}{\lambda}, \tag{8}$$

is the propagation constant. Unit vectors $\hat{\theta}_a$, $\hat{\varphi}_a$ express the polarization and are defined with respect to the local polar coordinates of each of the antennas. The following relations can be easily derived.

$$\hat{\theta}_r = \hat{\theta}_t, \tag{9}$$

$$\hat{\varphi}_r = -\hat{\varphi}_t. \tag{10}$$

At the receiver, the matched filter $H_{MF}(f)$ is introduced to maximize the signal-to-noise ratio (SNR) of the receiver output, as shown in Figure 1.

$$H_{MF}(f) = \frac{H^*_{\text{c-Friis}}(f)}{\sqrt{\int_{-\infty}^{\infty} |H_{\text{c-Friis}}(f)|^2\,\mathrm{df}}}, \tag{11}$$

which satisfies the following constant noise output power condition

$$\int_{-\infty}^{\infty} |H_{MF}(f)|^2\,\mathrm{df} = 1. \tag{12}$$

In this case, the output waveform when $E_i = 1$, and the spectrum of the receiver output are $h_{\text{c-Friis}}(t)$ and $H_{\text{c-Friis}}(f)$, respectively. The waveform of the output from the matched filter $v_{MF}(t)$ and the spectrum of the output from the matched filter $V_{MF}(f)$ are

$$\begin{aligned}v_{MF}(t) &= h_{\text{c-Friis}}(t) * h_{MF}(t)\\ &= \frac{h_{\text{c-Friis}}(t) * h_{\text{c-Friis}}(-t)}{\sqrt{\int_{-\infty}^{\infty} h^2_{\text{c-Friis}}(t)\mathrm{d}t}},\end{aligned} \tag{13}$$

$$\begin{aligned}V_{MF}(f) &= H_{\text{c-Friis}}(f) H_{MF}(f)\\ &= \frac{|H_{\text{c-Friis}}(f)|^2}{\sqrt{\int_{-\infty}^{\infty} |H_{\text{c-Friis}}(f)|^2\,\mathrm{df}}},\end{aligned} \tag{14}$$

taking its maximum as

$$\begin{aligned}\max_t v_{MF}(t) &= \int_{-\infty}^{\infty} V_{MF}(f)\mathrm{df}\\ &= \sqrt{\int_{-\infty}^{\infty} |H_{\text{c-Friis}}(f)|^2\,\mathrm{df}}.\end{aligned} \tag{15}$$

Equation (15) is the UWB extension of Friis' transmission formula. It includes three elements, namely the frequency characteristics of the antennas, the frequency characteristics of free space propagation, and the spectrum of the transmit signal. It is clear from Eq. (15) that the transmission gain of the UWB signal can not be defined as the product of gains of antennas and a free space channel as Friis' formula (1). Instead, the total transmission gain including the effect of the waveform can be obtained as Eq. (15). For the normalization, the reference isotropic antenna with $H_{Iso}(f) = 1$ is considered. The UWB transmission gain can be defined as

$$G_{UWB} = \max_t v_{MF}(t) / \max_t v_{MF,Iso}(t). \tag{16}$$

3. DESCRIPTIONS OF EXPERIMENTS

3.1. Experimental Setup and Measurement Model

By using the vector network analyzer (VNA), complex transfer functions can be measured. However, this transfer

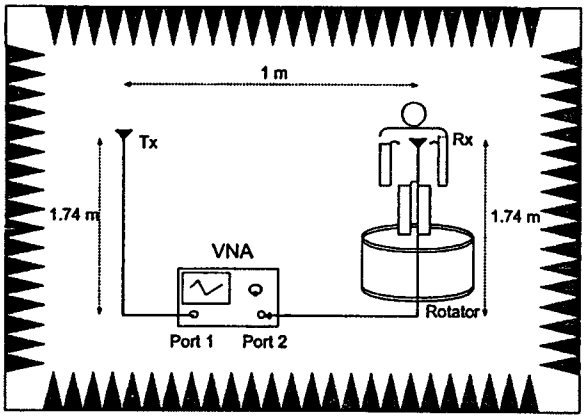

Figure 2. *The instrument setup.*

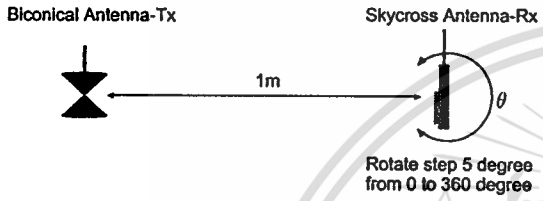

Figure 3. *Top view antenna setting.*

function is a product of transfer functions of Tx and Rx antennas as well as the free space channel. Among them, the free space transfer function is calculated from the distance between the antennas by using Eq. (7). The VNA was operated in the response measurement mode, where Port-1 was the transmitter port (Tx) and Port-2 was the receiver port (Rx), respectively. Biconical antennas with the maximum diameter of 65.3 mm and the length of 37 mm [8] and as the AUT is the broadband Skycross antenna [9]. The measurement was done in the anechoic chamber. Both Tx and Rx antennas were fixed at the height of 1.74 m and separated at a distance of 1 m. The setup is sketched for top view and side view in Fig. 2 and Fig. 3, respectively.

Figure 3 shows the orientations of the S_{21}, transfer function measurement for Tx and Rx antennas. The Tx antenna is fixed at pointing angle 0° and the Rx antenna is rotated from pointing angle 0° to 360° with each step at 5°.

3.2. Parameters of Experiment

The important parameters for the experiments are listed in Table 1.

It is noted that the calibration is done at the connectors of the cables to be connected to the antennas. Therefore, all the impairments of the antenna characteristics are included in the measured results.

3.3. UWB waveform Transmission

The effect of the waveform distortion is more obvious when the bandwidth is wider. We considered the impulse radio signal that fully covers the FCC band [10], i.e., 3.1 ~ 10.6 GHz. The center frequency and the bandwidth

Table 1. *Experimental setup parameters.*

Parameter	Value
Frequency range	3 GHz to 11 GHz
Number of frequency points	1601
Dynamic power range	80 dB
Tx antenna height	1.74 m
Rx antenna height	1.74 m
Distance between Tx and Rx	1 m
Rx rotate range	0° to 360°
Rx rotate step	5°

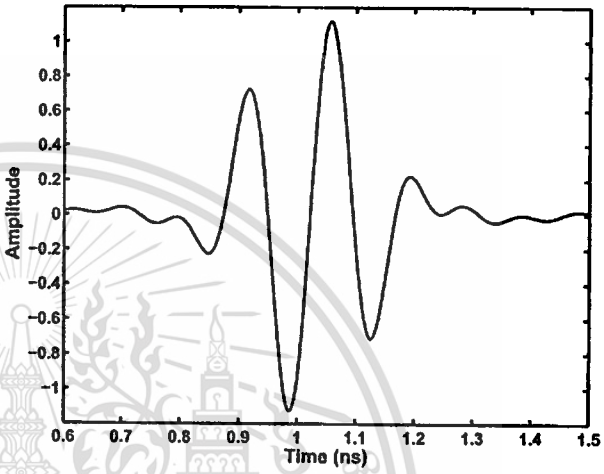

Figure 4. *The transmission waveform of UWB signal.*

were therefore set to be $f_0 = 6.85$ GHz and $f_b = 7.5$ GHz, respectively. The transmit waveform assumed in the simulation was a single ASK pulse with the carrier frequency f_0. To satisfy the bandwidth requirement of f_b, the pulse length was set to be $\frac{2}{f_b}$. Then the signal was band-limited by a Nyquist roll-off filter with roll-off factor $\alpha = 0$ (rectangular window) and passband $\left(f_0 - \frac{f_b}{2},\ f_0 + \frac{f_b}{2}\right)$. Figure 4 shows the transmit pulse waveform. The transmission process of the pulse waveform is simulated based on the measured transfer function of the antenna.

4. EXAMPLE RESULT AND DISCUSSION

We can particularly see the delay spread at each pointing angle. As the AUT is the broadband Skycross antenna, the ideal linear phase is almost realized, except for the null directions which change by the frequency.

The UWB signal shown in Fig. 4 is used as the transmission waveform. The received waveforms at the output of the matched filters is evaluated. The relative gain is defined as Eq. (16). In practice, it is quite complicated and is not feasible to implement the adaptive matched filter to adjust for the antennas. Therefore, the matched filter designed for an isotropic antenna is also considered and is compared with the ideal matched filter.

Figures 5 and 6 shows the UWB transmission gain ver-

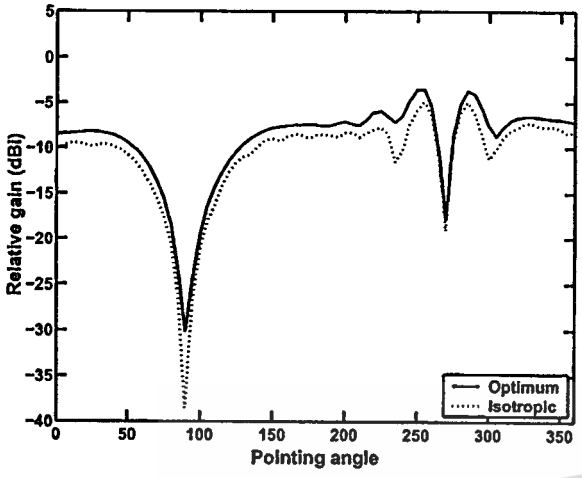

Figure 5. *UWB transmission gain without human body.*

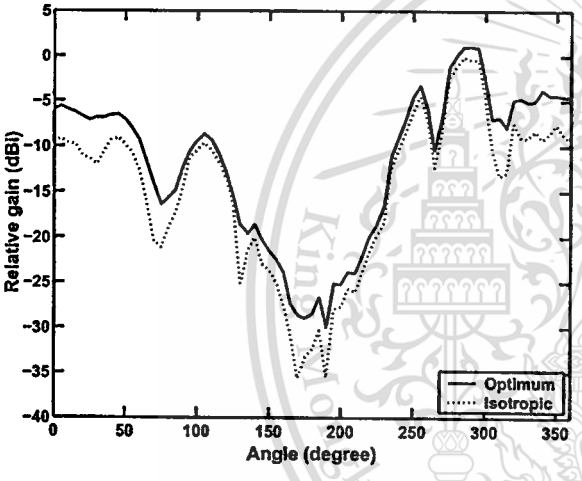

Figure 6. *UWB transmission gain with human body.*

sus antenna pointing angle that uses the optimum matched filter compared with the matched filter for an isotropic antenna.

5. CONCLUSION

This paper presented the effects of the human body shadowing on the UWB transmission gain, which is an extension of Friis' transmission formula in order to take into account the transmit waveform and the matched filter into the system for the free space link budget evaluation of UWB-IR for WBAN. The experimental examples using the biconical antennas for transmitter and the receiver is skycross antennas are presented.

6. REFERENCES

[1] K. Siwiak, "Impact of UWB Transmission on Generic Receiver," Proc. 2001 Spring IEEE Veh. Tech. Conf. (VTC), May 2001.

[2] H.F. Harmuth and S. Ding-Rong, "Antennas for Non-sinusiodal Wave — Part I: Radiators," IEEE Trans. Elec. Mag. Compat., vol. EMC-25, no. 1, pp. 13–24, Feb. 1983.

[3] H.F. Harmuth and S. Ding-Rong, "Antennas for Non-sinusiodal Wave — Part II: Sensors," IEEE Trans. on Elec. Mag. Compat., vol. EMC-25, no. 1, no. 2, pp. 107–115, May 1983.

[4] H.T. Friis, "A Note on a Simple Transmission Formula," Proc. IRE, vol. 34, no. 5, pp. 254–256, May 1946.

[5] United States of America, "Path Loss Calculations for Ultra-Wideband Signals in Indoor Environments," ITU-R Document 3K/30-E, pp. 1–14, Nov. 2003.

[6] J. Takada, S. Promwong and W. Hachitani, "Extension of Friis' Transmission Formula for Ultra-Wideband Systems," IEICE Tech. Rep., WBS2003-8/MW2003-20, May 2003.

[7] A.H. Mohammadian, A. Rajkotia, and S.S. Soliman, "Characterization of UWB Transmit-Receive Antenna System," Proc. IEEE Conf. Ultra Wideband Syst. Tech. (UWBST) 2003, Nov. 2003.

[8] S. Promwong, W. Hachitani, and J. Takada, "Free Space Link Budget Evaluation of UWB-IR Systems," *2004 International Workshop on Ultra Wideband Systems Joint with Conference on Ultra Wideband Systems and Technology* (Joint UWBST&IWUWBS2004), to be presented, May 2004.

[9] Skycross, Inc., "3.1-10 GHz Ultra-Wideband Antenna for Commercial UWB Applications" http://www.skycross.com/

[10] Federal Communications Commission, "Revision of Part 15 of the Commission's Rules Regarding Ultra-Wideband Transmission Systems," First Report and Order, FCC 02–48, Apr. 2002.

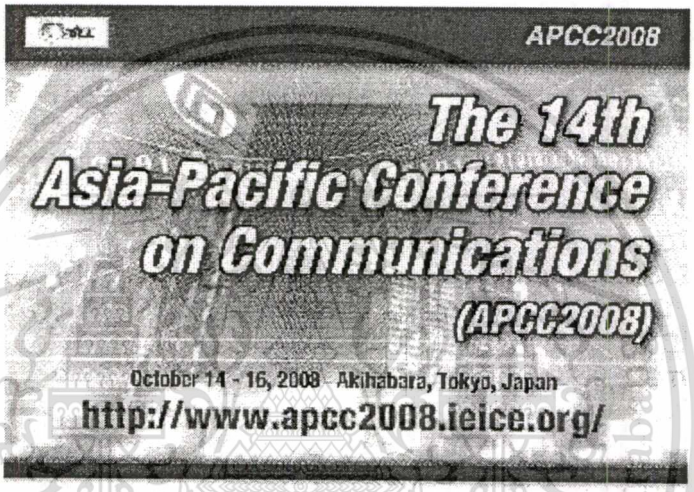

PROCEEDINGS

ISBN978-4-88552-231-4 C3055

SNR Gain Analysis of Ultra Wideband Template Receiver for Wireless Personal Area Networks

Sengaloun Keoalounxay†, Sathaporn Promwong†,††, Wiphanee Boonsing†, Nikorn Sukutamatanti†, and Jun-ichi Takada††

† Department of Information Engineering, Faculty of Engineering,
King Mongkut's Institute of Technology Ladkrabang, Bangkok 10520, Thailand.
††Graduate School of Science and Engineering, Tokyo Institute of Technology
O-okayama Minami 6 Bldg., 2–12–1, O-okayama, Meguro-ku, 152–8550, Tokyo, Japan.
E-mail: kpsathap@kmitl.ac.th

***Abstract*—In this paper, we evaluated the signal to noise ratio (SNR) gain of ultra wideband (UWB) receivers performance for wireless personal area network. The optimum and isotropic template receivers are considered based on the data measurement. The biconical antennas are used as the transmitter (Tx) and receiver (Rx) antennas. The rectangular passband, which is satisfied the full band of UWB signal definition and Federal Communications Commission (FCC) indoor and outdoor limit spectral masks, is used as the transmitted UWB signal. The channels are measured in an anechoic chamber by using a vector network analyzer (VNA). The SNR gains of optimal and isotropic template receivers are shown and compared in results.**

I. Introduction

Recently, ultra wideband (UWB) radio technology has become an important topic for microwave communication because of its low cost and low power consumption potentials [1]-[3]. The UWB is different from other radio frequency (RF) technologies. UWB transmits very short pulse and power spectral density (PSD) in the range of ultra wide frequency spectrum instead of using narrow band radio frequency in traditional RF tecnologies. The UWB is a unique and new usage of recently legalized frequency spectrum. The FCC specified that UWB signal has frequency spectrum ranging from 3.1 GHz to 10.6 GHz [4], and have a fractional bandwidth equal or greater than 0.20, or occupied bandwidth equal or greater than 500 MHz. The fractional and occupied bandwidth are defined as

$$\text{Fractional bandwidth} = \frac{2(f_H - f_L)}{f_H + f_L}, \quad (1)$$

$$\text{Occupied bandwidth} = f_H - f_L, \quad (2)$$

where f_L and f_H are the lowest and highest frequencies at the -10 dB point, respectively.

The PSD of UWB signal does not exceed the FCC part 15 limits or -41.3 dBm/MHz, so that the PSD of UWB signal is considered as the noise for other radio communication systems. Therefore, the UWB radio technology can coexist with other RF communications without interference. Moreover, the UWB radio technology is an ideal candidate that can be utilized for commercial, short-range, low power, low cost indoor communication systems such as wireless personal area networks (WPANs) [5].

The Friis' transmission formula is widely used to calculate the free space path loss for narrowband communications [6]. After that, the complex form of Friis' transmission formula is developed for UWB communications [7]-[9]. The matched filter receiver is used as the UWB receiver [10]-[12]. Although, the rectangular waveform distorted by UWB free space channel is used to derive the theoretical SNR gains [13], there are no considerations about the measured channel and UWB antennas.

In this paper, we evaluated the SNR gains of UWB receivers performance. The optimum and isotropic template receivers satisfied constant noise power condition between input and output are considered. The biconical antennas are used as the transmitter (Tx) and receiver (Rx) antennas. The rectangular passband, which is satisfied the full band of UWB signal definition and FCC indoor and outdoor limit spectral masks, is used as the transmitted UWB signal. The channels are measured in an anechoic chamber by using a vector network analyzer (VNA). The frequency range of measurement is form 3 GHz to 11 GHz. The path losses are evaluated and investigated for considering the SNR gains. The SNR gains of optimal and isotropic template receivers are shown and compared. The results are discussed in the conclusion.

This paper is organized as follows. Section 2, the evaluation of SNR gain for UWB systems. Section 3, the UWB template receiver. Next, the evaluation results are illustrated in Section 4. Finally, the conclusions are discussed in Section 5.

II. SNR Gain Evaluation Scheme for UWB Systems

A. UWB Signal Waveform Model

For UWB waveform signal, the rectangular passband waveform is considered as the UWB transmitted signal. The expression of UWB transmitted signal (v_t) in time domain is given by

$$v_i(t) = \frac{A}{f_b}[f_H \text{sinc}(2f_H t) - f_L \text{sinc}(2f_L t)], \quad (3)$$

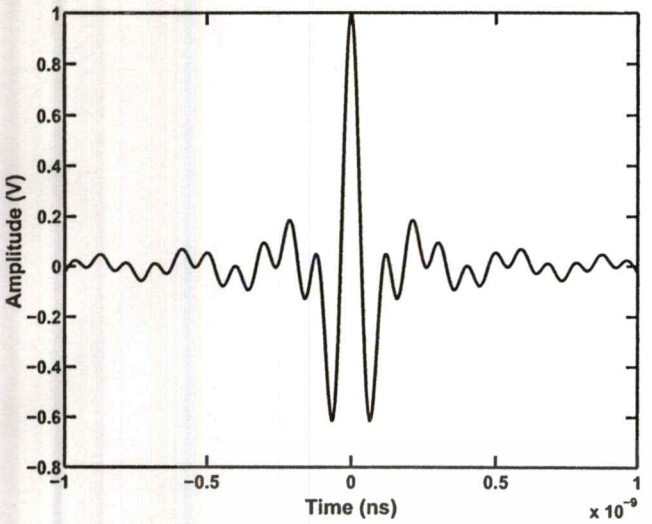

Fig. 1. Transmitted signal waveform of UWB.

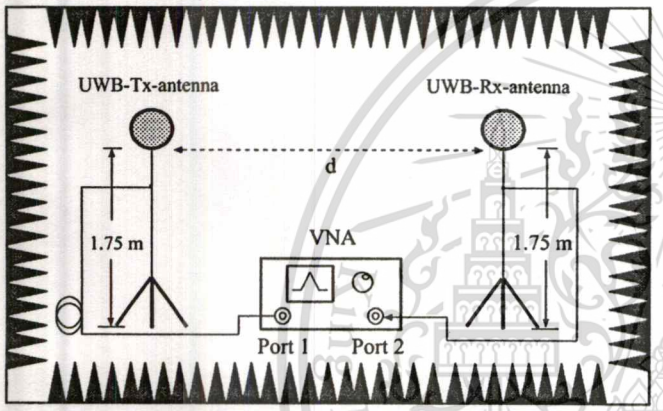

Fig. 2. The instrument setup.

where $A = 1$ V is the maximum amplitude, $f_b = 7.5$ GHz is the occupied bandwidth, $f_L = 3.1$ GHz and $f_H = 10.6$ GHz are the minimum and maximum frequencies. This transmitted UWB signal is shown in Fig. 1.

B. Measurement System

The UWB channel transfer function is measured in frequency domain by using VNA in an anechoic chamber. The VNA is operated in the response measurement mode, where Port-1 and Port-2 are the Tx and Rx ports, respectively. Both Tx and Rx antennas are fixed at the height of 1.75 m and separated by 1 m. This measurement setup is shown in Fig. 2.

The biconical antennas are used as the Tx and Rx antennas. These antennas are chosen because they are easy to fabricate and have low distortion property. The geometry and dimensions of the antenna is shown in Fig. 3. The upper cone is connected to the center conductor of a coaxial line while the lower cone is connected to the shield conductor. The maximum diameter is 65.3 mm and the length is 37 mm. Only Rx antenna is

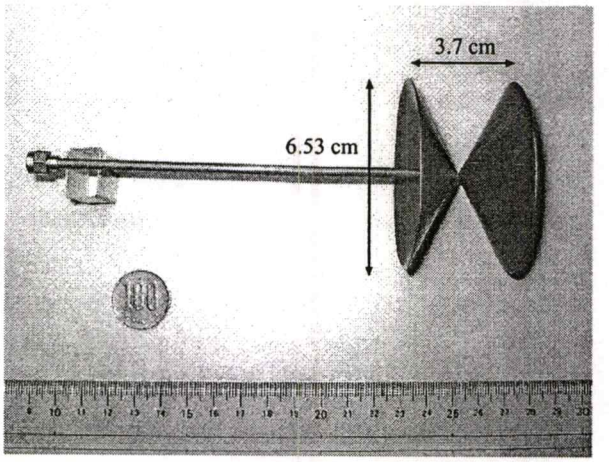

Fig. 3. Geometry and dimensions of the biconical antenna.

TABLE I
MEASUREMENT PARAMETERS.

Parameter	Value
Frequency range	3 GHz to 11 GHz
Number of frequency points	1601
Dynamic power range	80 dB
Tx and Rx antennas heights	1.75 m.
Distance between Tx and Rx antennas	1.00 m.
Rx rotation range	0° – 360°
Rx rotation step	5°
Polarization	horizontal

rotated from 0° to 360 ° with 5° rotation step. The horizontal polarization is measured.

The measurement parameters are listed in Table 1. It is note that the calibration of VNA is done at the connectors of the cables to be connected to the antennas. Therefore, all impairments of the antenna characteristics are included in the measurement results.

III. UWB Template Receivers

A. Optimum Signal Analysis

The template receiver is used at the receiver side as shown in Fig. 4. The optimum and isotropic template receivers satisfied constant noise power condition between input and output are considered. The optimum template receiver considered received signal from measured channel and it is an ideal case with maximum SNR gain, while the isotropic matched filter considered received signal from free space channel using Friss' transmission formula [7]-[9] with isotropic Tx and Rx antennas.

For constant noise power condition between input and output, the frequency transfer functions of optimum and isotropic template receivers, H_{opt} and H_{iso}, are normalized as

$$\int_{-\infty}^{\infty} |H_{opt}(f)|^2 df = \int_{-\infty}^{\infty} |H_{iso}(f)|^2 df = 2f_b. \quad (4)$$

Therefore, the output noise power is a constant as $N_0 f_b$, where $N_0/2$ is the PSD of additive white Gaussian noise (AWGN).

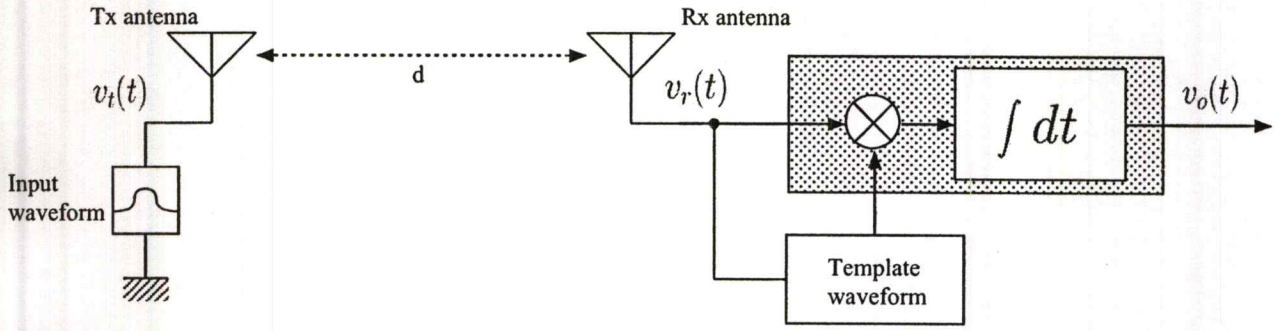

Fig. 4. Block diagram of SNR gain for UWB system.

Under this condition, the frequency transfer functions of optimum and isotropic template can be respectively written as

$$H_{\mathrm{opt}}(f) = \frac{\sqrt{2f_{\mathrm{b}}}V_{\mathrm{r}}^{*}(f)}{\sqrt{\int_{-\infty}^{\infty}|V_{\mathrm{r}}(f)|^{2}\mathrm{d}f}}, \quad (5)$$

$$H_{\mathrm{iso}}(f) = \frac{\sqrt{2f_{\mathrm{b}}}V_{\mathrm{r-iso}}^{*}(f)}{\sqrt{\int_{-\infty}^{\infty}|V_{\mathrm{r-iso}}(f)|^{2}\mathrm{d}f}}, \quad (6)$$

where * is the complex conjugate operator, V_{r} and $V_{\mathrm{r-iso}}$ are the spectral densities of received signals from measured channel and free space channel with isotropic Tx and Rx antennas, respectively. They can be evaluated from

$$V_{\mathrm{r}}(f) = H_{\mathrm{c}}(f)V_{\mathrm{t}}(f), \quad (7)$$

$$V_{\mathrm{r-iso}}(f) = H_{\mathrm{f}}(f)V_{\mathrm{t}}(f), \quad (8)$$

where V_{t} is the spectral density of transmitted signal calculated from

$$V_{\mathrm{t}}(f) = \int_{-\infty}^{\infty} v_{\mathrm{t}}(t)e^{-j2\pi ft}\mathrm{d}t, \quad (9)$$

H_c is the frequency transfer function of measured channel measured from Sec. 2.2 and H_f is the frequency transfer function of free space channel given by

$$H_{\mathrm{f}}(f) = \frac{c}{4\pi d|f|}e^{-j2\pi fd/c}, \quad (10)$$

where d is the distance and c is the velocity of light.

B. SNR Gain Analysis

Because of the frequency transfer functions of optimum and isotropic matched filter receivers are satisfied the constant noise power condition between input and output, the ratio between average powers of output and input signals of matched filter receiver, v_{o} and v_{r}, is the SNR gain. Therefore, SNR gain can be defined as

$$G_{\mathrm{SNR}} = \frac{\int_{-\infty}^{\infty}|v_{\mathrm{o}}(t)|^{2}\mathrm{d}t}{\int_{-\infty}^{\infty}|v_{\mathrm{r}}(t)|^{2}\mathrm{d}t}. \quad (11)$$

The output signal of matched filter receiver can be computed from

$$v_{\mathrm{o}}(t) = \int_{-\infty}^{\infty} H_{\mathrm{a}}(f)V_{\mathrm{r}}(f)e^{j2\pi ft}\mathrm{d}f, \quad (12)$$

where a is opt or iso, which is presented to optimum and isotropic, respectively.

The input signal of template receiver or received signal is calculated by using inverse Fourier transform of its spectral density

$$v_{\mathrm{r}}(t) = \int_{-\infty}^{\infty} V_{\mathrm{r}}(t)e^{j2\pi ft}\mathrm{d}f. \quad (13)$$

IV. Results

In this section, the evaluation results of SNR gains are shown. First, the path losses based on average power losses of received signal and output signals of optimum and isotropic template receivers are considered.

Figure 5 shows the path losses of received signal and output signals of optimum and isotropic template receivers along pointing angle from 0° to 360°. The path losses at 0°, 180° and 360° pointing angles are low because they correspond to the broadside direction of biconical antenna and they are high at 90° and 270° pointing angles. The path losses of output signals of both template receivers are lower than that of received signal. This improvement is considered in the term of SNR gain.

The SNR gains of optimum and isotropic template receivers along pointing angle from 0° to 360° are shown in Fig. 6. The average SNR gain of optimum and isotropic template receivers are about 2.99 and 2.56 dB, respectively. Therefore, the SNR gain of optimum template receiver is better that that of isotropic template about 0.43 dB. Considering this, the bit error rate performance of the optimum and isotropic template shown in Fig.7. It can be seen that the different is low. As described above, by this scheme, it becomes possible to detect several types of UWB signals.

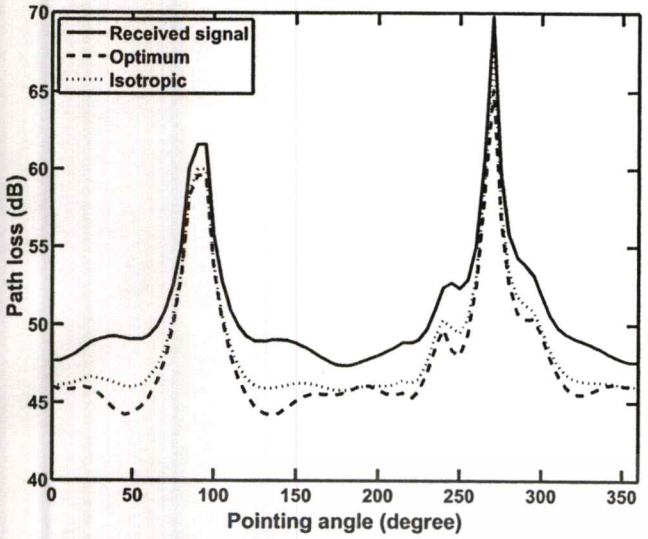

Fig. 5. Path loss of received signales and output signals of optimum and isotropic template receivers along pointing angle from 0° to 360°.

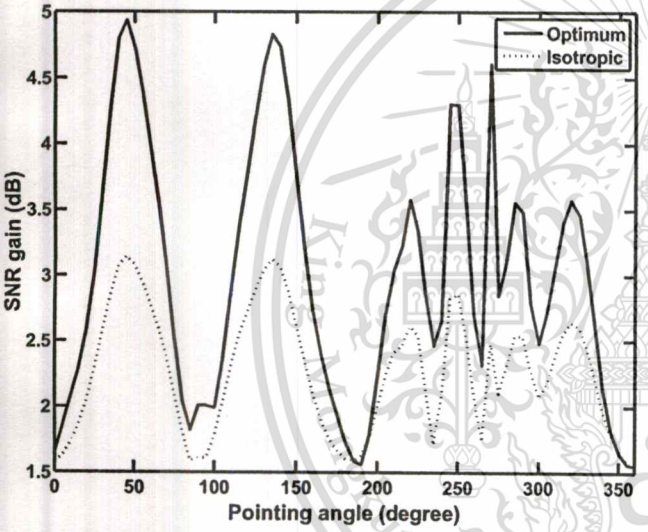

Fig. 6. SNR gains of optimum and isotropic template receivers along pointing angle from 0° to 360°.

V. Conclusion

In this paper, we discussed the SNR gains of UWB template receivers performance are evaluated for WPANs. The optimum and isotropic template receivers are considered. The biconical antennas are used as the Tx and Rx antennas. From the results, the SNR gains of optimum and isotropic template receivers are about 2.99 and 2.56 dB, respectively. The difference is low, that is only 0.43 dB. That because the channel is measured in the anechoic chamber, which can assume to be free space channel, and the biconical antennas have low distortion characteristics. In the future work, the SNR gains of indoor environment and other UWB antennas are investigated.

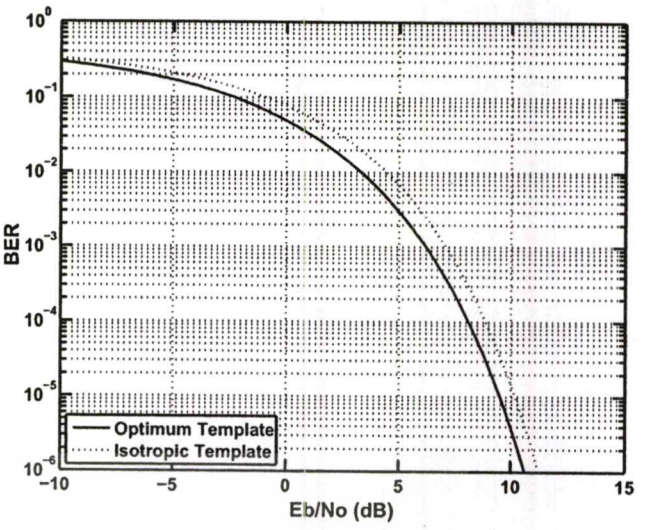

Fig. 7. Bit error rate of the optimum template and isotropic template performance are shown.

References

[1] K. Siwiak, "Ultra-Wide Band Radio: Introducing a New Technology," *2001 Spring IEEE Vehicular Technology Conference (VTC)*, vol. 2, pp. 1088-1093, May 2001.

[2] K. Siwiak, "Ultra-Wide Band Radio: The emergence of an Important RF Technology," *2001 Spring IEEE Vehicular Technology Conference (VTC)*, vol. 2, pp. 1169-1172, May 2001.

[3] K. Siwiak, "Impact of ultra wide band transmissions on a generic receiver," *2001 Spring IEEE Vehicular Technology Conference (VTC)*, vol. 2, pp. 1181-1183, May 2001.

[4] Federal Communications Commission, "Revision of Part 15 of the Commission's Rules Regarding UWB Transmission Systems," First Report, FCC 02-48, Apr. 2002.

[5] J. Farserotu, A. Hutter, F. Platbrood, J. Gerrits and A. Pollini, "UWB Transmission and MIMO Antenna Systems for Nomadic User and Mobile PAN," *Wireless Personal Communications*, no. 22, pp. 197-317, 2002.

[6] H. T. Friis, "A Note on a Simple Transmission Formula," *Proc. IRE*, Vol 34, no 5, pp. 254-256, May 1946.

[7] J. Takada, S. Promwong and W. Hachitani, "Extension of Friis' Transmission Formula for UWB Systems," *Technical Report of IEICE*, WBS2003-8/MW2003-20, May 2003.

[8] S. Promwong, W. Hachitani and J. Takada, "Experimental Evaloation Scheme of UWB Antenna Performance," *Technical Meeting on Instrument and Measurement*, IEE Japan, IM-03-35, June 2003.

[9] S. Promwong, W. Hachitani, J. Takada, P. Supanakoon and P. Tangtisanon, "Experimental Study of Ultra-Wideband Transmission Based on Friis' Transmission Formula," *The Third International Symposium on Communications and Information Technology (ISCIT) 2003*, vol. 1, pp. 467-470, Sept. 2003.

[10] S. Promwong, J. Takada, P. Supanakoon and P. Tangtisanon, "Path Loss and Matched Filter Gain for UWB System," *2004 International Symposium on Antenna and Propagation (ISAP)*, pp. 97-100, Aug. 2004.

[11] S. Promwong, J. Takada, P. Supanakoon and P. Tangtisanon, "Path Loss and Matched Filter Gain of Free Space and Ground Reflection Channels for UWB Radio Systems," *IEEE TENCON 2004 on Analog and Digital Techniques in Electrical Engineering*, pp. 125-128, Nov. 2004.

[12] F. Tufvesson and A. F. Molisch, "Ultra-Wideband Communication Using Hybrid Matched Filter Correlation Receivers," *2004 IEEE 59th Vehicular Technology Conference (VTC)*, vol. 3, pp. 1290-1294, May 2004.

[13] P. Supanakoon, K. Teplee, S. Promwong, S. Keawmechai and J. Takada, "Theoretical SNR Gain and BER Performances of UWB Communications with Matched Filter and Correlation Receivers," *The International Technical Conference on Circuits/Systems, Computers and Communications (ITC-CSCC 2006)*, no. 3, pp. 269-272, July 2006.

VITA

Sengaloun Keoalounxay, was born on October 17, 1976, at Attapeu province, Lao PDR. In 1996, he joined the four-year Bachelor of Engineering degree program in Civil Engineering, Faculty of Engineering and Architecture, National University of Laos (NUOL) and graduated in June 2000. Since September 2000, he was a lecturer at the Faculty of Engineering and Architecture, NUOL. Due to his interest in Information Technology (IT), he jointed 2 years studies to the upgrading to the Bachelor of Information Technology (B.IT.) in the IT bridging course established in the Faculty of Engineering (FE), NUOL and graduated in December 2004. After receiving an award from the ASEAN University Network Southeast Asia Engineering Education Development Network (AUN/SEED-Net), In May 2007 he joined King Mongkut's Institute of Technology Ladkrabang (KMITL) in Thailand for his Masters in Information Engineering. His area of interest is in the field of Information and Communications Technology (ICT) which led him to this work in ultra wideband (UWB) communications.